Appendix V9-3A

2013 Bathurst Inlet Marine Diesel Fuel Spill Modelling Report

Rescan™
an ERM company

Sabina Gold & Silver Corp.

BACK RIVER PROJECT
2013 Bathurst Inlet Marine Diesel Fuel Spill Modelling

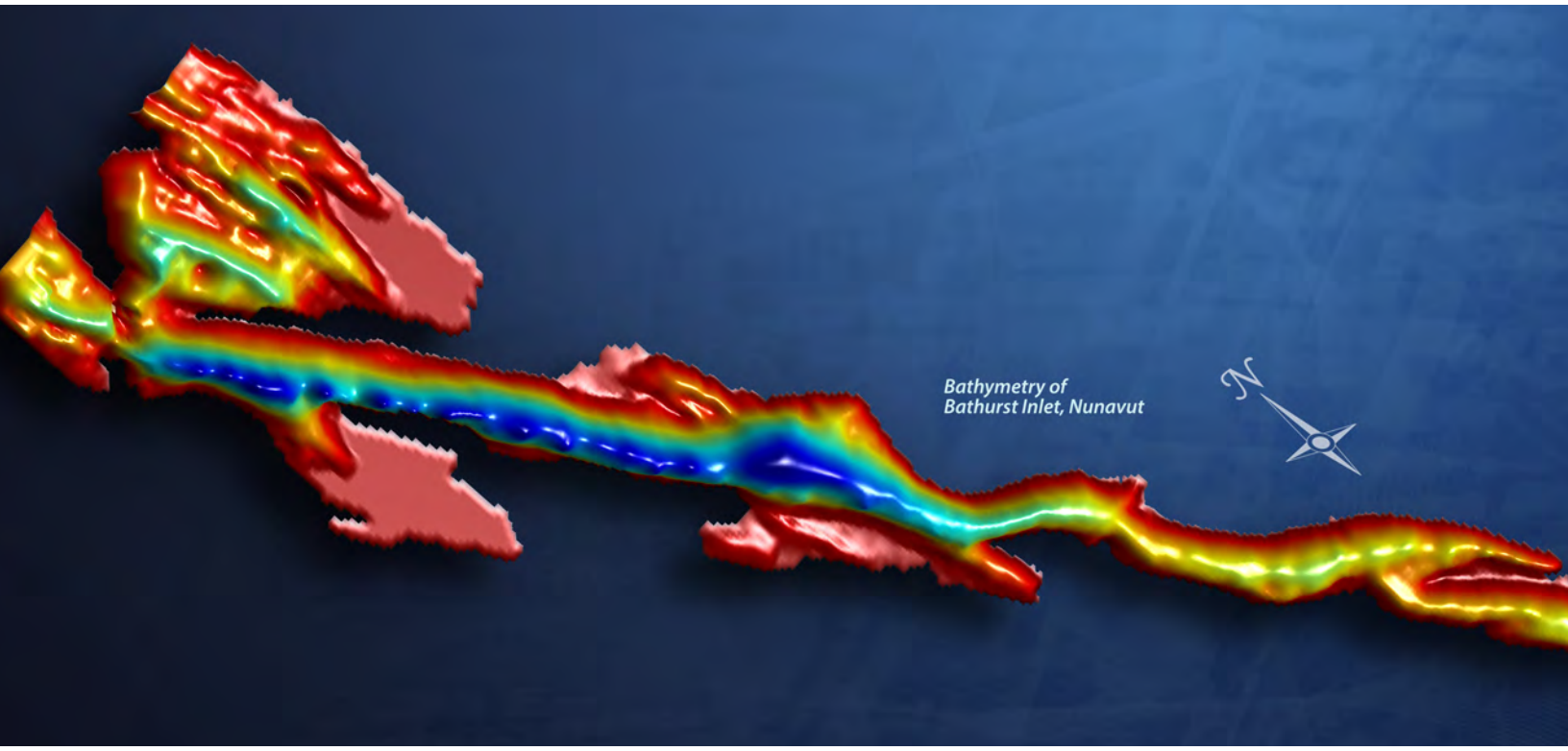

Rescan™ Environmental Services Ltd., an ERM company
Rescan Building, Sixth Floor - 1111 West Hastings Street
Vancouver, BC Canada V6E 2J3
Tel: (604) 689-9460 Fax: (604) 687-4277

September 2013

BACK RIVER PROJECT

2013 BATHURST INLET MARINE DIESEL FUEL SPILL MODELLING

September 2013
Project # 0194096-0038

Citation:

Rescan. 2013. *Back River Project: 2013 Bathurst Inlet Marine Diesel Fuel Spill Modelling*. Prepared for Sabina Gold & Silver Corp. by Rescan Environmental Services Ltd., an ERM company

Prepared for:

Sabina Gold & Silver Corp.

Prepared by:

Rescan Environmental Services Ltd., an ERM company
Vancouver, British Columbia

Executive Summary

Rescan™
an ERM company

Executive Summary

This report presents the modelling study that was completed to predict the fate of potential diesel fuel spills near the Marine Laydown Area (MLA) in Bathurst Inlet during the open-water season (i.e., ~ July to October). The spills were assumed to originate near the MLA site, where diesel would be stored on fuel barges anchored near the shore. Two types of fuel volumes were assessed during simulations: 1) a large spill of 5 ML that could hypothetically occur as a result of a serious collision accident, and 2) a smaller 20 kL spill that would represent the typical volume being transferred between a marine vessel and the shore.

The DHI MIKE3 3D numerical fluid model, coupled with the DHI Oil Spill Module, was used to run the simulations. The main results of the modelling work are summarized below.

2012 Baseline Simulation (Model Calibration)

A 3D numerical fluid model was constructed in order to accurately model potential diesel fuel spills in southern Bathurst Inlet. The model was shown to reasonably reproduce the conditions observed during August and September 2012 (Rescan 2012c). The circulation pattern was mainly driven by a combination of wind forcing and river freshwater discharges, in agreement with the observations from past studies (Rescan 2012c). The thermohaline structure was adequately simulated for the measurement period, and the currents were of the same magnitude order as the field observations.

Diesel Fuel Spill Simulations

The diesel volume scenarios were modelled under hundreds of different wind conditions, from which spill probability distribution figures were drawn. Results from the 5 ML simulations showed a significant proportion of the simulations did not result in much movement of diesel fuel outside of the MLA area; however, a minority of spills caused vast spreading of the diesel slicks across southern Bathurst Inlet. Most of the diesel deposits were limited to the southern portion of the modelled inlet, and over two-thirds of the diesel quickly weathered out within the first 10 days of all simulations. The diesel probability distributions and spread resulting from the 20 kL diesel spills were of much smaller scale compared to the 5 ML simulations. High probabilities were only recorded directly near the MLA site; diesel very rarely spread in the areas outside of the MLA.

High winds (i.e., >8 m/s) and large freshwater discharges were commonly associated with the far spreading of diesel fuel slicks. Prevalent southern winds resulted in northward currents moving the diesel fuel towards Kingaok, while northern winds generated southern currents which moved diesel fuel slicks towards the proposed BIPR port location. Regardless of diesel amounts, spills occurring in mild to moderate wind conditions generally did not progress past a few kilometres from the spill origin near the MLA.

Marine Birds Sensitivity Analysis

Marine bird observations in Bathurst Inlet were compared with the shoreline residual probability distributions resulting from the diesel fuel spill simulations. The MLA region had the highest diesel residual probability for the 5 ML spill simulations, however very few bird observations were correlated with that high diesel fuel spill probability area. Large amounts of geese and ducks were observed in the cove directly south of the MLA, but simulation probabilities indicated than <10% of simulations had some diesel remaining at or near the shore in that area. Other regions with frequent bird observations had similar shoreline probability distributions. Marine bird observations were also compared with

results from the 20 kL spill simulations. The residual shoreline probabilities were very similar to 5 ML simulations near the MLA, thus limited sensitive bird areas would be affected. Furthermore, almost all sensitive bird areas outside of the MLA were not affected by diesel fuel spills. Thus it is assumed that diesel spills of the order of ~<20 kL would have minimal impacts on the marine bird populations of Bathurst Inlet.

Acknowledgements

Rescan™
an ERM company

Acknowledgements

This report was prepared for Sabina Gold and Silver Corp. (Sabina) by Rescan Environmental Services Ltd. (Rescan). The modelling work was conducted by Philippe Benoit (M.Sc.). The report was written by Philippe Benoit and was reviewed by Mike Henry (Ph.D.) and Deborah Muggli (Ph.D., M.Sc., R.P.Bio.). The project was managed by Deborah Muggli. Field data used for calibrating the model was collected by Rescan field staff with the site and logistical support of Sabina.

Table of Contents

Rescan™
an ERM company

BACK RIVER PROJECT
2013 BATHURST INLET MARINE DIESEL FUEL SPILL MODELLING

Table of Contents

List of Figures

FIGURE **PAGE**

List of Tables

TABLE **PAGE**

List of Appendices

Glossary and Abbreviations

Rescan™
an ERM company

Glossary and Abbreviations

Terminology used in this document is defined where it is first used. The following list will assist readers who may choose to review only portions of the document.

ADCP	Acoustic Doppler Current Profiler
Baroclinic/Baroclinity	Characteristic of a stratified fluid that has misaligned pressure and density gradients, a fundamental requirement for the generation of eddies.
BIPR	Proposed Bathurst Inlet Port and Road project
CHS	Canadian Hydrographic Service
CTD	Conductivity, temperature, and depth profiler
Current velocity	Speed of the water movement at a given water depth. By convention, the direction of a current (in degrees) is given as the direction towards which the current is heading.
Density	Weight of water per unit volume (kg/m^3); calculated from temperature, salinity and pressure.
Diesel fuel oil	Refined crude oil fraction obtained from petroleum distillation. This is the type of oil that would be stored at the MLA and is modelled in this report.
Lagrangian	In fluid dynamics, refers to the frame of reference where an observer follows an individual fluid parcel as it moves through space and time (see Kundu [1990] for details).
'Negative' estuary	An estuary where freshwater losses from evaporation or ice formation exceed freshwater additions (e.g., river discharge, rain, ice melting). This leads to a landward longitudinal density gradient that drives a strong surface volume inflow from the ocean in response to the freshwater scarcity, and a correspondingly weaker near-bottom seaward outflow.
NOAA	National Oceanic and Atmospheric Administration
"Positive" estuary	An estuary where freshwater additions (e.g., river discharge, rain, ice melting) exceed freshwater losses from evaporation or freezing. This leads to a seaward longitudinal density gradient that drives a strong surface volume outflow to the ocean in response to the supplementary freshwater, and a correspondingly weaker near-bottom inflow of seawater.
PSS	Practical salinity scale
Pycnocline	Depth zone where density changes sharply.
Salinity	Dimensionless (i.e., no units) scaling used to represent the total mass of solid material dissolved in a sample of water divided by the mass of that sample. The scaling used is based the PSS-78 standard, which relates the conductivity ratio of a seawater sample to a KCl solution (for additional details see UNESCO [1985]).
UNESCO	United Nations Educational, Scientific and Cultural Organization

Thermocline	Depth zone where temperature changes sharply.
Thermohaline	Relating to temperature and salinity
Wind Velocity	Speed of wind, generally standardized at an altitude of 10 metres. By convention, the direction of a wind (in degrees) is given as the direction from which the wind is blowing.

1. Introduction

1. Introduction

The Back River Project (the Project) is a proposed gold mine that includes a Marine Laydown Area (MLA) within southern Bathurst Inlet, Nunavut (see Figure 1-1). Equipment, material, fuel and supplies would be delivered by annual sealifts and staged at the MLA during the open-water season and transported to the Goose and/or George properties via a winter road. Diesel fuel would be stored on fuel barges anchored near the MLA, and subsequently unloaded to shore by means of flexible hoses.

This report presents the results of a diesel fuel oil spill model that was developed to support the permitting of the Project. An oil spill may consist of a variety of materials, including crude oil, refined petroleum products (such as gasoline or diesel fuel), or by-products such as a ship's bunkers oily refuse. However, the oil spill model presented in this report is intended to simulate the expected behavior of diesel fuel, which is the oil type that will be stored at the MLA.

For this study, DHI's Oil Spill Module (DHI 2012a) was coupled to the MIKE3 Flow model (DHI 2012b, 2012c) to predict the fate of marine diesel fuel spills within southern Bathurst Inlet. The scenario modelled was a hypothetical accidental release of diesel fuel at the proposed MLA site in Bathurst Inlet during the open-water season. Although such an event is extremely unlikely in settings similar to the MLA (Anderson, Mayes, and LaBelle 2012), a spill could potentially occur as a result of a serious collision accident or while transferring fuel between a marine vessel and the shore. The following two diesel fuel spill scenarios were examined:

1. 5,000,000 L (5 ML)
2. 20,000 L (20 kL)

This report details the methodology used in the numerical model, results for the two spill scenarios and a shoreline environmental sensitivity analysis. Chapter 2 describes the theory and methodology used for the Bathurst Inlet hydrodynamic numerical model construction, Chapter 3 focuses on the diesel fuel parameterization coupled to the hydrodynamic model, Chapter 4 presents the graphical displays and analysis of the simulation results, Chapter 5 details how sensitive local marine bird areas could be affected by potential diesel fuel spills, and Chapter 6 summarizes the model findings in terms of the statistical probability fate of the diesel spills.

PROJECT #0194096-0038 GIS # BAC-28-014 VERSION # T2.0 September 16 2013

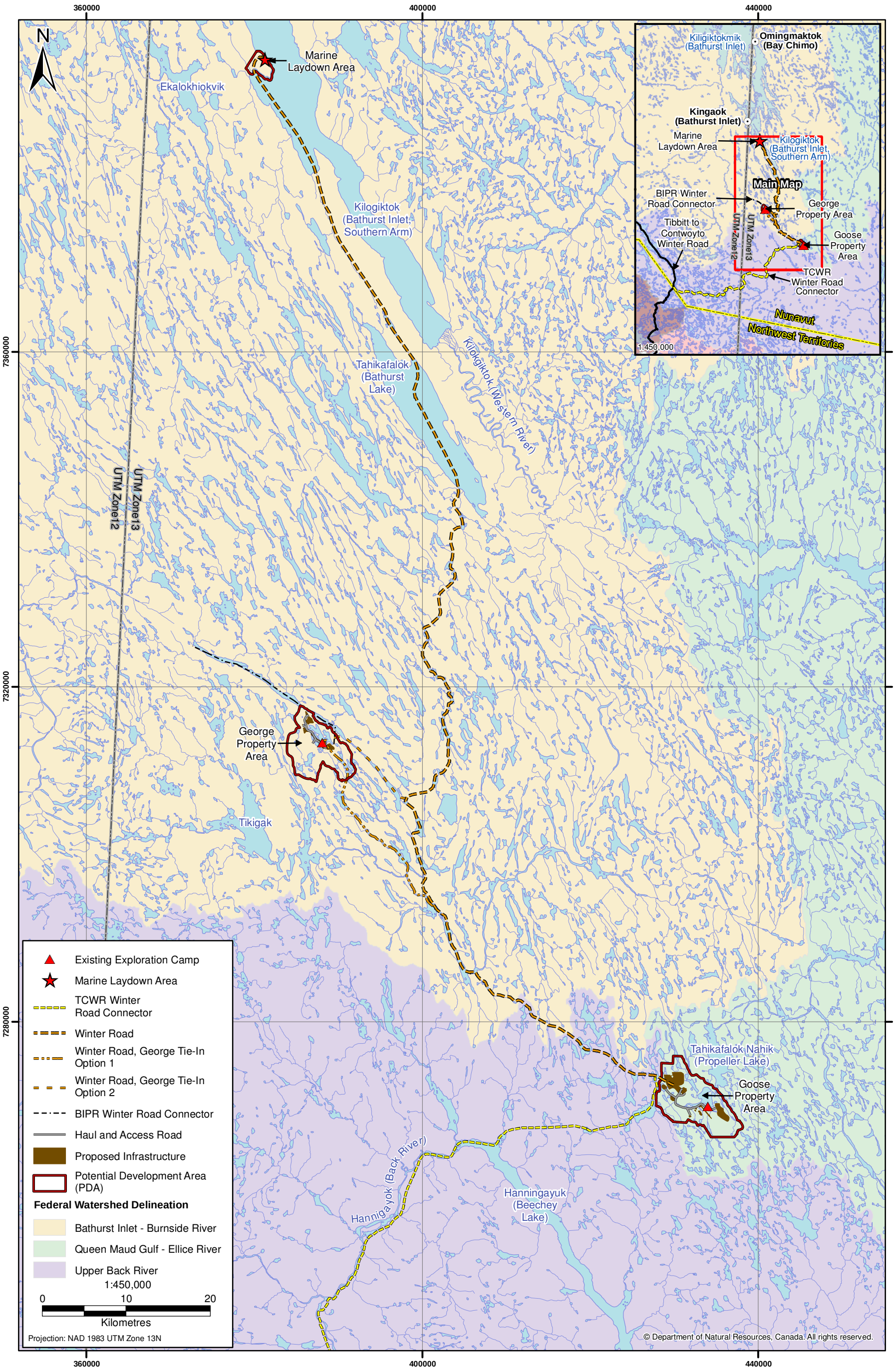

Figure 1-1

Sabina GOLD & SILVER CORP.

Back River Project Site Layout

Figure 1-1

Rescan™ Engineers & Scientists

2. Bathurst Inlet Flow Model

2. Bathurst Inlet Flow Model

2.1 NUMERICAL MODEL DESCRIPTION

The Bathurst Inlet marine waters were modelled using the DHI MIKE3 Flow Model (see www.mikebydhi.com for further details). MIKE3 is a three dimensional baroclinic fluid model that can simulate unsteady discretized flows while accounting for density variations, bathymetry and external forcings such as tides, boundary currents and meteorological inputs. Other built-in features of the model include flooding and drying of coastal land, sediment bed resistance, turbulence modelling, sources/sinks of external waters and heat exchange with the atmosphere.

The MIKE3 model is based on the numerical solution of the three dimensional Reynolds-averaged Navier-Stokes fluid equations (Gill 1982; Kundu 1990), including the effects of turbulence (using the Boussinesq approximation), variable density and the conservation equations for salinity and temperature. MIKE3 Flow model can solve the fluid equations using two different algorithmic modules: the hydrodynamic module (DHI 2012b) which incorporates water compressibility and the full vertical momentum equation, and the hydrostatic module (DHI 2012c) which assumes water incompressibility and invokes the hydrostatic assumptions (i.e., vertical velocities are presumed negligible compared to horizontal currents; Gill 1982; Kundu 1990).

The spatial discretization of the primitive equations is performed using a cell-centered finite volume method, e.g., see Patankar (1980). The spatial domain is discretized by subdivision of the fluid continuum into non-overlapping elements or cells. An unstructured grid is used in the horizontal plane while a structured mesh is used in the vertical. The elements can either be prisms with triangular horizontal faces or bricks with quadrilateral horizontal faces.

The model solves the pertinent time-dependent hydrodynamic and thermodynamic equations over the discretized regional grid. It therefore produces computed values of variables, such as temperature or current, in each grid cell throughout the model domain for each time step. The model's physical system is driven by environmental inputs comprised of time-series of winds, air temperatures and freshwater discharges. Other inputs are derived from the latitude of the domain such as incoming solar radiation.

The utility of a sophisticated modelling tool like MIKE3 is that, after the initial model setup, it is subsequently straightforward to evaluate varying scenarios, such as different wind or discharge magnitudes.

2.2 MODEL DEVELOPMENT FOR BATHURST INLET

This section provides a summary of the 2012 open-water field results that were used to calibrate the numerical model, and describes the assumptions taken while constructing the numerical model for the study.

2.2.1 Marine Physical Processes

The proposed MLA is on the western shore of southern Bathurst Inlet at approximately 66°38.59' N and 107°42.69' W (Figure 2.2-1). The site consists of a long cobble/sand beach with a shoreline generally following a 120 - 125° WSW heading. The water shelf extends orthogonally from the shore at a steep slope of approximately 20% 240 m offshore down to depths below 50 m. Beyond this distance, the seabed slopes more gently to depths below 150 m in the main inlet channel.

Numerous detailed studies of the region have been conducted by Rescan, and a recent one in 2012 between August 23 and September 21 (Rescan 2012c) collected physical oceanographic water column data (i.e., vertical profiles of temperature, salinity and dissolved oxygen), and the first available acoustic Doppler current profiler (ADCP) high-quality water current velocities at the three sampling stations within

southern Bathurst Inlet (Figure 2.2-1). This dataset was assembled specifically to monitor the areas of interest for a marine shipping route and potential marine built-in infrastructure within the southern portion of the inlet.

All water column observations within Bathurst Inlet showed a strongly stratified two-layered vertical structure with a sharp ~3 to 4 m thick pycnocline present at roughly 15 to 20 m depth that separated a warmer (10-13°C), fresher (salinity 17.8 – 19.5) upper layer from a colder (1 to -0.5°C) and more saline (salinity 26.9 - 27.7) oceanic bottom layer. The surface salinity in the inlet was highly dependent on the seasonal riverine inputs and precipitation conditions. The summer dissolved oxygen concentrations in the surface layer (> 9 mg/L) were lower than values previously recorded in winter (Rescan 2013a), but were near saturation (95 to 99%) due to the warmer surface temperatures. The deep water layer harboured lower oxygen concentrations (< 7.5 mg/L) compared to surface concentrations, with a minimum observed of 6.53 mg/L (53.6% saturation). This dissolved oxygen deficiency resulted from a combination of deep-water and sediment organic matter oxidation, and the mid-column stratification limiting mixing between both top and bottom water layers.

Measured water current velocities and directions were heavily influenced by their surrounding bathymetry. A two-layered positive estuarine flow structure was usually observed, although significant variability was recorded in both current speeds and directions at all times. Average velocities in southern Bathurst Inlet were less than 10 cm/s in the bottom layer, while in the top layer they ranged from 20 to 60 cm/s with maximum recorded magnitudes up to nearly 100 cm/s during strong wind events. Maximum surface significant wave heights were estimated at roughly 2 m height for the study region. The vast majority of currents were linked to wind-driven forcing. Tidal heights were found to be extremely low (i.e., ≤0.5 m) within southern Bathurst Inlet, while estimated tidal currents were generally very small (i.e., ~5 cm/s) compared to wind-driven currents.

2.2.2 Model Usage

The first step for the modelling was to simulate the 2012 conditions in southern Bathurst Inlet using the observed field measurements collected between August and September 2012 (Rescan 2012b; see Section 2.2.1). The following assumptions were used in the 3D hydrodynamic model:

- no ice-covered period was modelled. The simulations were thus restricted to the open-water season only;
- only the southern portion of Bathurst Inlet was modelled, i.e., below the Manning Channel latitude of ~ 66°55' N, or approximately the region contained within the Canadian Hydrographic Service (CHS) chart #7793 (CHS 2004). This includes physical oceanographic stations A and B previously sampled by Rescan (2012c), but excludes station C. The reason for this limitation was two-fold:
  - The flow characteristics observed at station C differed notably from the other two sampled stations: the estimated tidal currents were much larger, and strong currents were present at all depths of the water column. It was surmised in Rescan (2012c) that the presence of a shallow sill near the mouth of Manning Channel caused strong upwelling and flow acceleration within the channel. Accurately modelling this feature is well beyond the scope of this work.
  - While the general bathymetry within the main navigable channel is well-known (i.e., see Figure 2.2-1), there is a dearth of information regarding most of the tributaries and small bays attached to Bathurst Inlet. Furthermore, the majority of the freshwater catchments along the inlet have never been studied and their flows remain unknown. Preliminary modelling attempts using a much larger model domain that included the northern hamlet of Omingmaktok yielded such poor results compared to the available measured currents as to render any oil spill simulation completely unrealistic.

PROJECT # 0194096-0038 GIS # BAC-28-007 September 09 2013

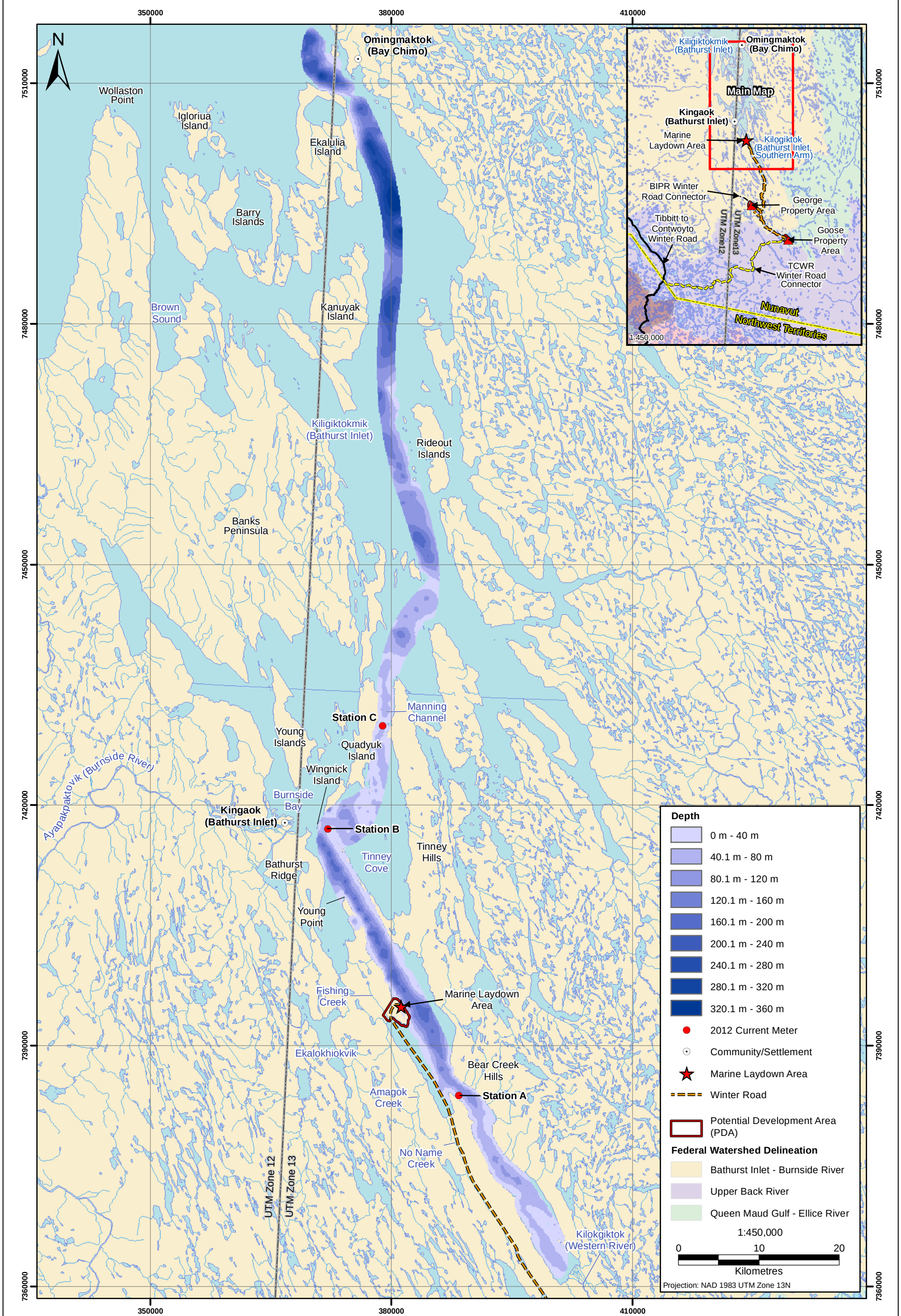

Figure 2.2-1

Sabina GOLD & SILVER CORP.

Baseline Stations and Bathymetric Data Used for Model Calibration

Figure 2.2-1

Rescan™ Engineers & Scientists

- measured data inputs were used within the model whenever available, and included: winds, freshwater discharges, atmospheric temperatures, relative humidity, etc. All other climactic and oceanographic variables were taken as either constants or were modelled using physical models.

2.3 SPECIFIC MODEL DETAILS

This section provides additional information on the input parameters needed to construct the Bathurst Inlet numerical model.

2.3.1 Bathymetry

Depths within the model domain were digitized with bathymetric data from field surveys previously conducted both by the CHS and Rescan. Figure 2.3-1 shows the model region and bathymetry data used for the simulations, as well as the approximate location of the MLA and the community of Kingaok.

For the Bathurst Inlet simulation, a three dimensional rectilinear grid was used covering the complete southern inlet area. The grid cells were selected at 200 m square dimensions; preliminary tests done at 100 m grid sizes yielded almost exactly the same results while taking significantly longer to complete simulations. Vertical layering of the model was designed to emphasize the top 12 m of the water column compared to the bottom depths, since the model's primary objective was to predict surface diesel fuel spill behavior. Hence, four parallel vertical layers were used to represent the water column: the first three vertical layers were set at 4 m thickness, while at the lowest layer depth was permitted to vary. This arrangement was the best configuration found that reproduced reasonably well both the inlet stratification and large surface currents while maximizing computational efficiency.

Two model boundaries are present in the northern limit of the domain (Manning Channel and Burnside Bay). Both were implemented as zero-gradient open boundaries, i.e., water was allowed to freely flow through the boundary to conserve momentum and mass balances within the model.

2.3.2 Winds

Wind speed and direction were logged continuously near Bathurst Inlet at approximately 17 km south of the MLA since 2007; the records for these are described in detail (Rescan 2012a, 2012c). Winds measured at this site were applied across the entire model domain. During model calibration, only the winds available during the 2012 water current measurement period (i.e., August 23 to September 19, 2012) were used. For the diesel fuel spill simulations, most of the available wind measurements were used (see Chapter 4).

2.3.3 Freshwater Influx

Including freshwater discharge flow within the numerical model is a critical step in being able to reproduce realistic flows for Bathurst Inlet as it is the combination of freshwater inputs and wind forcing that creates horizontal pressure gradients in the surface waters of the inlet, which in turn drive the positive estuarine circulation. Five freshwater discharge points were implemented in the model: Amagok Creek, No Name Creek, Bear Creek, Fishing Creek, and the Western River at the southern tip of the inlet (see Figure 2.2-1). Only the outflow of Amagok and No Name creeks have been studied in any detail (Rescan 2012d). The other freshwater inflows were estimated based on the known available data: both Bear and Fishing creeks are estimated to have roughly the same catchment size as Amagok Creek; therefore, the same discharge amounts were used.

Inferring the flow discharge for the Western River was more challenging. It is arguably one of the most important sources of freshwater into Bathurst Inlet (CHS 1994). A thorough analysis of all available GIS databases revealed that the catchment size and flow of the Western River would realistically be between 10 to 20 times the amounts previously measured near Amagok Creek.

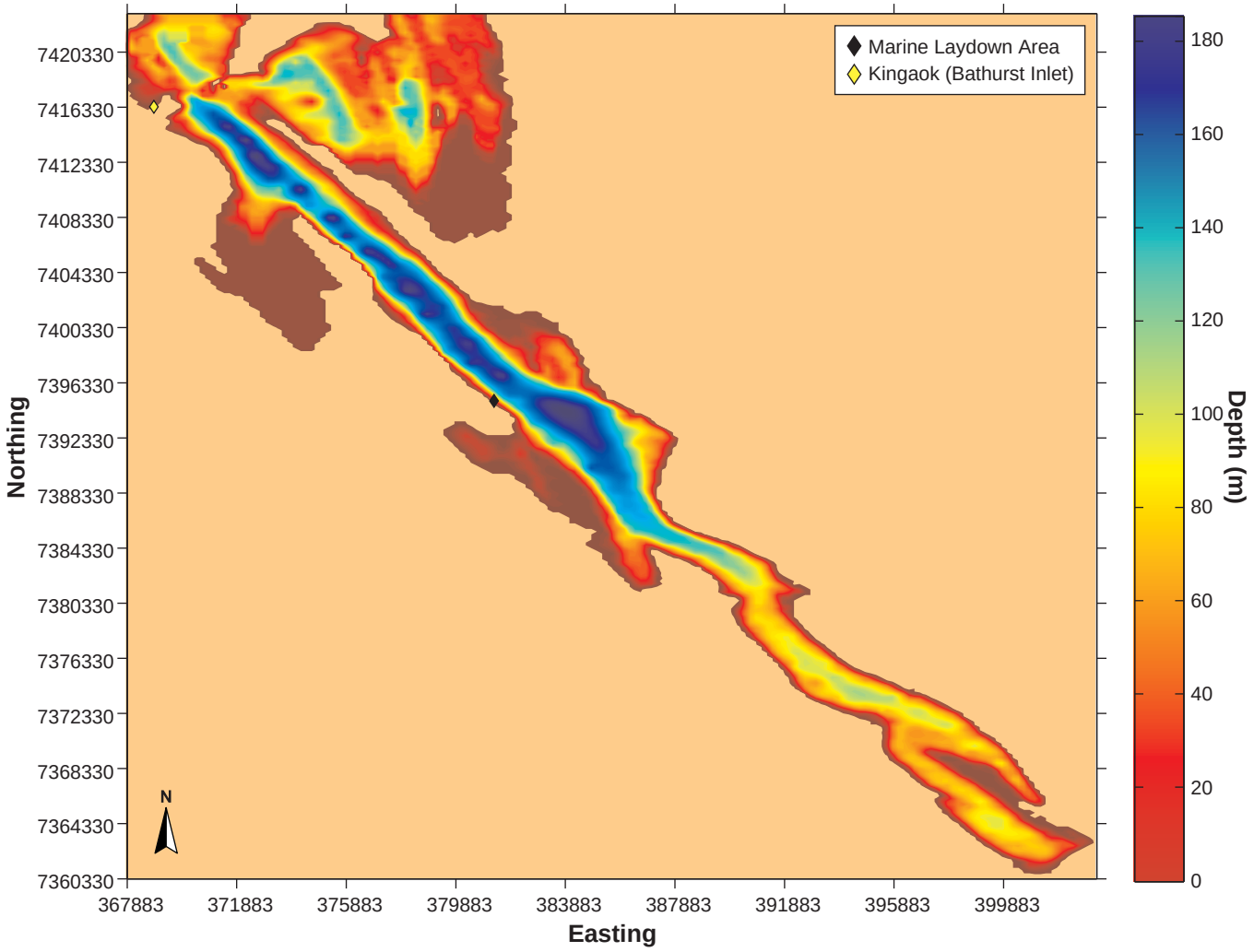

Figure 2.3-1

Bathurst Inlet Bathymetry Used in the Numerical Model

Sabina GOLD & SILVER CORP.

Rescan Engineers & Scientists

2.3.4 Other Meteorological Inputs

Relative humidity, air temperatures and solar intensity were all continuously recorded with winds in 2012, thus they were implemented as time-varying components in the model.

2.3.5 Water Temperature and Stratification

Background temperatures and salinity were assumed to be initially constant for each layer (see values in Table 2.3-1). Once a simulation was started, both temperatures and salinities were set to vary spatially and temporally. The temperature and salinity of waters coming into the inlet from the model boundaries (i.e., waters assumed to be coming in from the northern part of the inlet) were initially set to be identical to the starting background model temperature and salinity. After a simulation start, they were forced to decrease linearly through time to replicate the general decrease in temperature and increase in salinity observed from measurements taken between August and September 2012 (Rescan 2012c). The values are indicated in Table 2.3-1.

Table 2.3-1. Important Model Input Parameters

Parameter Name	Values	Comment
Horizontal Grid Size	200 m	
Vertical Grid Size	4 m	Bottom layer varies
Number of Layers	4	
Time Step	5 s	
Simulation Duration	28 days	
Bed Roughness Length	0.05 m	
Smagorinsky vertical coefficient	0.176	
Horizontal Eddy Viscosity Limits	0.01 to 33.3 m^2/s	Smagorinsky formulation
Vertical Eddy Viscosity Limits	0.0001 to 0.003 m^2/s	Smagorinsky formulation
Wind Friction	0.0128	Drag coefficient
Initial Background Salinity		
Layer 1	19.66	Top
Layer 2	20.24	
Layer 3	20.42	
Layer 4	20.89	Bottom
Initial Background Temperature		
Layer 1	10.46°C	Top
Layer 2	9.72°C	
Layer 3	9.47°C	
Layer 4	9.13°C	Bottom
End Boundary Salinity		
Layer 1	22.14	Top
Layer 2	22.38	
Layer 3	23.08	
Layer 4	25.91	Bottom
End Boundary Temperature		
Layer 1	7.46°C	Top
Layer 2	7.08°C	
Layer 3	6.57°C	
Layer 4	4.15°C	Bottom

2.3.6 Tides

Tidal heights and currents were previously found to be very weak (i.e., less than 0.4 m and 5 cm/s, respectively) south of Manning Channel within Bathurst Inlet when compared to wind-driven currents (see Rescan 2012c for details), so tides were not included in this model to save computational time.

2.3.7 Model Time: Calibration and Simulation Periods

The model was set to run at a 5 s time step for 28 days between August 23 and September 19, 2012. This range was defined as the simulation period, where the calculated model currents could be compared to the measured field data.

2.3.8 Module Selection

Numerous testing runs were done using either the hydrodynamic or hydrostatic module for the numerical model. Given that the model architecture was *a priori* built-up to simulate horizontal currents within the inlet's surface mixed layer, differences in current magnitudes between both modules were usually less than 5%. Therefore, the hydrostatic module was chosen for most runs as it yielded slightly better computational times and more conservative salinity variations.

2.3.9 Turbulence Closure Scheme

In many numerical simulations, the small-scale turbulence cannot be resolved with the chosen spatial resolution, thus it needs to be approximated through other methods. Thus, the turbulence in MIKE3 is parameterized using an eddy viscosity concept (i.e., the Boussinesq approximation), which is described separately for the vertical and the horizontal transport. Several turbulence models can be applied in any given simulation, and two were extensively tested for this study: the Smagorinsky formulation (Smagorinsky 1963) that involves the eddy viscosity being linked to a filter size (i.e., the grid spacing) and the velocity gradients of the resolved flow field, and the k-ε formulation (Rodi 1984) that determines the velocity scale from a transport equation based on the isotropic energy dissipation rate, ε.

For complex applications, the k-ε model is inherently superior to the Smagorinsky formulation; however, it does take more computational time. For the current study though, both turbulence schemes resulted in nearly identical horizontal current results. Thus, the Smagorinsky formulation was used for convenience.

2.3.10 Other Model Parameters

Table 2.3-1 summarizes the inputs and model parameters used in the hydrodynamic model. Additional meteorological data used in the baseline simulation is presented in Appendix 2.

2.4 2012 BASELINE SIMULATION

2.4.1 Thermohaline Structure

The evolution of surface layer temperature and salinity values for the 2 available baseline stations (A and B; see Figure 2.2-1) is depicted in Figure 2.4-1 for August and September 2012. Also shown is the linear boundary temperature and salinity forcing for the model that was based on temperature-salinity profiles measured in 2012 (Rescan 2012c). While it is unfortunate that no *in situ* profiles of temperature and salinity were taken during the current measurement period (i.e. between August 23 and September 19, 2012), it can be seen from Figure 2.4-1 that the model values track the boundary conditions quite well for the baseline simulation, with model temperatures on average within ~ 2°C of boundary values and within 2 of salinity. A noticeable increase in salinity occurs around August 27 for the station A, when strong winds forced the upwelling of deeper waters in the surface layer. Of note are the large variations of salinity observed at both stations that were caused by large discharges of

freshwater from the river sources. These can provoke steep plunges in salinity (i.e., a loss of ~3) that can linger for days due to the natural buoyancy of freshwater preventing easy mixing with the deeper, more saline waters. This type of salinity variation in estuaries is a common occurrence in nature (Levinton 1995), thus it is an important feature replicated within the model.

2.4.2 Currents and Circulation

Model current velocities for the surface layer were plotted versus the top 4 m average of recorded ADCP observations for both station A (Figure 2.4-2) and station B (Figure 2.4-3) stations. Three subplots are shown on each figure: a) describes the east-west direction current timeseries; b) describes the north-south direction current timeseries and; c) shows the total current magnitude timeseries. In both stations, the model's effectiveness at simulating the measured currents varied during the entire simulation length. Despite some dissimilarity, the agreement between measured and modeled currents is excellent, particularly given the multiple simplifying assumptions taken in the model formulation. While the average coefficients of correlation R between both sets of current magnitudes was 0.52 for station A and 0.51 for station B, there were several instances within the run where measured and modelled data correlated extremely well (i.e., over 0.90). For example, the eastern currents after September 11 on Figure 2.4-2 a), or the northern currents between August 30 and September 3 in Figure 2.4-3 b). There are some current spikes in the model that are not observed in the measured dataset; the best example is found around September 7 at station B on Figure 2.4-3. Such inconsistencies are likely explained by the measured wind from only one location is applied over the complete model domain; in reality, wind and wave strength/direction can vary at the sub-metre scale.

Another important feature can be gleaned from Figures 2.4-2 and 2.4-3: the magnitudes of the model currents are on the same scale (i.e., average difference < 5 cm/s) as the near-surface ADCP measurements. This suggests that the model output currents are a reasonable and realistic approximation to the largest observed currents in the dataset, a critical threshold that needed to be established before starting the marine diesel fuel spill simulations.

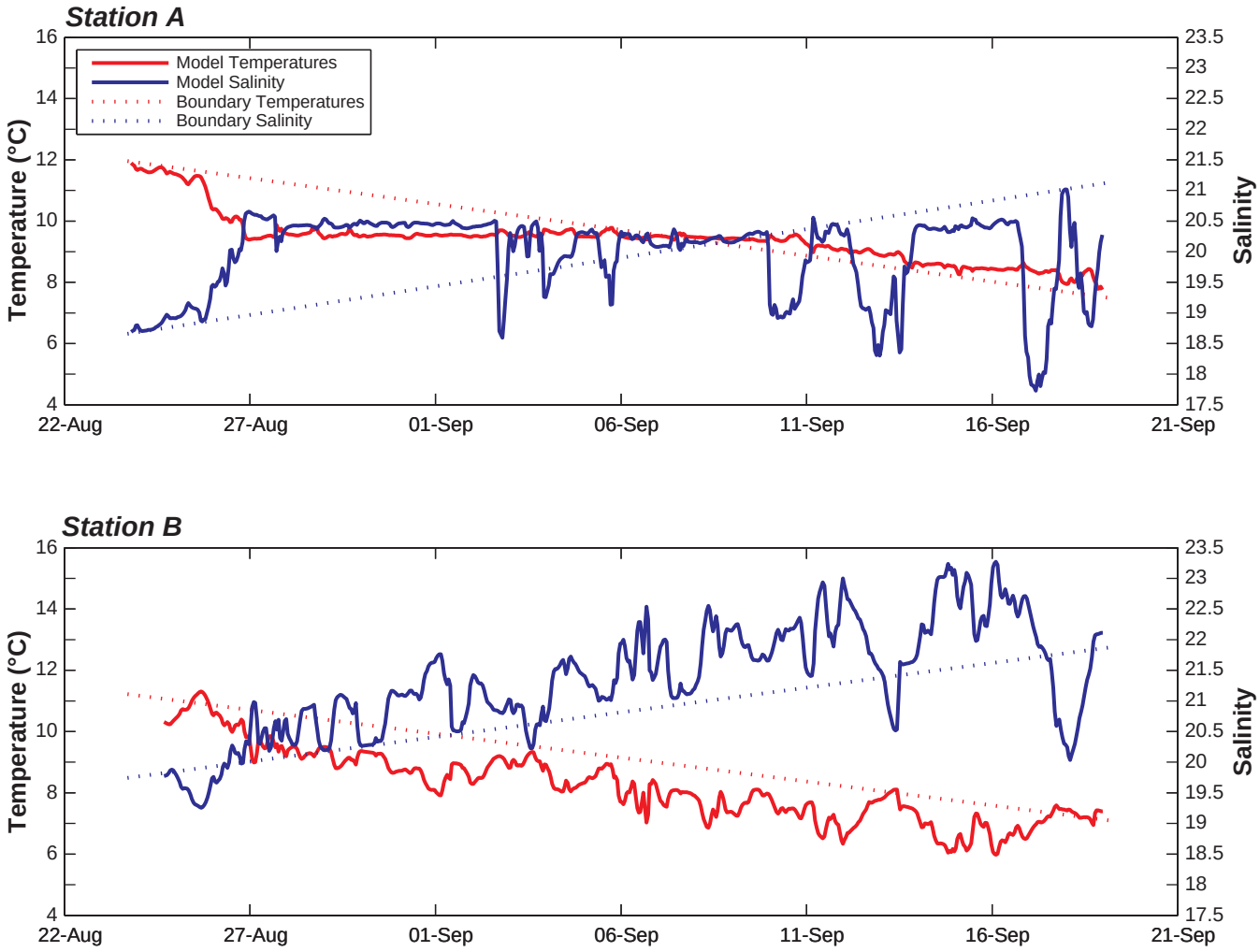

Temperature and Salinity Comparison between Measured and Modelled Data in Bathurst Inlet, Back River Project, August to September 2012

Figure 2.4-1

Sabina GOLD & SILVER CORP.

Rescan Engineers & Scientists

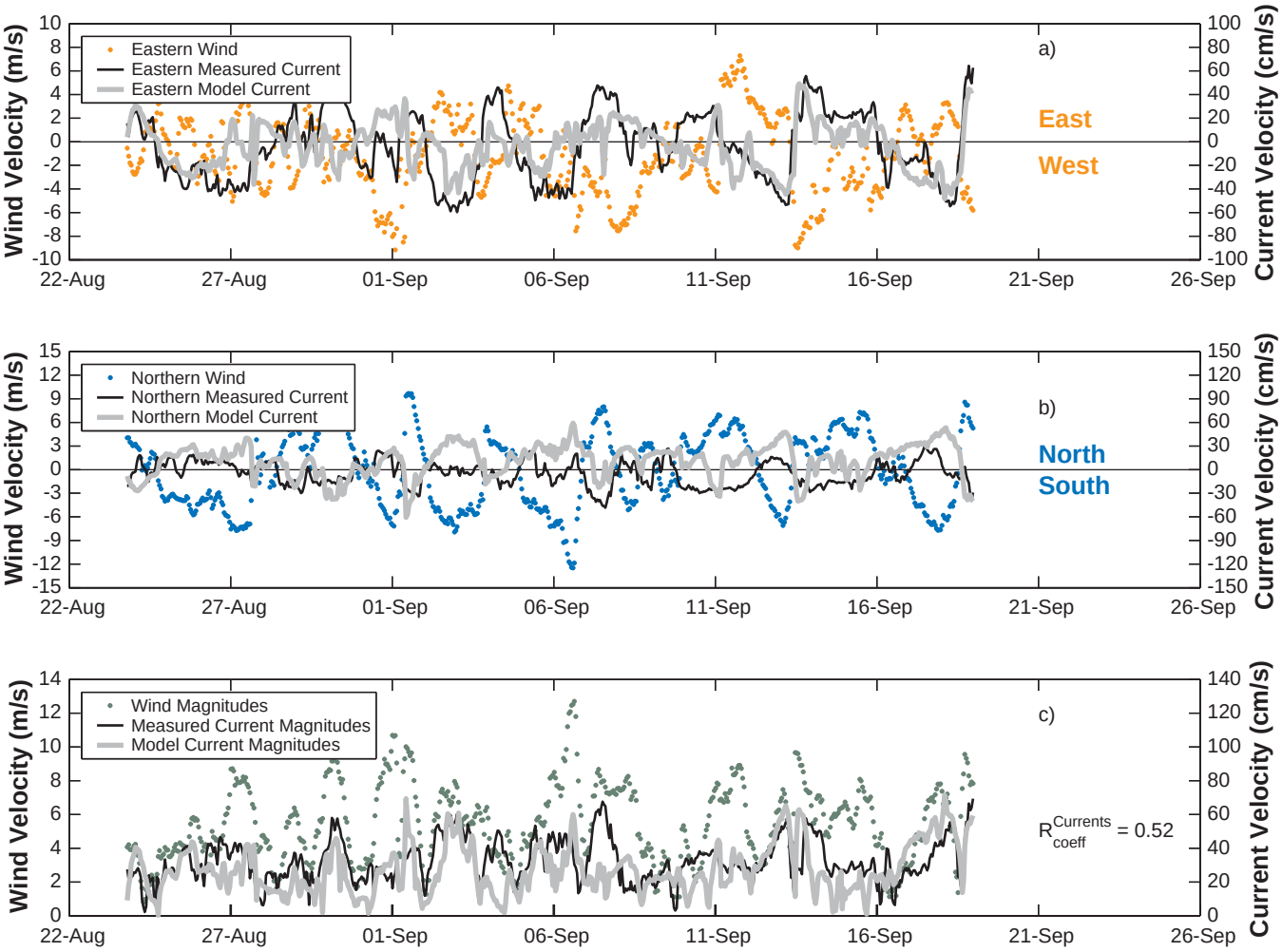

Notes: Wind direction is given as the direction FROM which the wind is blowing.
Current direction is given as the direction TOWARDS which the current is moving.

Comparison of Current Velocities between Measured and Modelled Data, Station A, August to September 2012

Figure 2.4-2

Sabina GOLD & SILVER CORP.

Rescan Engineers & Scientists

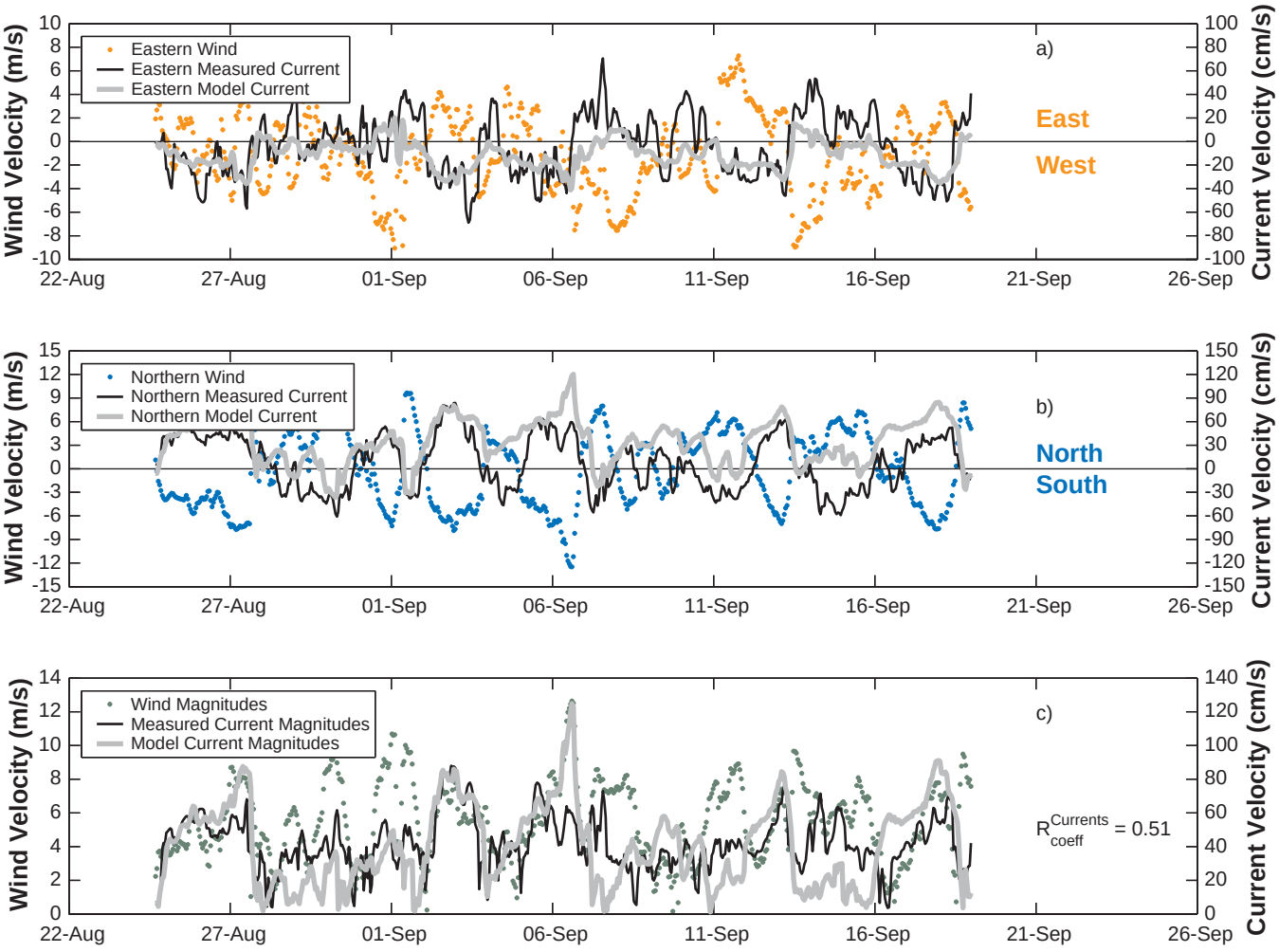

Notes: Wind direction is given as the direction FROM which the wind is blowing.
Current direction is given as the direction TOWARDS which the current is moving.

Comparison of Current Velocities between Measured and Modelled Data, Station B, August to September 2012

Figure 2.4-3

Sabina GOLD & SILVER CORP.

Rescan Engineers & Scientists

3. Diesel Fuel Oil Spill Model

3. Diesel Fuel Oil Spill Model

3.1 MODEL DESCRIPTION

An oil spill is the release of liquid petroleum hydrocarbons into the environment, most likely due to human activity. The term often refers to marine oil spills, where oil is released into the ocean or coastal waters. The oil may be a variety of materials, including crude oil, refined petroleum products (such as gasoline or diesel fuel), or by-products such as a ship's bunkers oily refuse.

For this study, DHI's Oil Spill Module (DHI 2012a) was coupled to the MIKE3 Flow model output (see Section 2) as a tool to predict the fate of marine oil spills within southern Bathurst Inlet, covering both the transport and the changes in chemical composition of oil products with time. The simulations reflect the behavior expected of diesel fuel, which would be the main type of oil stored at the MLA. The model is a Lagrangian model of advection/diffusion (see Kundu 1990) that runs decoupled from the fluid dynamics simulated by the MIKE3 model.

The changes in chemical composition of oil residues over time is a result of physical and biological processes and is often referred to as 'weathering' of the oil. As such, the more closely the chemical composition of a residue resembles that of the pre-spilled oil, the 'fresher' it is. This chapter will briefly describe each weathering process implemented within the DHI model, followed by the specific parameter details included within the Bathurst Inlet diesel fuel spill scenarios.

3.2 DIESEL FUEL PARAMETERIZATION

For better prediction of the weathering processes within numerical models, oil types are often split up into fractions of certain properties (so-called pseudo components; Mackay et al. 1980). This usually requires detailed knowledge about the chemistry of each oil type such as content of each pseudo-component and its properties. Therefore, for the diesel fuel modelling purposes detailed in this work, it is required to find specific diesel oil characteristics, either from a database or by performing additional calculations based on distillation data, if applicable.

The oil spill templates used in the DHI Oil Spill module describes the diesel by two fractions only: a light volatile fraction and a heavier fraction. The light volatile fraction is defined as the mass of hydrocarbons with molecular weights below 160 g/mol and a boiling point well below 300°C. The heavy fraction is defined as hydrocarbons of molecular weights above 160 g/mol and boiling points from 250°C - 300°C and upwards, including wax and asphaltene components. The latter two are considered special conservative fractions of the oil, i.e., they are not subject to weathering and invariably end up beached on the shoreline.

The model describes the total amount of spilled diesel fuel as an assemblage of smaller diesel fuel amounts represented by individual diesel particles of a pre-selected volume or mass. These particles are tracked across the model domain as they are subjected to the weathering processes and the drift due to currents flows.

3.3 WEATHERING PROCESSES

Once diesel fuel is spilled in the marine environment, it becomes subject to a number of different processes that are dependent on each other and collectively referred to as 'weathering'. These include evaporation, dispersion, dissolution, photo-oxidation, emulsification, spreading, biodegradation and sedimentation. Weathering eventually changes the physical and chemical properties of the spilled diesel fuel, which may lead to its disappearance from the water surface. Figure 3.3-1 shows a

schematic view of the processes acting on a given diesel fuel slick, while Figure 3.3-2 shows the relative importance of each weathering element versus time from the initial spill period. The following sections describe how each process is integrated within the DHI Oil Spill module.

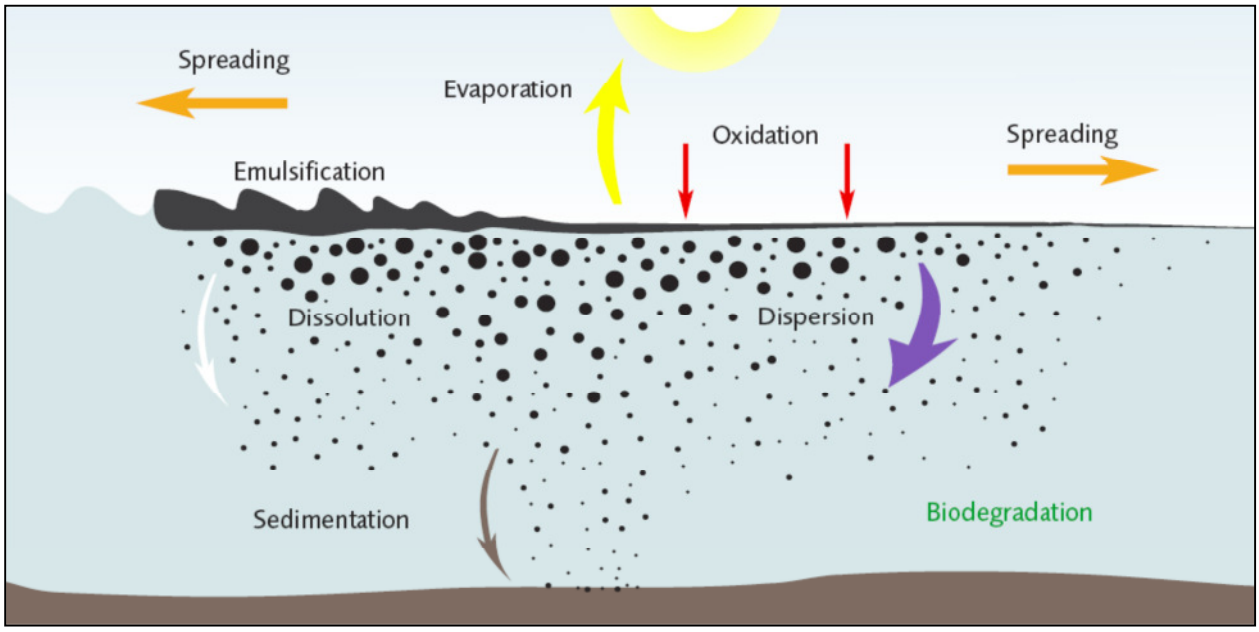

Figure 3.3-1. Schematic of Weathering Processes Acting on Spilled Diesel Fuel, Adapted from ITOPF (2011) and DHI (2012a)

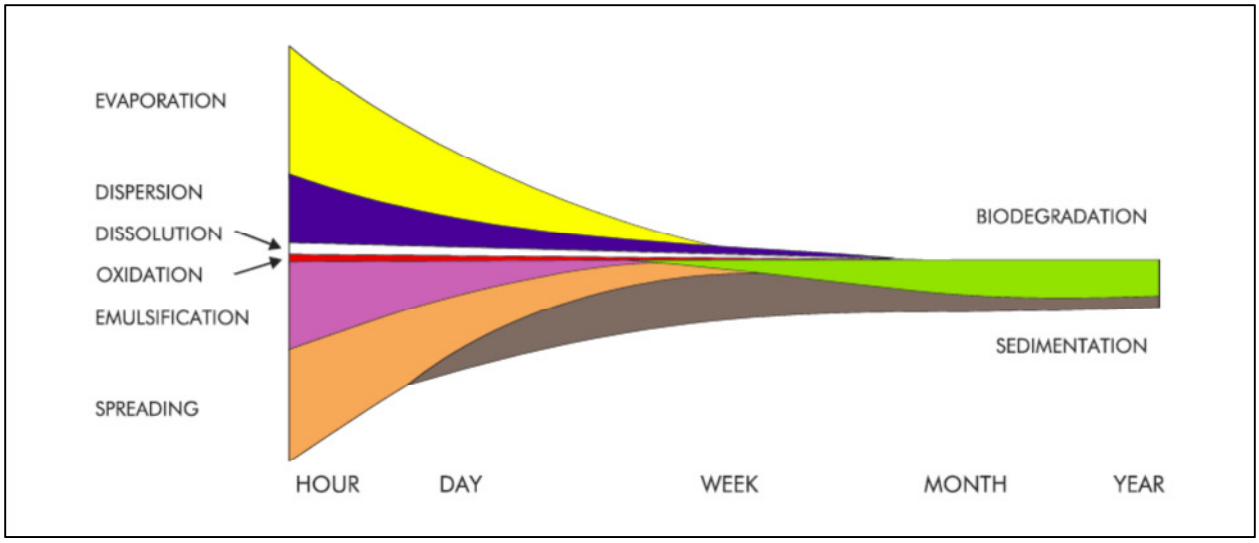

Figure 3.3-2. Heuristic Representation of the Relative Importance of Each Weathering Process on a Given Spill through Time – the Width of Each Band Indicates the Importance of the Process, Adapted from ITOPF (2011) and DHI (2012a)

3.3.1 Evaporation

In the first hours and days of the spill, evaporation at the surface of an diesel fuel slick is the dominant weathering process (French-McCay 2004). If the spill consists of a lightweight, highly refined product like gasoline, evaporation can very effectively remove nearly all of the spill contamination in as little as 24 hours. For spills of most medium-weight crudes, the removal is less complete, but substantial nevertheless. Typically, 10-30% of the material from these spills can be removed through evaporation in the first 24 hours. Other external factors affecting the evaporation of a spill include the amount of the spill exposed at the surface of the slick, wind and sea surface conditions.

Two types of evaporation models are used by the DHI Oil Spill module: a detailed boundary regulated method as originally implement by Reed (1989) and Betancourt, Palacio, and Rodriguez (2005), and a time-dependent percentage loss model developed by Fingas (1996, 1997). Given that one of the major goals of this study was to assess the potential maximum amount of diesel fuel spreading within the inlet, the most conservative Fingas quadratic-type loss model was used for the simulations.

3.3.2 Dispersion

The horizontal and vertical dispersion of diesel fuel into the water by natural forces are important processes controlling the long-term fate of diesel fuel slicks at sea. In conjunction with evaporation, this process reduces the volume of diesel fuel on the water surface, thereby influencing the potential extent of surface and shoreline contamination. In slick dispersion, diesel droplets are dispersed from the slick into the water by oceanic mixing. The larger of these droplets, which are buoyant, resurface quickly and rejoin the slick. The smaller droplets remain in suspension in the water column. Lighter, more water soluble hydrocarbons partition from these droplets into the water phase. Clouds of the entrained dissolved and particulate diesel fuels then spread horizontally and vertically by diffusion and other long-range transport processes.

Although natural dispersion is a poorly understood process, it is known that oil/water interfacial tension, oil viscosity, oil buoyancy and slick thickness each inversely affect the ability of a particular oil to disperse naturally (Mackay et al. 1980). Sea state is also an important factor controlling the rate and amount of dispersion. Even light, non-viscous oils do not rapidly disperse under calm conditions. On the other hand, even the heaviest, emulsified oils can disperse over a period of time in heavy seas with frequent breaking waves (Al-Rabeh 1994). The net dispersion rate of oil from a slick into the water will vary greatly depending on the properties of the spilled oil and mixing energy.

Dispersion within the DHI model is treated separately for the horizontal and vertical directions. For horizontal flow, dispersion is parameterized through a dispersion coefficient formulation that depends on the current magnitudes at each model grid point. A dispersion coefficient of 3 m^2/s (good value for moderately energetic waterways (see Kuiper and Van den Brink 1987) was pre-selected for all simulations within Bathurst Inlet. For vertical dispersion, the main mechanism causing diesel fuel droplets to move downwards is the breaking of surface waves. The entrainment of diesel fuel from the sea surface into the water column is quantified using the wave breaking model of Delvigne and Sweeney (1988), using the surface wave parameterization of Demirbilek, Bratos, and Thompson (1993).

3.3.3 Dissolution

Some part of the diesel fuel slick is removed as the water-soluble portion of the petroleum hydrocarbons are dissolved into the surrounding seawater. The factors affecting the dissolution of a spill include the amount of the spill exposed at the surface of the slick, wind and sea surface conditions, air temperature, insolation intensity and emulsification amount.

The dissolution in DHI's Oil Spill module is implemented as a 1st-order mass dissolution rate equation for both volatile and heavy oil fractions, and is dependent on oil density, slick area and oil/water solubility.

3.3.4 Photo-oxidation

Chemical oxidation of the spilled diesel fuel also occurs, and this process is facilitated by exposure of the diesel fuel to sunlight. Oxidation contributes to the total water-soluble fraction of diesel fuel components. Less complete oxidation also contributes to the formation of persistent petroleum compounds called tars. However, the overall contribution of photo-oxidation to diesel fuel spill removal is small compared to other weathering processes (DHI 2012a); even strong continuous sunlight (e.g., approximately 700 W/m^2) only results in photo-oxidation breaking down about 0.1% of an exposed slick in a day within the numerical model. Given its negligible contribution within the modelling time frame, photo-oxidation was not implemented of the Bathurst Inlet simulations.

3.3.5 Emulsification

Emulsification is the formation of a mixture of two distinct liquids: seawater and diesel fuel in the case of a marine diesel spill. Fine diesel fuel droplets are suspended within (but not dissolved into) the water and the emulsification formed occupies a volume that can be up to four times that of the diesel fuel it formed from (Mackay et al. 1980). Moreover, the viscous emulsion is considerably more long-lived within the environment than the source diesel fuel, and its formation slows subsequent weathering processes. Emulsification tends to occur under conditions of strong winds and/or waves, once a diesel fuel spill has persisted on the water for at least several hours.

The DHI model describes the emulsification as an equilibrium process between the two stages diesel fuel + water and water in diesel fuel, following the work of Xie, Yapa, and Nakata (2007). In essence, the model uses a first order water release formula to assess the potential to form emulsions in any given model grid point, and then evaluates the stability of existing emulsions. Hence, unstable and mesostable emulsions will release water, and will completely demulsify in calm waters.

3.3.6 Spreading

Diesel fuel spilled in the water surface immediately spreads over a slick of mm-scale thickness that can quickly span in the 100 m^2 scale or more, depending on spill volumes. Marine spills usually do not spread uniformly but are composed of thick patches (usually a few mm thick) that contain about 90% of the spill's volume that are surrounded by sheens (about 1 to 10 μm or 0.001 to 0.01 mm thick). The thick patches spread and thin over time and feed diesel fuel into the surrounding sheen. The spreading is especially promoted by gravity and surface tension; however, many spills of varying size quickly reach a similar average thickness of about 0.1 to 1 mm (Kuiper and Van den Brink 1987).

Spreading in the DHI Oil Spill module is implemented as a non-linear areal growth model initially formulated by Mackay et al. (1980) that takes into account a constant rate of spreading for each diesel fuel particle to simplify model computations.

3.3.7 Biodegradation

Microbial oil degradation is a critical late-stage step in the natural weathering of petroleum spills as it is the stage that gradually removes the last of the petroleum pollutants from the marine environment. Degradation of petroleum compounds occurs most rapidly via the oxidative metabolic pathways of the degrading organisms. As such, biodegradation is predicted to occur fastest in environments with ample oxygen, high temperatures and containing a diverse and healthy oil-degrading flora (Marchal et al. 2003). Conversely, oxygen-depleted marine sediments that are often sites of petroleum contamination

are among the habitats where aerobic metabolism is severely limited and microbial oil breakdown must therefore proceed via slower anaerobic pathways.

The biodegradation process in the DHI model is calculated as a simple 1st order decay process involving a predetermined biodegradation rate constant.

3.3.8 Sedimentation

Very few oil types are dense enough to sink on their own in seawater, and few of them weather fully enough to yield a residue dense enough to do so either (unless the oil is ignited, in which case sufficiently dense residues may be formed). The DHI model however can handle the vertical movement of diesel fuel driven by buoyancy forces from differences in diesel fuel density and water density in both upward and downward direction, using an implementation based on Stoke's Law (Kundu 1990).

3.4 BATHURST INLET SPILL CHARACTERISTICS

The diesel fuel property data, spill flow rates and volumes, and weathering processes (Section 3.3) parameters used in the spill behaviour and trajectory model for Bathurst are described in this section.

3.4.1 Diesel Fuel Properties

The main type of oil being transported, stored and used at the Back River MLA will be diesel fuel, the properties of which have been obtained from Environment Canada's online oil property database (see Environment Canada 2013) for use in this modelling exercise. Numerous types of diesel are listed in the database, most of which could conceivably be used for the Back River project. The fresh and weathered properties of Canada-specified Diesel Fuel Oil (see Appendix 3) were used in the numerical model, which incorporates a range of characteristics generally seen in diesel fuels used in Canada.

Unlike gasoline, which is primarily a light and extremely volatile petroleum product, diesel is a more intermediate fuel oil that can contain up to 35% of a 'heavy' oil fraction when considered through DHI Oil Spill module templates (see Section 3.2 for details). The selection of a heavy component fraction is somewhat arbitrary, as likely the total would change depending on the refinery of origin for each barrel of diesel. For this study, a light volatile fraction of 72% was chosen to best represent the relative amount of fuel being subject to intense weathering immediately after the spill, which left a heavy fraction of 27% as the more resistant component that ends up beached along the shoreline. The remaining 1% was set to be a conservative wax amount that follows the heavy fraction. Asphaltene content is usually negligible in diesel fuel, thus it was omitted from the spill model.

The parameters necessary for the DHI Oil Spill module to predict the transport and weathering of diesel are detailed in Table 3.4-1.

3.4.2 Spill Volumes and Particle Sizes

Two volume amounts were used for the Bathurst Inlet marine spill modelling, situated at each end of the spectrum of likely spill volumes. The first scenario volume was set at 5 ML of diesel, which is assumed to be the maximum credible spill of a transport barge set at the MLA. Spills of such volume are statistical extremely unlikely in any given locality (Anderson, Mayes, and LaBelle 2012), as modern vessels have multiple failsafe mechanisms that would prevent a full tanker load to easily discharge. However, it is useful to consider such amounts in numerical modelling exercises to present the most conservative results. The second scenario considered spills on the order of 20 kL, which was deemed the potential maximum lost during a loading operation at the MLA. The 5 ML spills were released into the marine waters over a 3 hour period, while 20 kL spill were assumed to occur instantaneously.

Table 3.4-1. Parameter Values from the DHI Oil Spill Module Used in the Back River Marine Diesel Spill Modelling

Basic Characteristics	State Variable	Unit	Diesel Fuel
Weights	Volatile oil fraction	wt%	72
	Heavy oil fraction	wt%	27
	Asphaltene	wt%	0
	Waxes	wt%	1
Tracked particle size	Particle weight	kg	1000
	Average surface area	m^2	100
Processes	**Class Constants**		
Evaporation	Schmidt number		2.7
	Average molecular weight of volatile fraction	g/mol	123
	Vapor pressure of volatile fraction	atm	0.005
	Distillation percentage at 180°C	wt%	23
	Distillation equation constant		0.31
	Temperature-dependent distillation constant	1/T	0.018
Spreading	Terminal thickness	mm	0.1
	Growth rate constant	per sec	150
Biodegradation	Decay rate, volatile fraction	per day	5.00×10^{-3}
	Decay rate, heavy fraction	per day	5.00×10^{-4}
Emulsification	Maximum water fraction	m^3/m^3	0.5
	Kao constant		3.3
	Kaw constant		200
	Emulsion rate	s/m^2	2.00×10^{-3}
Buoyancy	Average diameter of oil droplets	m	0.001
	Density of oil at 20°C, volatile fraction	kg/m^3	789
	Density of oil at 20°C, heavy fraction	kg/m^3	878
Water solubility	Volatile fraction	kg/kg	2.00×10^{-5}
	Heavy fraction	kg/kg	2.00×10^{-7}
Volumetric temperature	Expansion coefficient, volatile fraction	1/°C	7.00×10^{-4}
	Expansion coefficient, heavy fraction	1/°C	7.00×10^{-4}
Dissolution	Dissolution rate, volatile fraction	per day	0.4
	Dissolution rate, heavy fraction	per day	0.4
Horizontal dispersion	Average dispersion coefficient	m^2/s	3
Vertical dispersion	Wind speed for wave breaking	m/s	5
	Wave energy dissipation rate	$J/m^3/s$	1000
Vertical limits	Max distance below surface	m	0.05
	Max distance above bed	m	0.05
Viscosity	Mooney constant		0.25
	Reference temperature	°C	20
	Dynamic water viscosity at reference temperature	cP	1.002
	Dynamic oil viscosity at reference temperature	cP	1.62
	Temperature-dependent exponential coefficient		-0.0462

Diesel fuel particles tracked by the model were set to be 1,000 kg for each scenario. Assuming an average density of 820 kg/m^3 (Table 3.4-1) for the diesel fuel, a ~1 mm thick slick generated by each particle could then conceivably cover an area over 1,200 m^2. In reality this does not occur, as particles do merge with one another and are constantly changing due to weathering effects. Given that each model grid covers 40,000 m^2 of surface waters, when a particle enters a new grid it is impossible to determine where it is located within the grid point. To circumvent this ambiguity, it is assumed that particles cover the entire surface area of any grid points they reside in.

3.4.3 Particle Beaching

When diesel fuel slicks encounter shorelines and shallow coastal waters, the diesel can become stranded in the intertidal zone and above, depending on the sea state at the time of the stranding. If subjected to large tidal cycles, the diesel fuel in the intertidal zone may be remobilized as slicks or as an diesel/sediment mixture deposited in the shallow nearshore littoral zone. However in low tidal cycle/low mixing energy coasts, the diesel fuel may subsequently penetrate into the shoreline substrate and remain there indefinitely until weathered out.

In the Bathurst Inlet numerical model, two outcomes are possible when tracked particles reach a position close to shore. First, the particles can get shore-locked; that is, the diesel fuel remains on the water surface, but no longer moves within the model domain as the currents are not strong enough to dislodge the slick. This situation will often occur in shallow waters and/or small nooks found within bays. The second outcome occurs when the near-shore cross currents are very strong: particles can get 'beached', i.e., they leave the water surface and remain immobilized on shore. Beached particles are thus removed from further transportation within the marine system, a valid assumption given that the gentle gravel beaches found in Bathurst Inlet would not be conducive to the reflection of incoming diesel fuel particles back into the inlet waters. Beached particles are also treated differently in terms of weathering processes; due to the absence of emulsification, dispersion, and the greater exposure to weather elements, they generally weather more rapidly than the particles remaining in marine waters (Kuiper and Van den Brink 1987).

4. Diesel Fuel Spill Simulation Results and Discussion

4. Diesel Fuel Spill Simulation Results and Discussion

4.1 BATHURST INLET SPILL MODEL OVERVIEW

The diesel fuel spill model described in Chapter 3 was used to provide a prediction of potential diesel fuel spill behaviour originating at the Back River MLA location. The simulations were designed to identify a range of probable spill outcomes issued from typical to extreme weather conditions found on site. To properly assess the statistical likelihood of the spills occurring in Bathurst Inlet, a large number of simulation scenarios must be run, each using a variety of input datasets. Generally, this means one or more parameters of the standard model is set to change before each simulation, and then the results are compiled into probability distribution figures that show the probable extent of any given spill through time.

For the current study, the main parameter varying between simulations was the wind input; all other parameters as described in Chapters 2 and 3 remained the same. Winds were chosen for Bathurst Inlet because years of continuous measurements are readily available for the region, and it is the single most important element that drives current speed and direction within the inlet (Rescan 2012c). To be consistent with the baseline simulation as detailed in Section 2.4, simulations were run in periods of 28 days set between August 23 and September 19, 2012 using wind conditions measured from 10 periods taken between 2007 and 2012. Thus, a total of 280 simulations of varying winds were run for each spill volume scenario. Using such a large number of simulations yields good confidence in the overall spill probability due to the wide range of weather conditions inherently sampled. More details on the wind data used in the model are found in Appendix 4-1 and 4-2.

In the probability distribution figures shown in this chapter, every model grid is attributed a probability percentage that details the likelihood of a diesel fuel particle reaching that grid point. Thus, a grid point with an example value of 20% indicates that in 56 of the 280 scenarios tested, diesel fuel particles circulated at that location.

4.2 5 ML SIMULATION RESULTS

The probability distribution plots of the diesel 5 ML spill scenarios are shown in Figures 4.2-1, 4.2-2 and 4.2-3 for the spread occurring 3 hours, 12 hours and roughly 10 days after the initial spill. In practice, very little movement of diesel fuel occurs after the first couple of days in a simulation, as the diesel fuel particles are generally beached or moored close to shore by then. In all three figures it can be easily seen that the most probable spill distribution location is the shoreline in the immediate vicinity of the MLA. This result is not surprising, as the grid points next to the spill source quickly get inundated by the slick in nearly 100% of all scenarios. Furthermore, it appears that in nearly 40% of the cases tested by the model, nearly all of the diesel fuel spill remains within 2 to 3 km of the source point during the simulation run time: either the inlet waters are too calm to move the diesel fuel slick much, or the western cross-shore currents are strong enough to maintain most of the diesel fuel near the source to be shore-locked or beached.

Probability distributions of up to 3 hours after the spill (Figure 4.2-1) show a nearly radial distribution of diesel fuel particles around the spill source location, with <20% of the scenario particles reaching waters up to 4 km away from the MLA. There is a noticeable preferential eastern direction to the spill distribution, as a ~2 km band with probabilities around 10-15% reaching the eastern shore directly opposite the MLA. This is clear evidence of the strong cross-shore currents sometimes present in the inlet, which can rapidly distribute the spill material east of the source location.

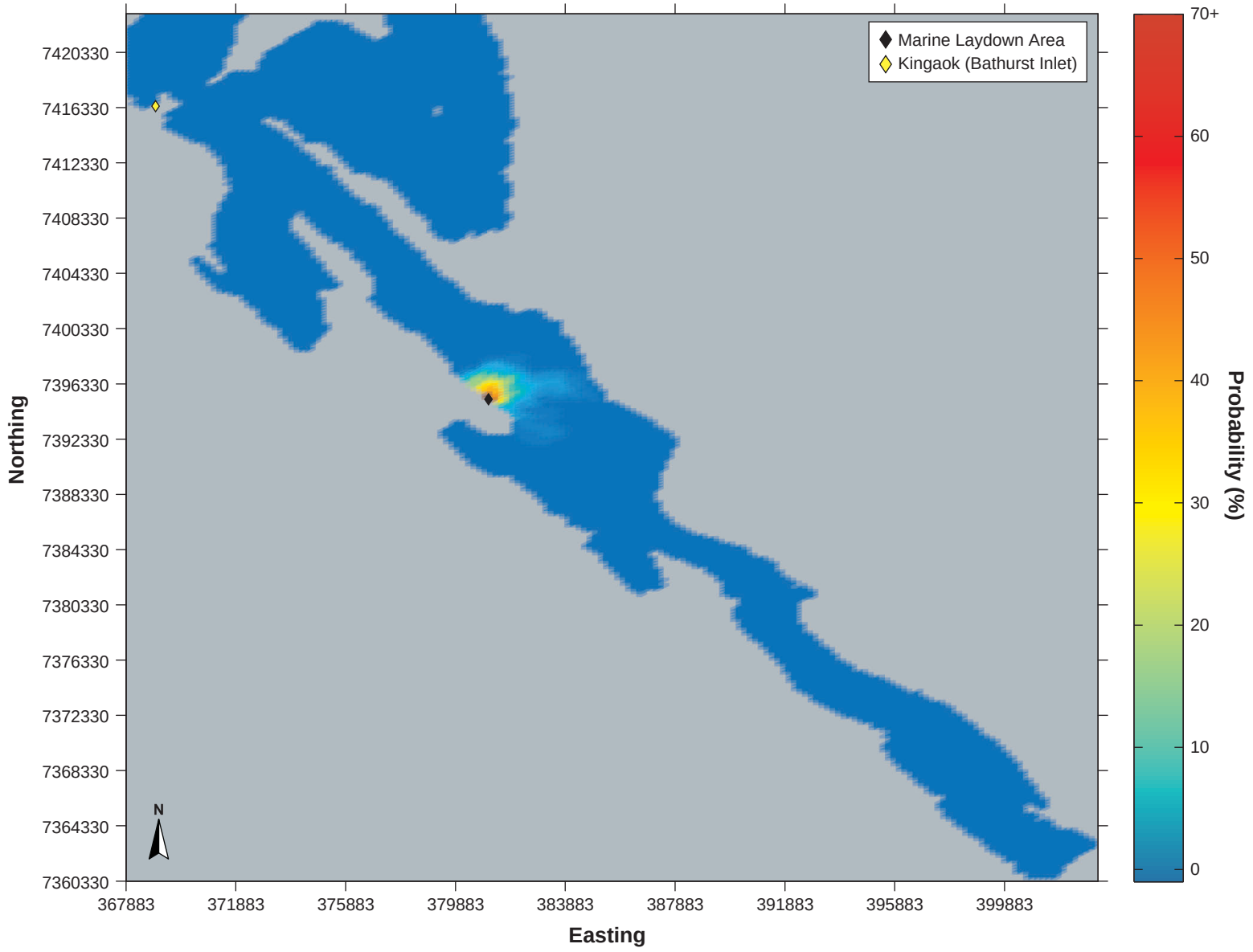

Figure 4.2-1

Sabina GOLD & SILVER CORP.

Diesel Fuel Spill Probability Distribution, 5 ML: 3 Hours after Spill

Figure 4.2-1

Rescan Engineers & Scientists

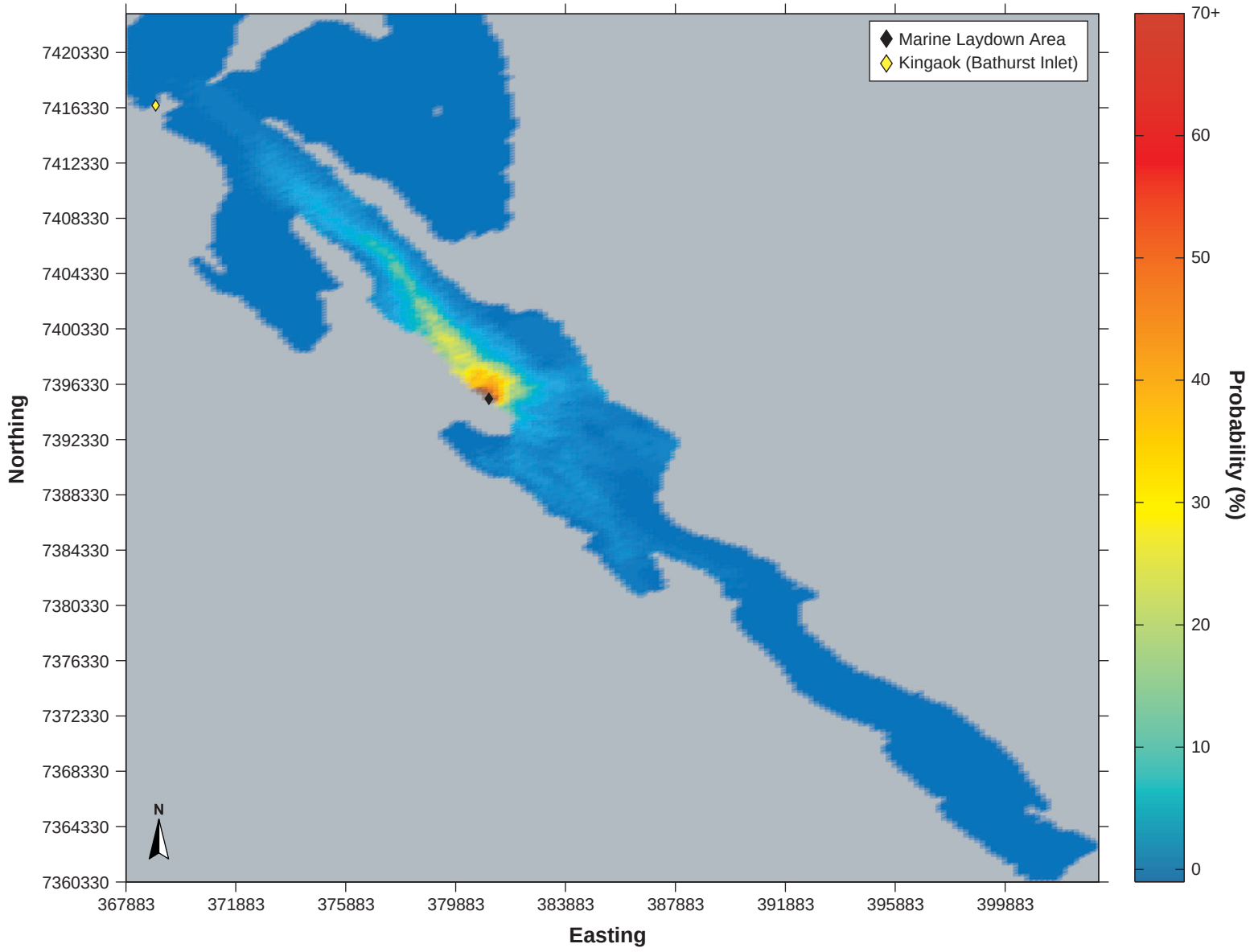

Figure 4.2-2

Sabina GOLD & SILVER CORP.

Diesel Fuel Spill Probability Distribution, 5 ML: 12 Hours after Spill

Figure 4.2-2

Rescan Engineers & Scientists

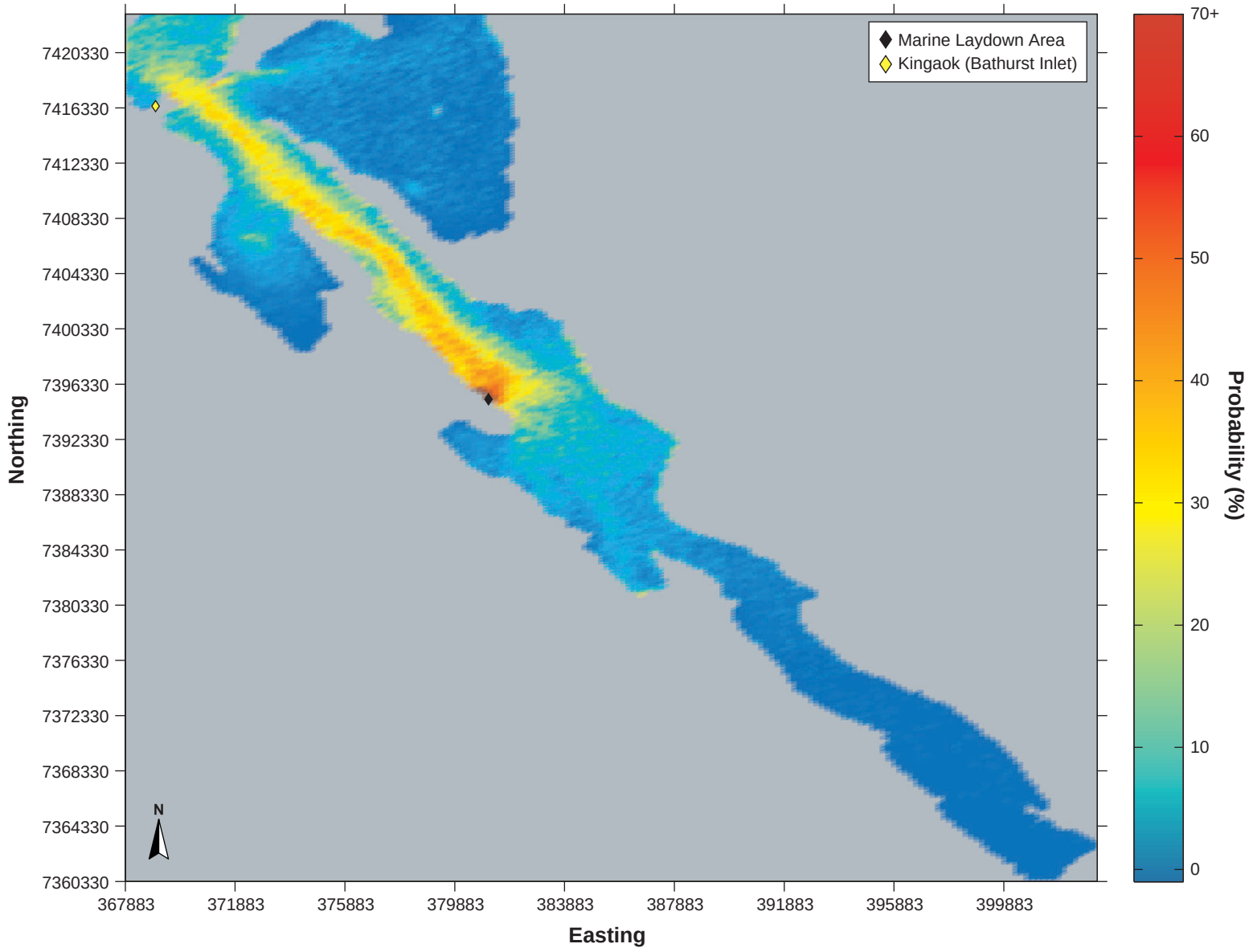

Figure 4.2-3

Sabina GOLD & SILVER CORP.

Diesel Fuel Spill Probability Distribution, 5 ML: 10 Days after Spill

Figure 4.2-3

Rescan Engineers & Scientists

After a period of 12 hours, the spill can propagate much further away from the MLA. While the highest probabilities (>70%) remain near the MLA area, there is direct evidence of the positive estuarine flow prevalent in Bathurst Inlet (see Rescan 2012c) that moves the diesel fuel outside of the southern inlet confines. For example, in Figure 4.2-2, there is an approximately 22 km long north-western spill tendril of probabilities, ranging between 25 and 35%, that reaches the outskirts of Tinney Cove. However, even after a half-day after the initial spill, less than 10% of diesel slicks actually reach Burnside Bay roughly 26 km from the MLA, near Kingaok.

The probability distribution after 10 days of spill is plotted in Figure 4.2-3. It clearly shows that, aside from the area near the source location, spills predominantly spread in the north-western direction, and that in nearly 50% of all cases, diesel fuel would escape the lower portion of Bathurst Inlet and move into either Burnside Bay or Tinney Cove. This situation generally occurred when strong (>8 m/s) southern and south-eastern origin winds were present in the inlet, or when large freshwater discharges propagated northward from the southern rivers: both situations tended to generate strong (>30 cm/s) northern currents. The vast majority of northward-bound diesel fuel particles appeared to either move into Burnside Bay or get caught in strong alongshore currents starting near Tinney station, where the diesel tended to get caught in the shores of Wignit Island and the southern beaches of Quadyuk Island before spreading much further away. While most of the modelled diesel fuel spill displayed in Figure 4.2-3 generally remained within the main channel of Bathurst Inlet, there was a ~30-40% chance that slicks of diesel would circulate around Burnside Bay and reach the shores of Kingaok. High uncertainty is associated with this region, however, given the scarcity of data collected outside the main channel of Bathurst Inlet. Less than 15% of simulation results displayed in Figure 4.2-3 had any diesel fuel particles that escaped the model domain as most particles tended to get shore-locked or beached before this. These out-of-domain particles comprised less than 5% of the total mass of the spills.

As previously mentioned, by the 10th simulation day almost no mobile diesel fuel particles were left in the simulation and most of the volatile diesel fuel content had weathered out. This rate of weathering was largest in the first couple simulation days, and was highly dependent on the initial spreading rate of the diesel slick. This fact is illustrated in Figure 4.2-4, which shows the general evolution of the volatile diesel fuel mass (a) and maximum diesel fuel slick area (b) in marine waters through simulation time for a selected series of simulations using 2012 data. Volatile mass will generally decrease exponentially, primarily through evaporation (Figure 4.2-4 a). The most rapid weathering occurred in the first day of simulation, where on average a third of the diesel fuel is lost. However, in some simulations (e.g., August 25), up to 85% of diesel fuel was lost during the first simulation day from the model. This occurred when large currents caused significant amounts of both slick spreading and particle beaching during the initial particle release. The former can be examined by computing the maximal diesel fuel slick spread area in Figure 4.2-4 b) and comparing those to the volatile diesel fuel mass in Figure 4.2-4 a). The typical mild-condition wind run (e.g., August 23, September 2) would show relatively slow weathering through time and have a spill remain in an area less than 5 km^2 centred on the MLA. In the runs when the spill was transported far into the inlet (e.g., July 31, August 8, August 25), nearly 20 km^2 (i.e., over 500 200 m^2 grid points) could be covered by diesel fuel particles at any given time. Conversely, these runs had weathering rates 2 to 3 times more elevated than runs with limited spreading. Thus, while increased spreading generally meant a larger diesel fuel slick area, it can also be associated with faster weathering (due to the increase amount of diesel exposed to the elements) and increased loss of volatile diesel fuel mass within the model.

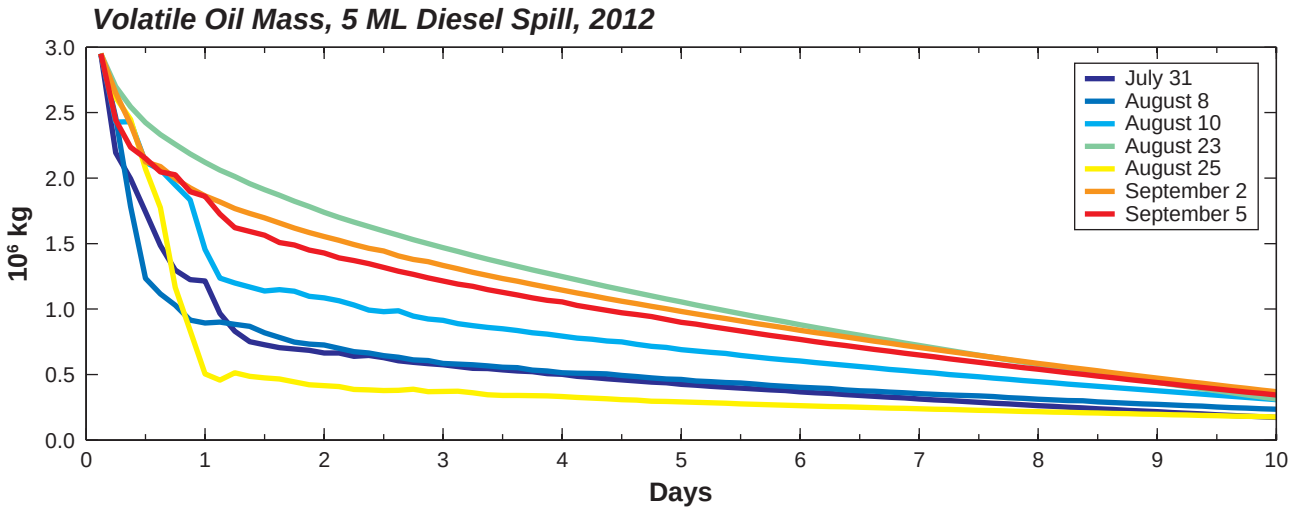

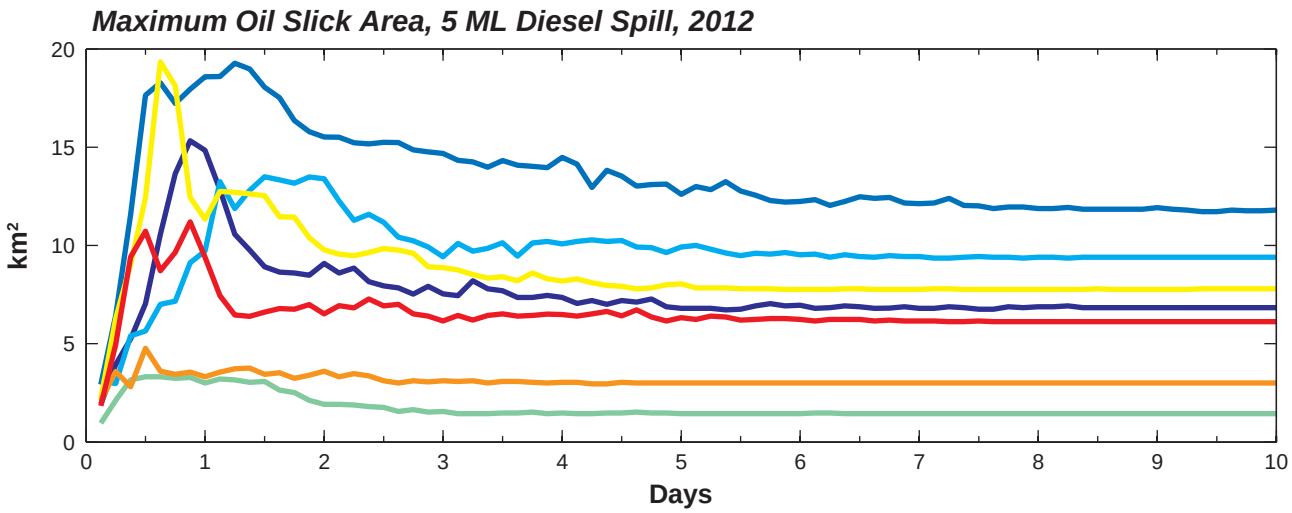

Note: Legend indicates simulation start dates.

Sample 2012 Diesel Fuel Spill Simulation Results of Volatile Diesel Fuel Mass Fraction Weathering vs. Time Lapsed from Initial Spill, and Maximum Area Covered by Diesel Fuel Slick vs. Time Lapsed From Initial Spill

Figure 4.2-4

Sabina GOLD & SILVER CORP.

Rescan Engineers & Scientists

Once all diesel fuel particles are either shore-locked or beached, the remainder of volatile mass quickly weathered out, and only the 'residual' heavy diesel fraction was left. As detailed in Chapter 3, this fraction could typically take weeks to months to weather naturally, although in practice most of the material would eventually disperse or end up beached. For practical reasons, simulations were not run that long for this study. An assessment of where those residual diesel fuel particles finish up after 10 simulation days is shown in Figure 4.2-5, where probabilities are displayed in nearshore locations throughout the model area. Not surprisingly, the highest probabilities are near the MLA shoreline, with probabilities over 95%. Afterwards, the highest probabilities are in the northern and southern shores of the main southern Bathurst Inlet channel and at the entrance of Burnside Bay, with some locations ending up with diesel fuel particles in nearly 40% of the simulations. The shores in the northern portion of the model along Burnside Bay and Quadyuk Island also have broad distribution profiles, with select location ending up with particles in 15 to 30% of simulations.

While Figure 4.2-5 concerns itself with the probability distribution of residual diesel fuel along the shores of Bathurst Inlet, it does not provide information on the actual mass of diesel present in the model. This information is presented in Figure 4.2-6, which mimics the probability distribution of Figure 4.2-5 but displays the average diesel mass at each grid point instead of the distribution probabilities. Most grid points end up with less than 1,000 kg of diesel throughout the domain (i.e., less than 0.03% of the initial 5 ML spill), with a few notable exceptions. The area next to the MLA has some of the highest deposited masses, which could be surmised by examining the distribution probabilities in Figure 4.2-6. However, large probabilities in Figure 4.2-5 do not necessarily translate in large mass distributions in Figure 4.2-6. This interesting feature is most notable in the shores directly south of the MLA (e.g., at the Amagok Creek source). While most of the nearshore locations in that area have probabilities less than 15%, average mass deposition amounts could exceed 100,000 kg of diesel. In other words, the diesel fuel slicks are less likely to be transported in the southern portion of the inlet; however, when they do travel south, the slicks are comprised of a large quantity of particles. The latter is due to south-southeastern currents in the inlet generally being of lower magnitude than the north-northwestern currents (Rescan 2012c), hence south propagating slicks will not spread and/or fragment as much as the north propagating ones. Figure 4.2-6 also clearly shows that the majority of the diesel fuel mass tends to remain below the Kingaok latitude (i.e., south of northing 7414330). Likely diesel fuel deposits around Burnside Bay are ~ 20,000 kg or less, as a large portion of the diesel slicks gets fragmented before reaching the Bay.

4.3 20 KL SIMULATION

The spills simulated using 20 kL of diesel were modelled using the same particle sizes and properties as the 5 ML simulations, despite the volumes having over 2 orders of magnitude in difference. This was done to provide consistency between both sets of results, and facilitate comparisons. However, the basic model grid size of 200 m was chosen to efficiently model extremely large (i.e., > 1 ML) quantities of diesel. Because 20 kL is much smaller than 5 ML, there are many fewer particles within the model, and the total spill amount can easily remain within one grid point for an entire simulation. Probability distribution figures therefore appear much more pixelated than in the 5 ML figures.

The probability distribution plots of the diesel 20 kL spill scenarios are plotted in Figures 4.3-1, 4.3-2 and 4.3-3 for the spread occurring 3 hours, 12 hours and roughly 10 days after the initial spill, exactly in the same manner as the 5 ML spill simulations except for the probability scaling. Because the simulations were run using the same winds as the 5 ML simulations, the results are generally qualitatively similar, with one important difference: outside of the immediate vicinity of the MLA, the probabilities are much lower. Roughly 70% of all 20 kL simulations had all diesel fuel remaining within ~21 km of the MLA location. Furthermore, only 15% of all simulations had particles reaching the northern portions of the modelling domain, like Burnside Bay and Tinney Cove. None of the particles managed to escape the model domain.

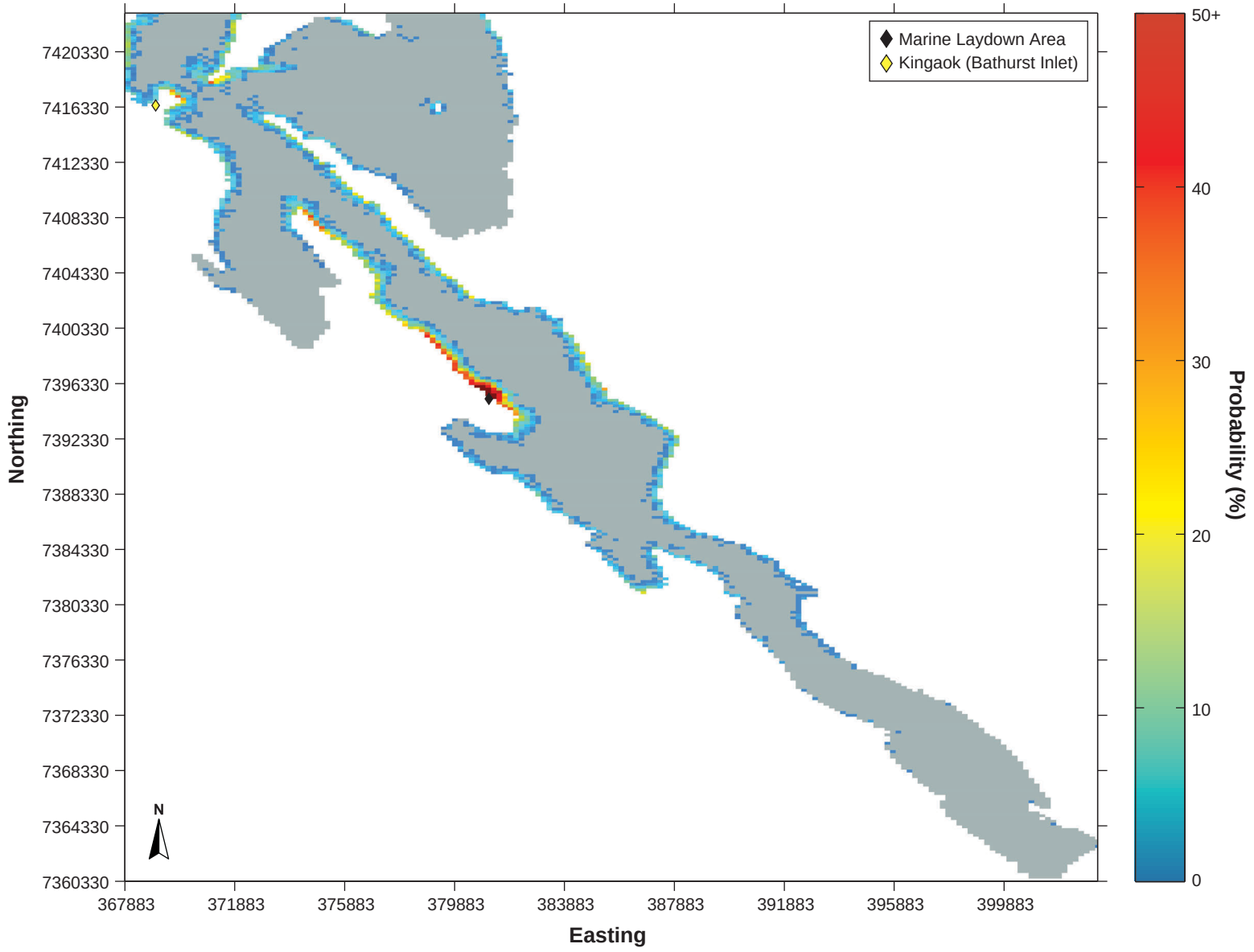

Figure 4.2-5

Sabina GOLD & SILVER CORP.

Diesel Fuel Spill Shore Residual Probability Distribution, 5 ML: 10 Days after Spill

Figure 4.2-5

Rescan Engineers & Scientists

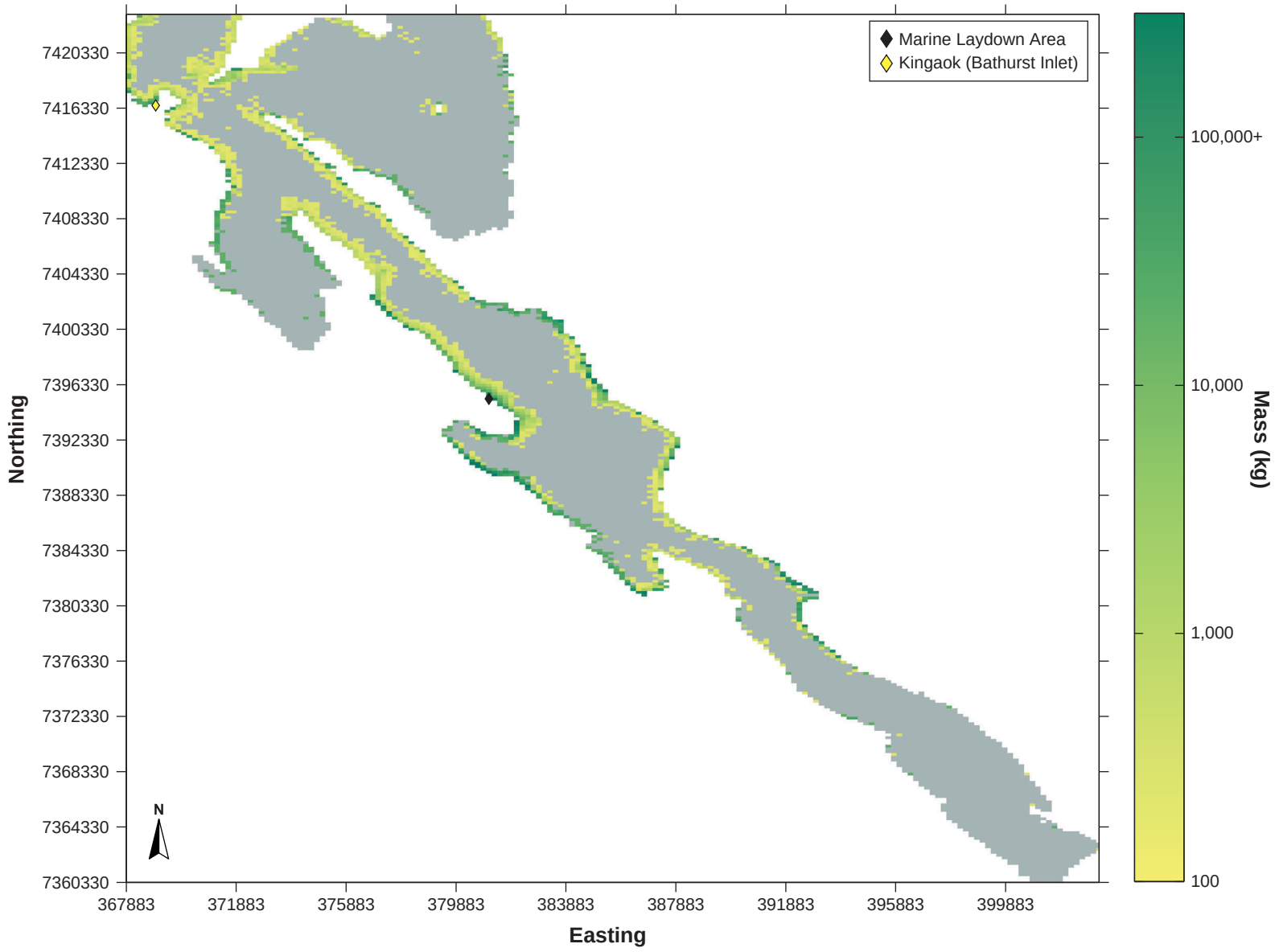

Figure 4.2-6

Sabina GOLD & SILVER CORP.

Diesel Fuel Spill Shore Residual Average Mass Distribution, 5 ML: 10 Days after Spill

Figure 4.2-6

Rescan Engineers & Scientists

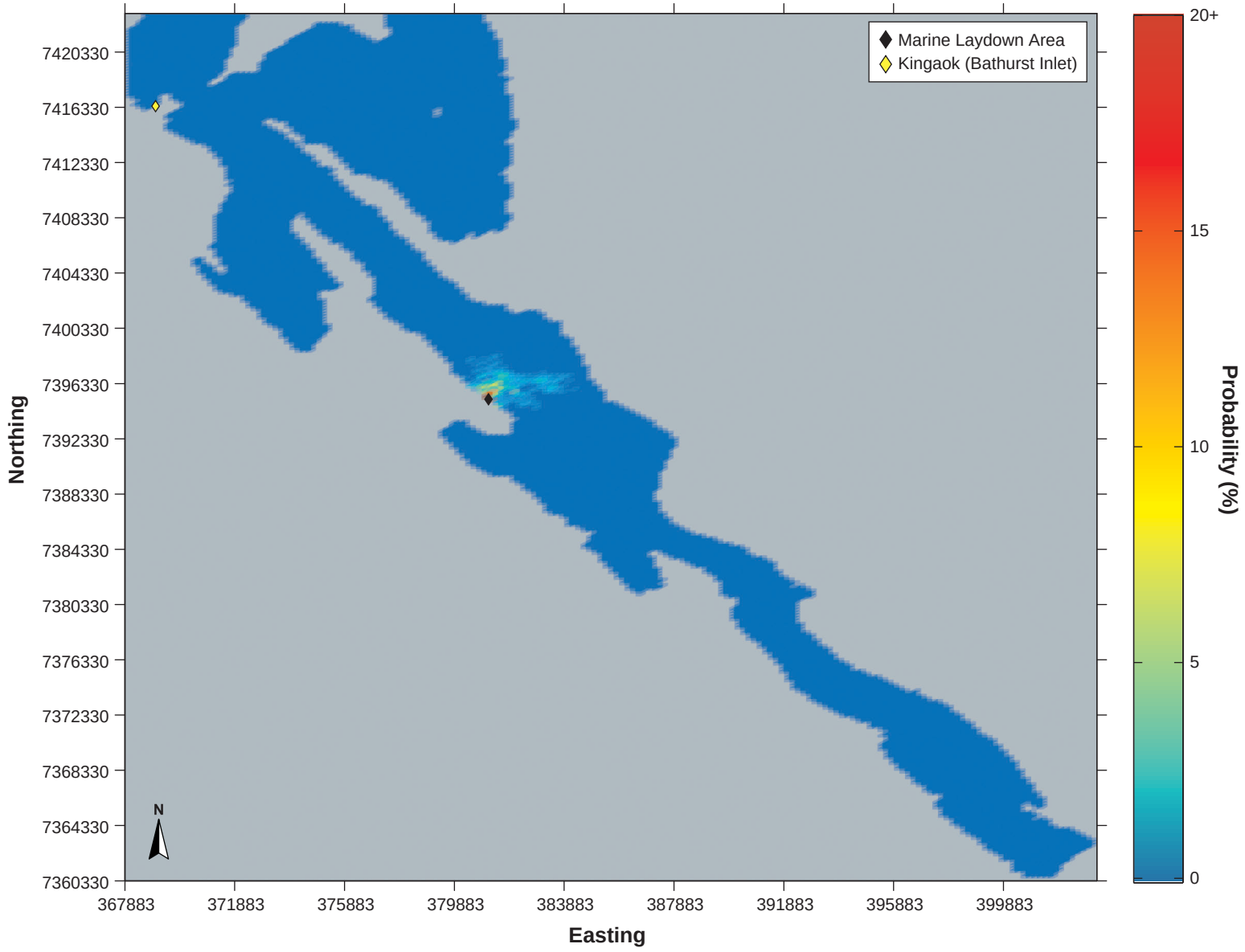

Figure 4.3-1

Sabina GOLD & SILVER CORP.

Diesel Fuel Spill Probability Distribution, 20 kL: 3 Hours after Spill

Figure 4.3-1

Rescan Engineers & Scientists

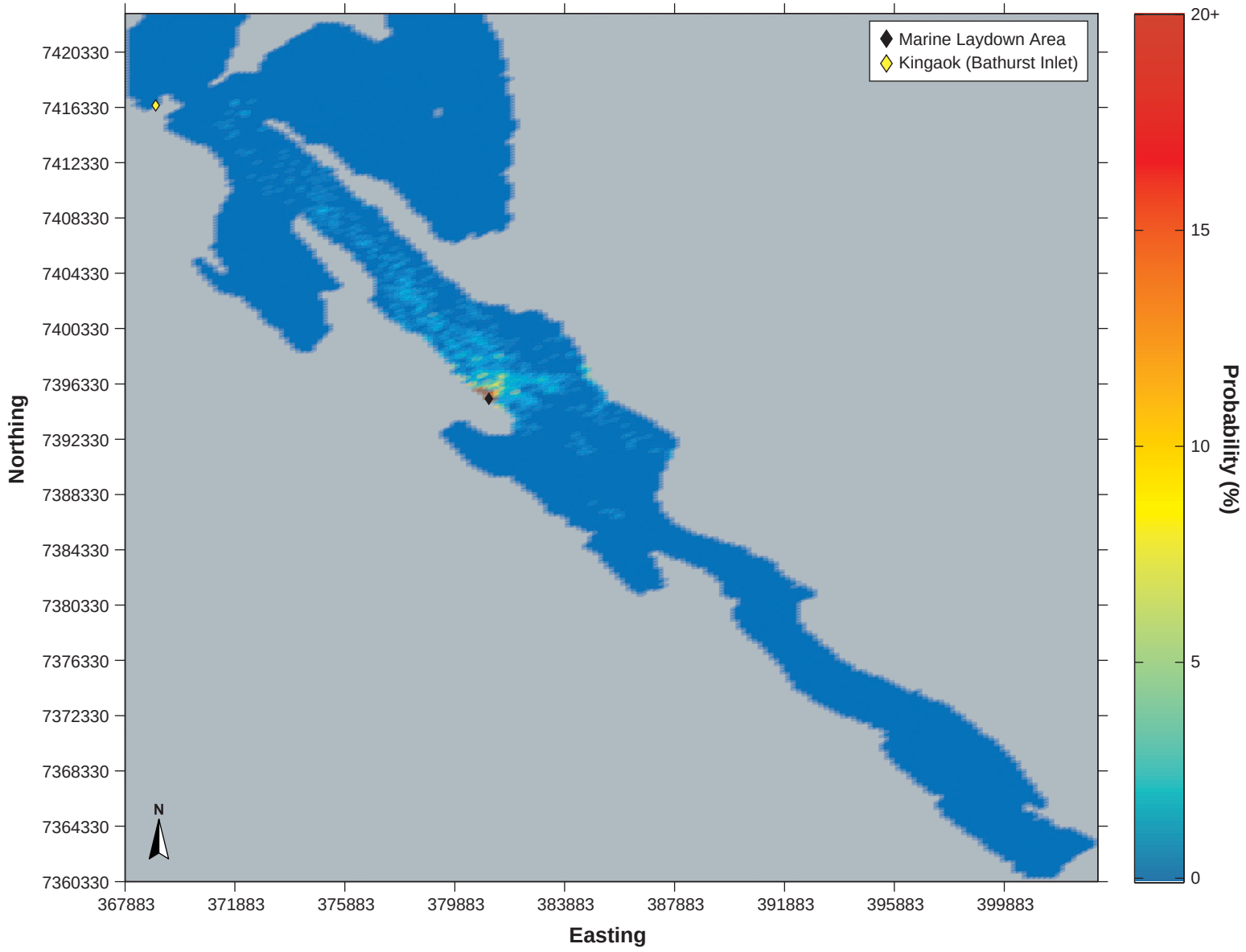

Figure 4.3-2

Sabina GOLD & SILVER CORP.

Diesel Fuel Spill Probability Distribution, 20 kL: 12 Hours after Spill

Figure 4.3-2

Rescan Engineers & Scientists

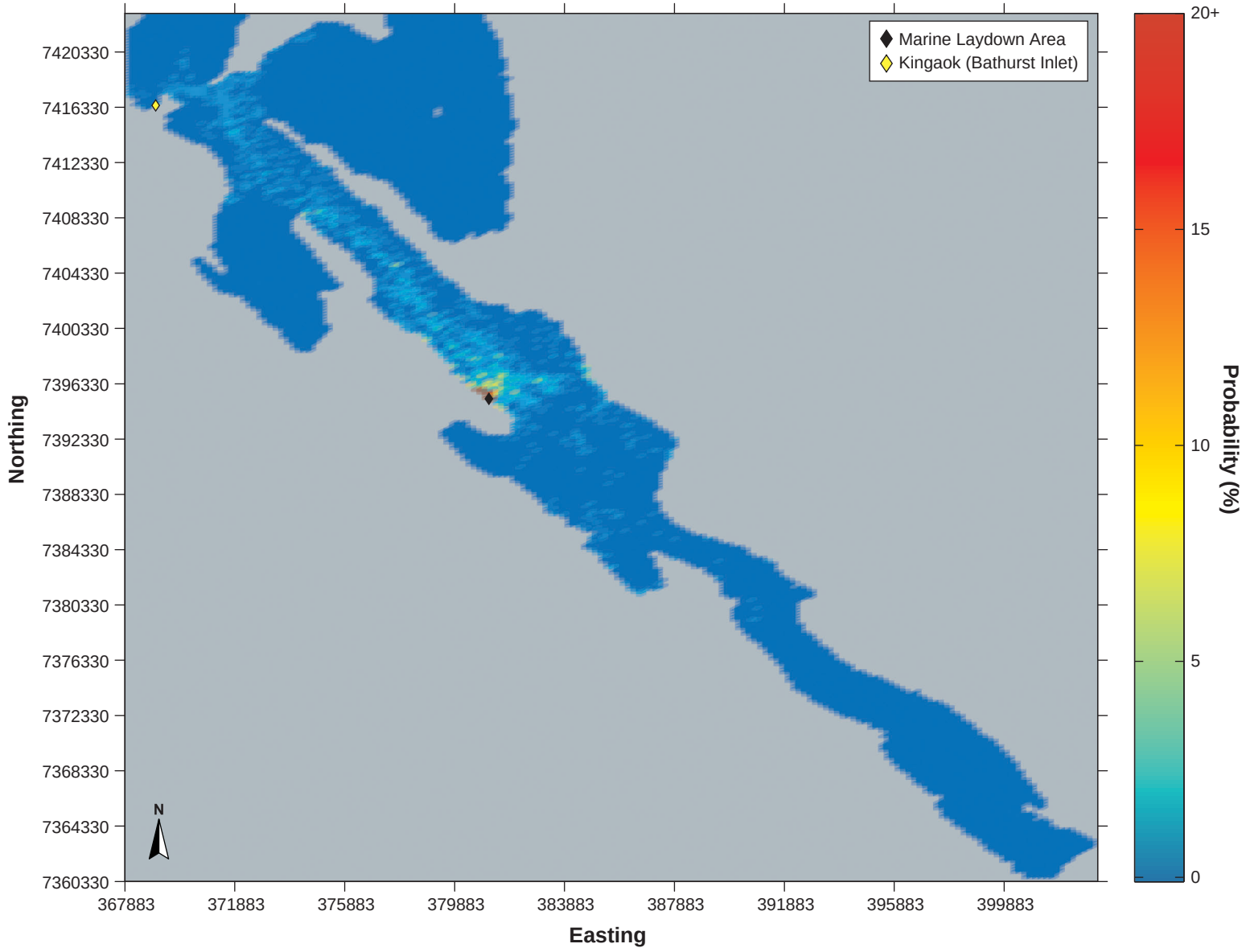

Figure 4.3-3

Sabina GOLD & SILVER CORP.

Diesel Fuel Spill Probability Distribution, 20 kL: 10 Days after Spill

Figure 4.3-3

Rescan Engineers & Scientists

Shore distribution probabilities and average mass residuals are plotted in Figures 4.3-4 and 4.3-5, respectively. Outside the MLA region, the residuals were generally minuscule compared to the 5 ML calculations with scattered probabilities <5% relatively common, including inside Burnside Bay. The highest probabilities were recorded along the shorelines directly north of the MLA and on the eastern shores across the main channel, but these rarely reached 10%. In terms of mass residuals, the largest deposition occurred near the MLA with depositions upwards of 5000 kg; however most of the scattered beached diesel fuel slicks around the model domain had residual masses below 500 kg.

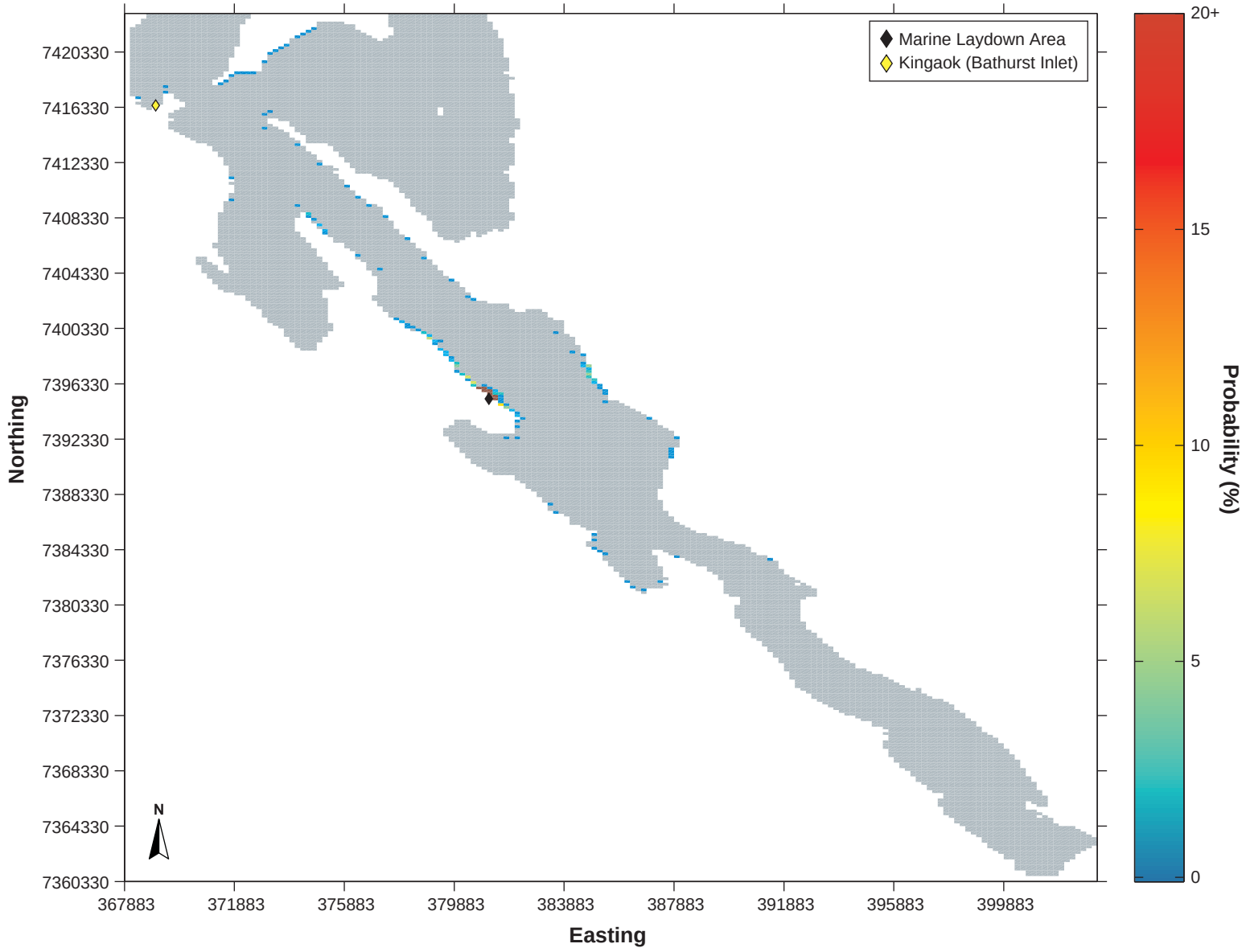

Figure 4.3-4

Sabina GOLD & SILVER CORP.

Diesel Fuel Spill Shore Residual Probability Distribution, 20 kL: 10 Days after Spill

Figure 4.3-4

Rescan Engineers & Scientists

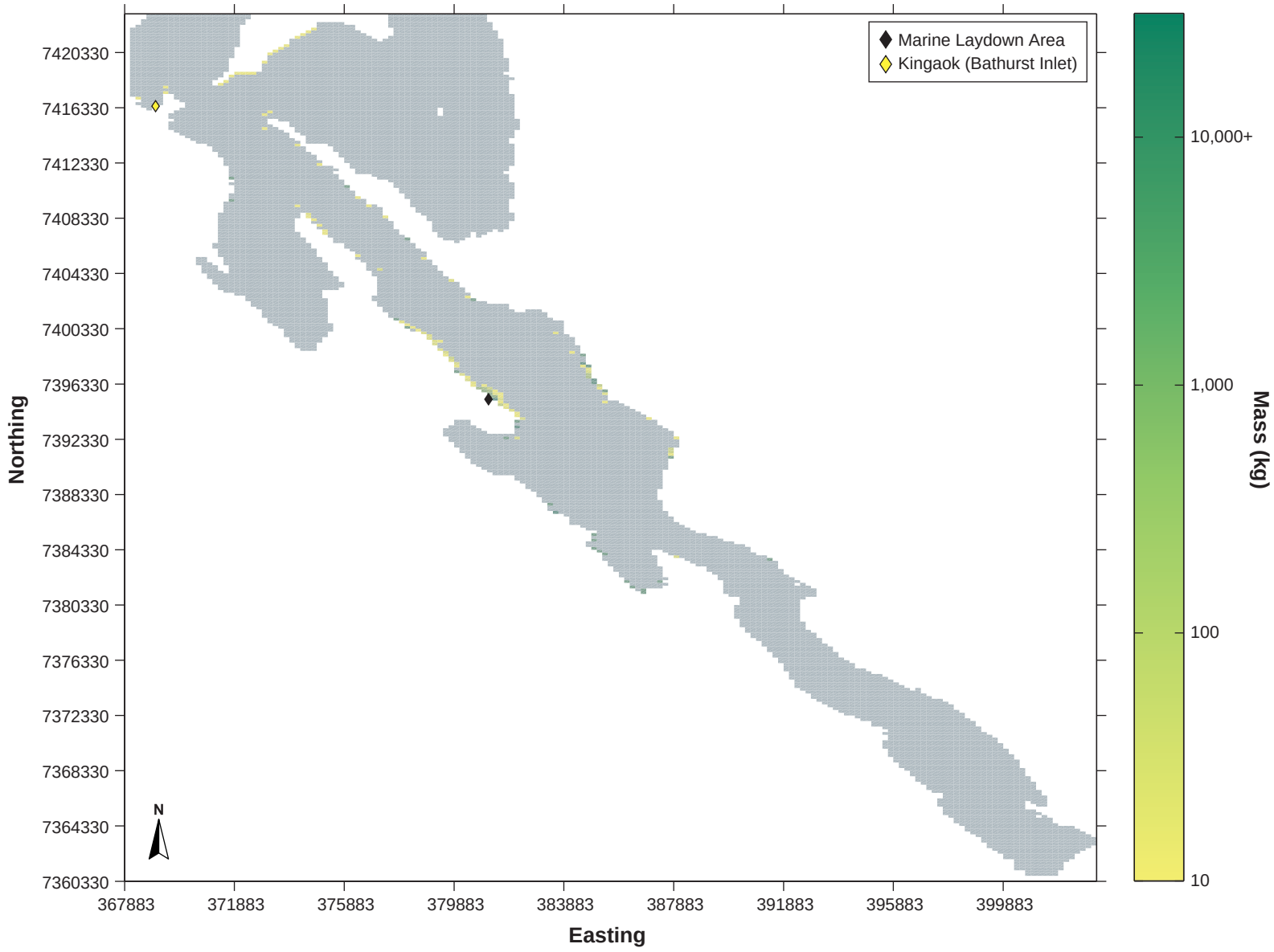

Figure 4.3-5

Sabina GOLD & SILVER CORP.

Diesel Fuel Spill Shore Residual Average Mass Distribution, 20 kL: 10 Days after Spill

Figure 4.3-5

Rescan Engineers & Scientists

5. Assessment of Potential Diesel Fuel Spills in Sensitive Marine Bird Areas

5. Assessment of Potential Diesel Fuel Spills in Sensitive Marine Bird Areas

5.1 GENERAL CONSIDERATIONS

This section addresses the potential for environmental damage from diesel spills resulting from transportation and storage of fuel near the proposed Back River MLA. In open-water diesel spills, a fraction of the diesel fuel becomes entrained into the upper water column immediately under slicks by direct solution or by entrainment of small oil droplets through current and wave action (Mackay et al. 1980; Kuiper and Van den Brink 1987; ITOPF 2011). Diesel fuel concentrations in this cloud of oil-contaminated water depend on the oil properties and the level of mixing energy (winds/waves). In theory, these concentrations may initially exceed the toxic thresholds of marine species present in the spill area. As the diesel fuel spreads under the influence of water currents, turbulent diffusion and weathering processes (see Chapter 3), the hydrocarbon concentrations within it are reduced. In time, these diesel fuel concentrations will fall below the threshold levels that cause toxicity to living organisms and ultimately decline to background levels.

5.2 RISKS TO MARINE BIRDS

Marine birds are one of the more vulnerable and sensitive of marine organisms to all types of oil spills; many bird species have a strong likelihood of contacting oil slicks if spills occur in their vicinity and all birds suffer adverse effects from exposures to small amounts of spilled fuel (see Murphy et al. 1997). However, unlike cruder distillates, diesel spills (particularly small ones ≤ 20,000 L) usually have limited impacts on marine bird wildlife due to the oil's high volatility (NOAA 2013). While diesel is highly toxic when in direct contact with marine birds, the number of birds affected is usually small due to the short residence times on surface waters. Serious impacts can occur though when currents rapidly transport 'fresh' diesel fuel directly into large nesting colonies or high bird concentration areas on the coastline. Thus, shore-locked or beached fuel material is surmised to be of a greater concern to marine birds than diesel fuel slicks primarily located in open waters.

Adults, juveniles, and fledglings are exposed to spilled diesel fuel either directly through exposure to slicks at sea or via ingestion of diesel fuel or oil-contaminated prey. Most marine birds have waterproof plumage; direct exposure to diesel fuel slicks on the surface results in oiling of plumage and subsequent loss of waterproofing. This in turn leads to a loss of insulating properties of plumage causing death by hypothermia. Oiling also leads to loss of buoyancy leading to death by drowning or reduction in swimming ability. Ingestion of hydrocarbons during preening or ingestion of contaminated food can lead to death or a variety of sub-lethal effects. The risk or vulnerability to oiling by spills appears to vary with differing bird habitats. Marine species that sit on the sea surface appear to be the most vulnerable; soaring birds, aerial divers, shorebirds and waders less so (French-McCay 2004). Once oiled, risk may vary with the birds' ability to leave the water and roost until the diesel fuel can be preened off and waterproofing restored.

A standardised threshold diesel toxicity level for numerous species of waterfowl has been established at approximately 10 g oil/m^2 (National Research Council 1985, 2005). This level is low when compared to modelling results as detailed in Chapter 4, e.g., a fresh spill of a 1000 kg of diesel slick in a 200 x 200 m model grid area technically leads to average surface diesel fuel concentration of 25 g oil/m^2. This value does not yet include weathering effects, a few hours or days after the spill will be sufficient to reduce the concentration below threshold levels in most weather conditions found in Bathurst Inlet.

5.3 BATHURST INLET BIRD POPULATIONS OF INTEREST

Numerous marine bird species have been documented in southern Bathurst Inlet (Rescan 2012b, 2013b). Ordered from commonly (i.e., over >200 individuals counted) to rarely (i.e., less than 30 individuals) observed, these are: Canadian goose; red-breasted merganser; greater scaup; black, white-winged and surf scoters; herring and glaucous gulls; long-tailed duck; pacific, red-throated and yellow-billed loons; and the common eider. Amongst these populations, the glaucous gull, long-tailed duck and common eider are all listed as sensitive species in Nunavut (CESCC 2010).

Aside from the eider, all of these species have been recorded to forage and/or nest within a few kilometres of the MLA and in multiple areas around southern Bathurst Inlet. The observations occurred mainly in the late summer and fall when a number of birds were present in marine habitats for molting and staging purposes. The approximate locality of each bird population within the study area is displayed in Figure 5.3-1 and 5.3-2. The birds were grouped up in a few basic taxons to simplify the color scheme: duck (incl. mergansers, scaups, scoters and long-tailed duck), goose, gull and loon. The unknown waterbird category is included to reflect bird observations that couldn't be identified properly in the field. Any large groups of marine birds that were documented during baseline studies from 2010 to the present during any time of the year were thus mapped (Rescan 2012b, 2013b). Large groups are defined as any observation of a group of more than 10 individuals for any species of duck, loon, or gull, or any observation of a group of more than 25 individuals of a goose species.

Figures 5.3-1 and 5.3-2 also display the shore residual probability distribution grid from the 5 ML diesel spill and 20 kL diesel spill scenarios respectively. The original model results from the raster graphics of Figures 4.2-5 and 4.3-4 were adapted through an interpolative contour procedure in order to align the cruder modelled coast to the high resolution map grid in Figures 5.3-1 and 5.3-2. Using this procedure, the likelihood of diesel spills interacting with sensitive birding areas can be assessed throughout southern Bathurst Inlet.

5.3.1 5 ML Spill Sensitivity Assessment

The most apparent feature of Figure 5.3-1 is the lack of bird populations located near the MLA, which has by far the highest spill probabilities. Only a medium flock of geese and a brief observation of an unidentified fowl have been recorded within 4 km of the on land MLA infrastructure. Conversely, the highest proportion of bird observations in the inlet is located in the small cove just south the MLA, which is seasonally inhabited by large groups of ducks and geese. Diesel particles appear to reach the cove only in <10% of simulations, and according to Figures 4.2-1 and 4.2-2 it would take several hours before a spill would reach the area. It is logical that birds would favor the southern cove relative to the MLA shoreline for nesting grounds, as the cove is relatively sheltered from the main currents driving the circulation in the main Bathurst Inlet channel. The alongshore currents near the MLA will disperse spills northwards, as is clearly seen in Figure 5.3-1.

Two other bird areas could potentially interact with diesel fuel spills in Figure 5.3-1: the northern shores directly across the main channel from the MLA, and the shores surrounding the peninsula to the south of the MLA. The former is largely inhabited by duck populations that span over 10 km of the coast. The diesel residual probabilities there still remain relatively low with respect to the MLA coast, some small areas can have probabilities as high as 30%, but on average most of the coast probabilities are <10%. The peninsula to the south, on the other hand, is far enough south to receive little diesel fuel overall, with only a few patches of <5% probabilities present.

PROJECT # 0194096-0040 GIS # BAC-23-224 September 16 2013

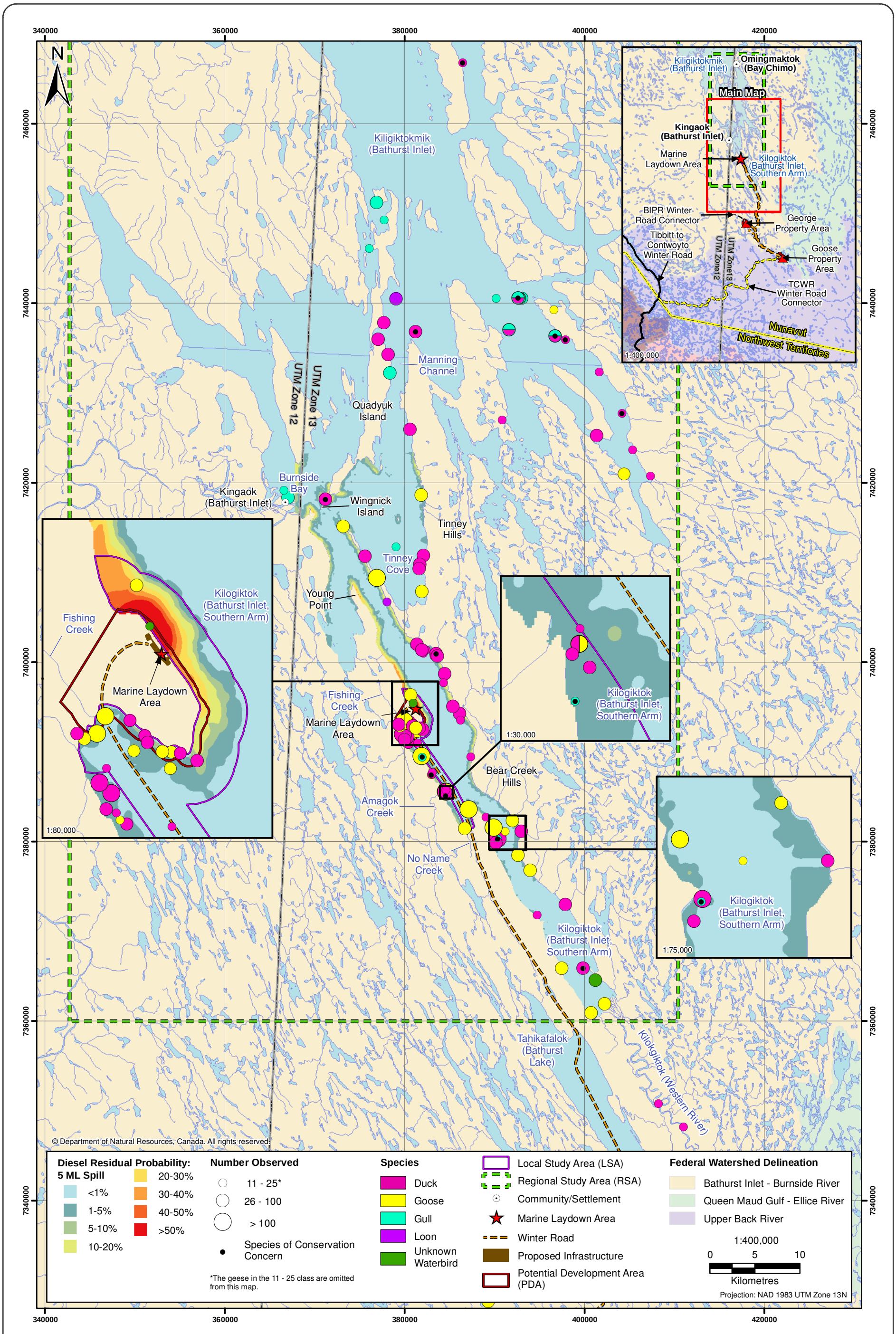

Figure 5.3-1

Sabina GOLD & SILVER CORP.

5 ML Spill Sensitivity in Relation to Migratory Bird Staging Areas in Bathurst Inlet

Figure 5.3-1

Rescan™ Engineers & Scientists

PROJECT # 0194096-0040 GIS # BAC-23-237 September 16 2013

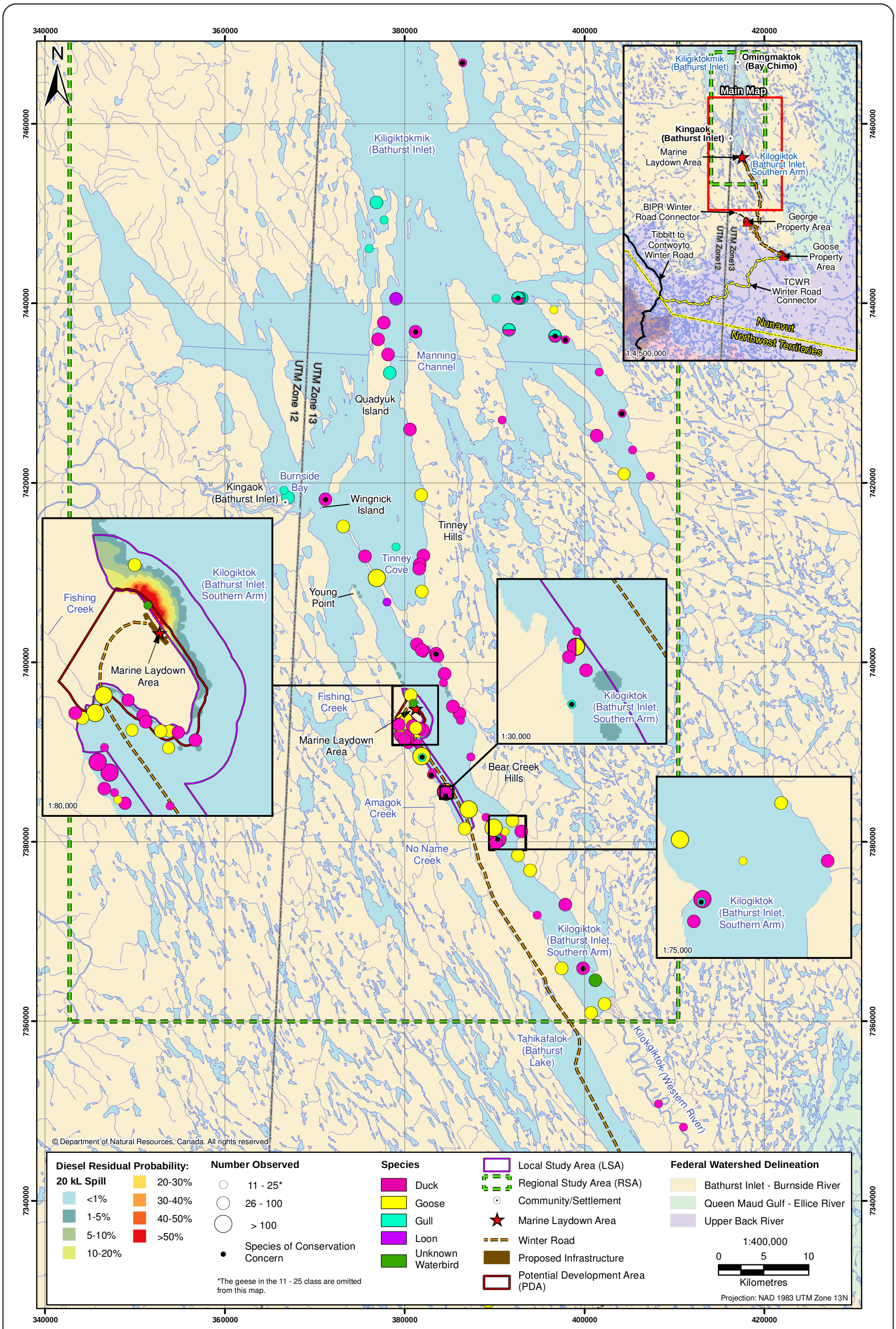

Figure 5.3-2

Sabina GOLD & SILVER CORP.

20 kL Spill Sensitivity in Relation to Migratory Bird Staging Areas in Bathurst Inlet

Figure 5.3-2

Rescan™ Engineers & Scientists

It can be surmised from Figure 5.3-1 that ducks and geese are the main species at risk of contact with a potential diesel spill. Loon observations are few and far between, as they mostly reside in the northern reaches of the inlet. The same situation applies for gull populations, with one notable exception: gulls are commonly observed near the community of Kingaok, which has a <30% probability of diesel spills reaching its shores. Gulls however are one of the species least likely to be affected by diesel fuel spills as soaring birds generally can easily escape contaminated areas (French-McCay 2004).

5.3.2 20 kL Spill Sensitivity Assessment

Shore residual probabilities for 20 kL spills are plotted alongside bird population observations in Figure 5.3-2. As previously detailed in Chapter 4, 20 kL spills probability distribution are much lower than the 5 ML spills due to the orders of magnitude difference in spill volumes. Consequently, the potential risk to marine birds is much less. The probabilities are still high around the MLA site, but again little to no diesel was found to reach the southern cove were geese and duck are plentiful (see left insert in Figure 5.3-2). Only a few areas along the northern shore have non-zero residual probabilities. Thus, it is surmised that diesel spills on the order of ~20 kL should have very little impacts on the marine bird population of Bathurst Inlet, similar to what has been observed during spills recorded in Alaska in the last 10 years (NOAA 2013).

6. Summary and Conclusions

6. Summary and Conclusions

A 3D numerical fluid model (MIKE3 by DHI) was used to develop a working model of southern Bathurst Inlet. The model was first calibrated using 2012 field data prior to conducting the diesel fuel spill scenarios. Despite the many simplifying assumptions made during model construction, the simulations were able to reasonably reproduce the surface thermohaline structure and current velocities of the inlet. The current depth structures modelled at the ADCP locations differed somewhat from instrument measurements, but the velocity magnitudes were of the same order and several shifts in current magnitudes were well-reproduced within the modelled data.

The Bathurst Inlet model was then coupled to a diesel fuel spill model (DHI's Oil Spill Module) to predict the fate of potential diesel fuel spills occurring at the MLA. Two scenarios of different volumes were considered during simulations: a 5 ML spill issued from a catastrophic event such as a sinking barge; and a 20 kL spill that could occur from a pipe failure during fuel transfers from barges. Each volume scenario was modelled under hundreds of different wind scenarios, producing adequate stochastic databases from which probability distribution figures could be drawn. The major results from the calculated simulations are summarized in Table 6-1.

Table 6-1. Summary of Results from the Marine Diesel Fuel Spill Modelling

Spill Scenario	Probability (%) 5 ML spill	Probability (%) 20 kL spill	General Bathurst Inlet Environmental Conditions
All diesel remains within <1 km of the MLA	~40%	~70%	Calm conditions (i.e., winds below 5 m/s). Periods with winds of predominantly northern and north-western origins
The majority of the diesel (i.e., <95%) remains south of Kingaok, within southern Bathurst Inlet	~52%	~85%	Similar to above, plus weak to moderate south-eastern winds.
Greater amounts of diesel get transported south of the MLA	~25%	<20%	Strong north-western winds (>8 m/s), driving large southern alongshore currents
Significant amounts of diesel reach Kingaok	<40%	<10%	Strong southern and south-eastern winds, generally above 8 m/s. Strong shifts in winds directions. Periods with strong freshwater flushing (i.e., freshet)
Diesel particles escaping the model domain	<15%	~0%	As above, also a small chance of occurring in any given wind/current condition, given the large number of diesel fuel particles in the system.

Probability distributions from the 5 ML simulations showed potential spreading of the diesel slick across southern Bathurst Inlet. While a significant proportion (i.e., over 40%) of the simulations did not result in much movement of diesel fuel outside of the MLA area, in high wind conditions large (>1,000 kg) masses of diesel could reach the community of Kingaok and beyond. Over two thirds of the diesel quickly weathered within the first 10 days of all simulations. The largest weathering rates occurred within the first couple of simulation days, with ~25 to ~85% loss of volatile material being loss,

depending on the weather conditions. Significant mass residual quantities were prevalent around the MLA area and in the shores located in the southern half of the modelled inlet.

The diesel probability distributions resulting from the 20 kL diesel spills were small compared to the 5 ML simulations. The only high probabilities were recorded directly near the MLA; diesel rarely spread to areas outside of the MLA. Spilled fuel reached Kingaok in less than 10% of all simulations, and the amounts were usually small (i.e., <1,000 kg).

Marine bird observations in Bathurst Inlet were compared with the shoreline residual probability distributions resulting from the diesel fuel spill simulations. The MLA region had the highest diesel residual probability for the 5 ML spill simulations, however very few bird observations were correlated with that high risk area. Large amounts of geese and ducks were observed in the cove directly south of the MLA, but simulation probabilities indicated than <10% of simulations had some diesel remaining at or near the shore in that area. Other regions with frequent bird observations had similar shoreline probability distributions. Marine bird observations were also compared with results from the 20 kL spill simulations. The residual shoreline probabilities were very similar to 5 ML simulations near the MLA, thus limited bird population would be affected in the area. Negligible amounts of diesel fuel were predicted to interact with bird population areas in the south of Bathurst Inlet. Thus it is assumed that diesel spills of the order of ~<20 kL would have minimal impacts on the marine bird population of Bathurst Inlet.

In summary, the wind conditions, current regime and overall spill volume play a critical role in determining the fate of diesel spills within southern Bathurst Inlet. Regardless of diesel amounts, spills occurring in mild to moderate wind conditions generally did not progress past a few kilometres from the source location. Thus, it is advisable that operations concerning the handling and transfer of fuel at the MLA be conducted during such calm periods to more easily mitigate the potential effects of potential spills.

References

References

Definitions of the acronyms and abbreviations used in this reference list can be found in the Glossary.

Al-Rabeh, A. 1994. Estimating surface oil spill transport due to wind in the Arabian Gulf. *Ocean Engineering*, 21: 461-65.

Anderson, C. M., M. Mayes, and R. P. LaBelle. 2012. *Update of Occurrence Rates for Offshore Oil Spills*. Bureau of Ocean Energy Management OCS Report 2012-069. Bureau of Ocean Energy Management: Hemdon, VA.

Betancourt, F., A. Palacio, and A. Rodriguez. 2005. Effects of the mass transfer process in oil spill. *American Journal of Applied Science*, 2: 939-46.

CESCC. 2010. *Wild Species 2010: The General Status of Species in Canada*. Canadian Endangered Species Conservation Council. http://www.wildspecies.ca/searchtool.cfm?lang=e (accessed August 2013).

CHS. 1994. *Arctic Canada*. Vol. 3 of *Sailing Directions*. Ottawa, ON: Canadian Hydrographic Services.

CHS. 2004. *Bathurst Inlet - Southern Portion/Partie Sud*. Nautical Chart #7793. Canadian Hydrographic Service: Ottawa, ON.

Delvigne, G. and C. Sweeney. 1988. Natural dispersion of oil. *Oil and Chemical Pollution*, 4 (doi:10.1016/S0269-8579(88)80003-0): 281-310.

Demirbilek, Z., S. M. Bratos, and E. F. Thompson. 1993. *Wind Products for use in Coastal Wave and Surge Models*. Miscellaneous Paper CERC-93-7. U.S. Army Engineer Waterways Experiment: Vicksburg, MS.

DHI. 2012a. *DHI Oil Spill Model: Oil Spill Template Scientific Documentation*. http://www.mikebydhi.com/Products/CoastAndSea/MIKE3/Ecosystems.aspx (accessed June 2013).

DHI. 2012b. *MIKE 3 Flow Model: Hydrodynamic Module Scientific Documentation*. http://www.mikebydhi.com/Products/CoastAndSea/MIKE3.aspx (accessed June 2013).

DHI. 2012c. *MIKE 3 Flow Model: Hydrostatic Module Scientific Documentation*. http://www.mikebydhi.com/Products/CoastAndSea/MIKE3.aspx (accessed June 2013).

Environment Canada. 2013. *Environmental Technology Centre, Oil Poperties Database*. http://www.etc-cte.ec.gc.ca/databases/oilproperties/Default.aspx (accessed June 2013).

Fingas, M. F. 1996. The evaporations of oil spills: Prediction of equations using distillation data. *Spill Science & Technology Bulletin*, 3 (doi: 10.1016/S1353-2561(97)00009-1): 191-92.

Fingas, M. F. 1997. Studies on the evaporation of crude oil and petroleum products: I. the relationship between evaporation rate and time. *Journal of Hazardous Materials*, 56 (doi: 10.1016/S0304-3894(97)00050-2): 227-36.

French-McCay, D. P. 2004. Oil spill impact modeling: Development and validation. *Environmental Toxicology and Chemistry*, 23: 2441-56.

Gill, A. E. 1982. *Atmosphere-Ocean Dynamics*. Vol. 30 of *International Geophysics Series*. San Diego, CA: Academic Press.

ITOPF. 2011. *Fate of Marine Oil Spills*. Technical Information Paper 2. The International Tanker Owners Pollution Federation Limited (ITOPF): London, UK.

Kuiper, J. and W. J. Van den Brink, eds. 1987. *Fate and effects of oil in marine ecosystems*. Dordrecht, NL: Martinus Nighoff Publications.

Kundu, P. K. 1990. *Fluid Mechanics*. San Diego, CA: Academic Press.

Levinton, J. S. 1995. *Marine Biology: Function, Biodiversity, Ecology*. New York, NY: Oxford University Press.

Mackay, D., R. Buist, R. Mascarenhas, and S. Paterson. 1980. *Oil spill processes and models*. Environmental Emergency Branch, Department of Fisheries and Environment, Environment Canada: Ottawa, ON.

Marchal, R., S. Penet, F. Solano-Serena, and J. P. Vandecasteele. 2003. Gasoline and diesel oil biodegradation. *Oil & Gas Science and Technology - Rev IFP*, 58: 441-48.

Murphy, S. M., R. H. Day, J. A. Wiens, and K. R. Parker. 1997. Effects of the Exxon Valdez Oil Spill on Birds: Comparison of Pre- and Post-Spill Surveys in Prince William Sound, Alaska. *The Condor*, 99 (2): 299-313.

National Research Council. 1985. *Oil in the Sea II: Inputs, Fates, and Effects*. Washington, D.C.: National Academy Press.

National Research Council. 2005. *Oil in the Sea III: Inputs, Fates, and Effects*. Washington, D.C.: National Academy Press.

NOAA. 2013. *Office of Response and Restoration: Small Diesel Spills (500-5000 gallons)*. http://response.restoration.noaa.gov/oil-and-chemical-spills/oil-spills/resources/small-diesel-spills.html (accessed August 24 2013).

Patankar, S. V. 1980. *Numerical Heat Transfer and Fluid Flow*. New York, NY: Hemisphere Publishing Corporation.

Reed, M. 1989. The physical fates component of the natural resource damage assessment model system. *Oil and Chemical Pollution*, 5: 99-123.

Rescan. 2012a. *Bathurst Inlet Port and Road Project: 2007 to 2011 Meteorology Baseline Report*. Prepared for the Bathurst Inlet Port and Road Project by Rescan Environmental Services Ltd.: Vancouver, British Columbia.

Rescan. 2012b. *Bathurst Inlet Port and Road Project: Marine Bird Baseline Study, 2010*. Prepared for the Bathurst Inlet Port and Road Project by Rescan Environmental Services Ltd.: Vancouver, British Columbia.

Rescan. 2012c. *Bathurst Inlet Port and Road Project: Physical Oceanography Baseline Study, 2012*. Prepared for the Bathurst Inlet Port and Road Project by Rescan Environmental Services Ltd.: Vancouver, British Columbia.

Rescan. 2012d. *Bathurst Inlet Port and Road Project: Surface Water Hydrology Baseline Study, 2010 and 2012*. Prepared for the Bathurst Inlet Port and Road Project by Rescan Environmental Services Ltd.: Vancouver, British Columbia.

Rescan. 2013a. *Back River Project: 2012 Marine Baseline Report*. Prepared for Sabine Gold & Silver Corp. by Rescan Environmental Services Ltd.: Vancouver, BC.

Rescan. 2013b. *Back River Project: Wildlife Baseline Report 2012*. Prepared for Sabina Gold and Silver Corp. by Rescan Environmental Services Ltd.: Vancouver, British Columbia.

Rodi, W. 1984. *Turbulence Models and Their Applications in Hydraulics*. Delft, NL: IAHR.

Smagorinsky, J. 1963. General circulation experiments with the primitive equations: I. the basic experiment. *Mon Wea Rev*, 91: 99-164.

Xie, H., P. D. Yapa, and K. Nakata. 2007. Modeling emulsification after an oil spill in the sea. *Journal of Marine Systems*, 68: 489-506.

Appendix 2

Hourly Meteorological Data Used in the Baseline Calibration Model

Rescan™
an ERM company

Appendix 2. Hourly Meteorological Data Used in the Baseline Calibration Model

Date	Average Air Temperature °C	Relative Humidity %	Average Wind Speed m/s	Average Wind Direction °(clockwise from North)
'8/23/2012 16:00'	10.86	67.84	3.98	15.14
'8/23/2012 17:00'	11.18	66.61	4.015	6.854
'8/23/2012 18:00'	11.22	68.56	3.919	5.374
'8/23/2012 19:00'	11.03	71.47	4	354.6
'8/23/2012 20:00'	10.38	77.95	4.336	346.2
'8/23/2012 21:00'	9.04	85.9	3.928	332.9
'8/23/2012 22:00'	8.56	86.8	2.713	332.4
'8/23/2012 23:00'	8.21	88.1	2.859	320.7
'8/24/2012 0:00'	7.836	91.1	4.086	318.1
'8/24/2012 1:00'	7.317	93.1	4.327	319.8
'8/24/2012 2:00'	7.059	95.4	3.97	318.8
'8/24/2012 3:00'	6.716	97	3.642	320
'8/24/2012 4:00'	6.555	98.1	3.353	323.7
'8/24/2012 5:00'	6.614	99	2.404	326.7
'8/24/2012 6:00'	5.598	99.4	1.82	264.9
'8/24/2012 7:00'	6.085	99.5	1.151	282.3
'8/24/2012 8:00'	6.953	99.6	1.001	36.94
'8/24/2012 9:00'	6.886	99.6	1.5	100.8
'8/24/2012 10:00'	7.393	98	1.645	87.7
'8/24/2012 11:00'	8.32	91.7	1.358	60.85
'8/24/2012 12:00'	9.81	82.1	1.647	47.16
'8/24/2012 13:00'	10.83	75.62	2.499	24.76
'8/24/2012 14:00'	10.95	74.39	2.89	20.11
'8/24/2012 15:00'	11.3	71.68	2.149	16.91
'8/24/2012 16:00'	12.11	66.29	1.617	44.83
'8/24/2012 17:00'	12.42	62.98	2.305	74.51
'8/24/2012 18:00'	12.47	62.01	3.357	111.2
'8/24/2012 19:00'	12.19	63.67	3.997	119.3
'8/24/2012 20:00'	11.93	64.2	3.483	128.3
'8/24/2012 21:00'	11.67	64.28	3.598	160.3
'8/24/2012 22:00'	11.02	65.03	3.493	169.4
'8/24/2012 23:00'	10.22	73.09	4.116	170.9
'8/25/2012 0:00'	10.3	75.79	3.849	175.5
'8/25/2012 1:00'	10.03	78.47	4.014	177.8
'8/25/2012 2:00'	10.18	74.34	3.536	180.9
'8/25/2012 3:00'	9.7	76.63	3.493	191.6
'8/25/2012 4:00'	9.11	78.21	3.574	206.4
'8/25/2012 5:00'	8.21	81	3.756	215.9
'8/25/2012 6:00'	8.47	83.8	3.95	212.3
'8/25/2012 7:00'	8.36	87.6	4.327	215.8
'8/25/2012 8:00'	9.2	85.3	3.989	202.3
'8/25/2012 9:00'	10.05	79.84	3.711	175.8
'8/25/2012 10:00'	10.53	78.71	4.345	152.3
'8/25/2012 11:00'	11.14	74.73	4.278	152.6
'8/25/2012 12:00'	12.06	69.27	4.196	159.6
'8/25/2012 13:00'	12.88	65.09	4.119	160.7
'8/25/2012 14:00'	13.74	61.46	4.193	166.9
'8/25/2012 15:00'	13.94	60.42	3.932	150.8
'8/25/2012 16:00'	14.25	58.76	3.842	150.9
'8/25/2012 17:00'	14.83	55.47	4.473	164.9

Appendix 2. Hourly Meteorological Data Used in the Baseline Calibration Model

Date	Average Air Temperature °C	Relative Humidity %	Average Wind Speed m/s	Average Wind Direction °(clockwise from North)
'8/25/2012 18:00'	14.82	54.12	5.336	159.1
'8/25/2012 19:00'	14.4	55.41	5.743	159.3
'8/25/2012 20:00'	13.42	61.08	5.885	168.2
'8/25/2012 21:00'	11.99	66.47	5.703	176.8
'8/25/2012 22:00'	11.47	66.57	5.847	198.9
'8/25/2012 23:00'	9.64	72.77	6.747	219.3
'8/26/2012 0:00'	8.96	75.99	5.533	217.5
'8/26/2012 1:00'	9.26	74.68	3.44	199.9
'8/26/2012 2:00'	8.95	77	4.612	209.6
'8/26/2012 3:00'	8.1	79.99	3.737	201.3
'8/26/2012 4:00'	8.01	81.5	4.091	194.1
'8/26/2012 5:00'	8.12	82.1	4.169	203.1
'8/26/2012 6:00'	8.92	80.1	4.375	205.8
'8/26/2012 7:00'	9.65	78.03	2.517	183.6
'8/26/2012 8:00'	9.91	77.76	2.64	192.6
'8/26/2012 9:00'	11.98	70.68	3.198	164.4
'8/26/2012 10:00'	13.94	60.73	5.077	188.6
'8/26/2012 11:00'	14.79	58.15	4.751	190.5
'8/26/2012 12:00'	15.44	52.61	4.65	211.9
'8/26/2012 13:00'	16.12	53.32	4.472	215.8
'8/26/2012 14:00'	17.05	50.2	4.502	224.8
'8/26/2012 15:00'	16.26	57	4.43	230.6
'8/26/2012 16:00'	17.6	47.75	3.145	221.4
'8/26/2012 17:00'	16.95	49.61	3.571	159.4
'8/26/2012 18:00'	16.73	50.51	5.389	152.3
'8/26/2012 19:00'	16.89	51.43	4.685	181.9
'8/26/2012 20:00'	15.94	58.28	8.04	195.5
'8/26/2012 21:00'	14.48	64.08	5.989	192.2
'8/26/2012 22:00'	14.21	66.7	6.28	200.8
'8/26/2012 23:00'	13.79	66.36	6.69	199.6
'8/27/2012 0:00'	12.47	69.74	8.71	207.4
'8/27/2012 1:00'	11.7	71.41	9.69	215.8
'8/27/2012 2:00'	10.99	73.03	9.48	214.2
'8/27/2012 3:00'	10.47	77.66	8.23	207.4
'8/27/2012 4:00'	9.86	83.5	6.076	160.6
'8/27/2012 5:00'	9.5	86.2	7.888	168.1
'8/27/2012 6:00'	8.92	88.4	8.72	164.3
'8/27/2012 7:00'	9.36	86.7	7.922	158.7
'8/27/2012 8:00'	9.62	87.8	7.857	156.4
'8/27/2012 9:00'	9.77	90.8	8.35	156.7
'8/27/2012 10:00'	9.72	93	8.68	154.2
'8/27/2012 11:00'	10.04	93.8	7.715	156.1
'8/27/2012 12:00'	10.12	95.4	7.813	150.5
'8/27/2012 13:00'	11.15	93.9	8.32	156
'8/27/2012 14:00'	12.57	91.7	7.336	157.5
'8/27/2012 15:00'	13.74	89.6	6.674	171.8
'8/27/2012 16:00'	12.56	92.2	8.04	335.8
'8/27/2012 17:00'	11.66	91.3	5.926	350.5
'8/27/2012 18:00'	11.47	88.2	6.544	345.6
'8/27/2012 19:00'	11.42	84.6	4.364	343.7

Appendix 2. Hourly Meteorological Data Used in the Baseline Calibration Model

Date	Average Air Temperature °C	Relative Humidity %	Average Wind Speed m/s	Average Wind Direction °(clockwise from North)
'8/27/2012 20:00'	11.33	82.4	2.238	306.9
'8/27/2012 21:00'	11.08	85.7	3.858	242.9
'8/27/2012 22:00'	11.02	81.8	5.073	250.2
'8/27/2012 23:00'	11.14	79.29	4.086	289.3
'8/28/2012 0:00'	10.74	77.95	4.861	300.1
'8/28/2012 1:00'	10.2	79.53	4.715	277.9
'8/28/2012 2:00'	10.09	78.19	4.286	283.6
'8/28/2012 3:00'	9.8	75.02	4.563	276.8
'8/28/2012 4:00'	9.34	75.76	2.384	293.2
'8/28/2012 5:00'	8.42	80.9	2.34	237.1
'8/28/2012 6:00'	7.32	86.4	4.795	232.8
'8/28/2012 7:00'	7.283	87.3	4.729	236.5
'8/28/2012 8:00'	8.54	84	2.553	203.4
'8/28/2012 9:00'	9.6	84.2	1.621	128.4
'8/28/2012 10:00'	10.75	81.6	1.537	88.8
'8/28/2012 11:00'	11.7	75.8	2.191	50.8
'8/28/2012 12:00'	12.21	69.14	2.119	40.8
'8/28/2012 13:00'	12.91	67.18	2.27	32.99
'8/28/2012 14:00'	13.61	65.46	2.858	15.53
'8/28/2012 15:00'	14.33	55.6	3.615	26.49
'8/28/2012 16:00'	14.66	55.08	3.282	19.36
'8/28/2012 17:00'	13.98	64.22	5.145	356.8
'8/28/2012 18:00'	13.21	69.57	6.194	348.3
'8/28/2012 19:00'	12.3	71.2	5.559	343.4
'8/28/2012 20:00'	10.82	77.89	5.829	317.4
'8/28/2012 21:00'	8.85	90.1	5.95	319.2
'8/28/2012 22:00'	8.47	89.3	5.837	317.4
'8/28/2012 23:00'	8.11	92.6	6.445	325.4
'8/29/2012 0:00'	7.636	96.4	6.198	326.8
'8/29/2012 1:00'	7.513	97.1	6.053	332.7
'8/29/2012 2:00'	7.211	97.8	5.704	326.9
'8/29/2012 3:00'	7.251	98.4	5.209	352.8
'8/29/2012 4:00'	6.858	98.3	3.155	51.05
'8/29/2012 5:00'	6.491	99.3	4.46	54.94
'8/29/2012 6:00'	6.618	99.4	4.407	54.31
'8/29/2012 7:00'	6.627	99.4	4.309	47.47
'8/29/2012 8:00'	6.971	98.9	3.314	23.52
'8/29/2012 9:00'	7.32	98	2.651	25.6
'8/29/2012 10:00'	7.541	94.9	3.14	89.6
'8/29/2012 11:00'	7.477	94	1.655	100.1
'8/29/2012 12:00'	7.896	91.7	1.375	31.97
'8/29/2012 13:00'	8.45	91.4	2.926	354.5
'8/29/2012 14:00'	9	89.1	3.775	0.033
'8/29/2012 15:00'	9.31	88.9	4.916	2.785
'8/29/2012 16:00'	10.05	79.63	5.25	48.33
'8/29/2012 17:00'	10.06	79.64	4.699	24.55
'8/29/2012 18:00'	10.17	80.1	5.715	14.82
'8/29/2012 19:00'	10.1	80.3	5.56	4.384
'8/29/2012 20:00'	10.02	80.8	5.609	354.1
'8/29/2012 21:00'	9.53	84.5	6.757	326.6

Appendix 2. Hourly Meteorological Data Used in the Baseline Calibration Model

Date	Average Air Temperature °C	Relative Humidity %	Average Wind Speed m/s	Average Wind Direction °(clockwise from North)
'8/29/2012 22:00'	9.58	83.3	8.2	342.5
'8/29/2012 23:00'	9.21	87.6	8.52	349
'8/30/2012 0:00'	8.56	93.8	7.779	341
'8/30/2012 1:00'	7.924	98	8.78	335.2
'8/30/2012 2:00'	7.856	99.4	8.45	347.7
'8/30/2012 3:00'	7.771	99.6	9.15	354.1
'8/30/2012 4:00'	7.392	99.8	10.08	354.8
'8/30/2012 5:00'	7.115	99.9	9.19	2.307
'8/30/2012 6:00'	7	99.1	9.65	1.154
'8/30/2012 7:00'	7.132	92.6	10.18	4.547
'8/30/2012 8:00'	7.092	93.5	8.79	9.67
'8/30/2012 9:00'	6.626	94	8.25	346.3
'8/30/2012 10:00'	6.54	89	7.76	345.6
'8/30/2012 11:00'	6.844	83.6	8.3	356.9
'8/30/2012 12:00'	7.131	79.47	7.405	358.7
'8/30/2012 13:00'	7.318	79.28	5.763	351.6
'8/30/2012 14:00'	7.773	75.76	5.869	356.6
'8/30/2012 15:00'	8.32	69.51	4.608	2.378
'8/30/2012 16:00'	8.65	66.81	4.42	16.06
'8/30/2012 17:00'	8.78	65.94	3.313	1.136
'8/30/2012 18:00'	8.92	67.08	2.729	5.664
'8/30/2012 19:00'	9.01	70.21	2.991	354.7
'8/30/2012 20:00'	8.62	73.15	1.785	337.1
'8/30/2012 21:00'	8.02	74.76	1.814	307.1
'8/30/2012 22:00'	7.854	76.03	1.384	261.5
'8/30/2012 23:00'	6.437	82.3	4.01	244
'8/31/2012 0:00'	6.333	79.91	4.045	262.1
'8/31/2012 1:00'	7.152	75.88	2.876	275.1
'8/31/2012 2:00'	8.13	71.19	2.449	264.6
'8/31/2012 3:00'	8.01	71.69	1.117	336.7
'8/31/2012 4:00'	8.38	70	4.035	288.5
'8/31/2012 5:00'	7.728	73.34	3.416	293.9
'8/31/2012 6:00'	6.73	78.07	3.365	234.6
'8/31/2012 7:00'	6.882	77.99	5.358	257
'8/31/2012 8:00'	8.37	73.52	3.109	227.1
'8/31/2012 9:00'	9.05	72.91	2.378	234.2
'8/31/2012 10:00'	11.26	64.56	3.794	282.3
'8/31/2012 11:00'	12.09	57.04	5.785	274.7
'8/31/2012 12:00'	12.75	51.02	7.794	254.1
'8/31/2012 13:00'	13.51	46.31	6.658	253.9
'8/31/2012 14:00'	14.05	43.93	7.562	243.1
'8/31/2012 15:00'	14.37	44.5	8.32	237.9
'8/31/2012 16:00'	14.71	44.39	7.787	234
'8/31/2012 17:00'	15.09	44.62	8.17	233.4
'8/31/2012 18:00'	15.19	45.79	9.38	237
'8/31/2012 19:00'	14.75	48.11	9.77	231.7
'8/31/2012 20:00'	13.49	54.31	8.99	227.9
'8/31/2012 21:00'	12.93	56.74	8.22	225.2
'8/31/2012 22:00'	11.59	62.51	8.4	224.9
'8/31/2012 23:00'	10.88	66.47	9.44	223.6

Appendix 2. Hourly Meteorological Data Used in the Baseline Calibration Model

Date	Average Air Temperature ˚C	Relative Humidity %	Average Wind Speed m/s	Average Wind Direction ˚(clockwise from North)
'9/1/2012 0:00'	11.16	65.28	11.81	230.6
'9/1/2012 1:00'	11.07	66.92	10.71	223.5
'9/1/2012 2:00'	11.2	67.84	12.69	239.9
'9/1/2012 3:00'	11.26	67.75	10.57	236.8
'9/1/2012 4:00'	12.12	63.71	3.916	218
'9/1/2012 5:00'	12.67	61.4	4.735	231.1
'9/1/2012 6:00'	12.19	64.14	2.346	186.1
'9/1/2012 7:00'	11.71	66.68	3.394	257.7
'9/1/2012 8:00'	11.9	67.59	10.81	256
'9/1/2012 9:00'	12.1	70.15	10.01	287.7
'9/1/2012 10:00'	9.98	96.2	8.41	338.4
'9/1/2012 11:00'	9.2	91.3	10.03	341.7
'9/1/2012 12:00'	8.62	86.1	9.8	357
'9/1/2012 13:00'	8.69	81.2	9.39	357.7
'9/1/2012 14:00'	8.43	77.06	9.72	359.2
'9/1/2012 15:00'	7.983	71.91	9.5	5.034
'9/1/2012 16:00'	7.835	67.56	8.32	1.843
'9/1/2012 17:00'	7.577	64.68	7.15	352.1
'9/1/2012 18:00'	7.405	63.89	6.727	343.5
'9/1/2012 19:00'	7.073	65.96	5.861	340.7
'9/1/2012 20:00'	6.24	69.85	5.071	327.7
'9/1/2012 21:00'	5.492	73.07	4.449	333.8
'9/1/2012 22:00'	4.757	74.88	3.191	336
'9/1/2012 23:00'	4.559	77.6	2.272	342.2
'9/2/2012 0:00'	4.576	79.82	1.567	331.9
'9/2/2012 1:00'	4.526	80.5	1.246	332.2
'9/2/2012 2:00'	4.279	82.9	0.344	8.24
'9/2/2012 3:00'	3.713	85.7	1.608	171.4
'9/2/2012 4:00'	3.133	89.5	3.541	173
'9/2/2012 5:00'	3.162	92.4	3.878	171.5
'9/2/2012 6:00'	3.778	89.8	4.885	164.6
'9/2/2012 7:00'	4.422	85.8	5.538	147.1
'9/2/2012 8:00'	4.735	85.6	6.023	152.1
'9/2/2012 9:00'	5.519	84.6	6.003	150.8
'9/2/2012 10:00'	6.459	81.6	5.63	147.9
'9/2/2012 11:00'	7.419	76.25	6.589	140.7
'9/2/2012 12:00'	8.51	69.22	7.257	145
'9/2/2012 13:00'	9.59	63.05	7.585	147
'9/2/2012 14:00'	9.81	60.94	7.258	150.8
'9/2/2012 15:00'	9.92	59.86	7.319	159.8
'9/2/2012 16:00'	10.02	60.21	6.956	156.1
'9/2/2012 17:00'	10.26	62.5	7.514	161.8
'9/2/2012 18:00'	10.68	62.26	7.689	152.5
'9/2/2012 19:00'	11.08	63.35	6.523	157.6
'9/2/2012 20:00'	10.86	67.14	6.012	165.4
'9/2/2012 21:00'	9.59	72.74	6.723	172.3
'9/2/2012 22:00'	9.04	73.06	8.01	175.1
'9/2/2012 23:00'	8.58	76.77	8.58	175.7
'9/3/2012 0:00'	8.86	81.6	7.817	165.8
'9/3/2012 1:00'	8.46	85.3	7.215	150.5

Appendix 2. Hourly Meteorological Data Used in the Baseline Calibration Model

Date	Average Air Temperature ˚C	Relative Humidity %	Average Wind Speed m/s	Average Wind Direction ˚(clockwise from North)
'9/3/2012 2:00'	8.15	87.1	5.29	159.7
'9/3/2012 3:00'	8.41	86.4	5.737	186.2
'9/3/2012 4:00'	8.29	87.2	5.222	170.6
'9/3/2012 5:00'	7.527	89.8	5.062	167.6
'9/3/2012 6:00'	6.604	93.3	5.739	167.8
'9/3/2012 7:00'	6.608	93.9	6.114	167.8
'9/3/2012 8:00'	7.641	90.9	5.289	157.8
'9/3/2012 9:00'	8.76	84.7	5.606	165.6
'9/3/2012 10:00'	10.46	78.03	5.411	140.8
'9/3/2012 11:00'	11.96	73.39	5.655	153.4
'9/3/2012 12:00'	14.36	65.36	5.45	165.8
'9/3/2012 13:00'	15.96	58.79	5.866	189.6
'9/3/2012 14:00'	17.72	50.47	4.978	196.8
'9/3/2012 15:00'	18.03	48.19	6.613	207.7
'9/3/2012 16:00'	18.63	46.41	6.491	223
'9/3/2012 17:00'	18.99	44.67	6.227	225.9
'9/3/2012 18:00'	19.01	42.42	5.742	239.4
'9/3/2012 19:00'	18.34	47.76	5.542	226.7
'9/3/2012 20:00'	16.06	58.58	6.102	230.8
'9/3/2012 21:00'	12.35	80.2	6.773	320.7
'9/3/2012 22:00'	10.95	86.7	6.529	327.5
'9/3/2012 23:00'	10.13	89.9	6.127	329.3
'9/4/2012 0:00'	9.73	91.4	4.786	323.9
'9/4/2012 1:00'	9.43	92.6	3.958	324.8
'9/4/2012 2:00'	9.47	94.2	3.524	334.8
'9/4/2012 3:00'	9.41	94.9	3.949	335.4
'9/4/2012 4:00'	9.32	95.4	3.895	332.1
'9/4/2012 5:00'	9.17	96.6	3.865	333.2
'9/4/2012 6:00'	8.98	97.8	3.463	331.3
'9/4/2012 7:00'	8.77	98.5	3.738	330.8
'9/4/2012 8:00'	8.76	99.1	3.266	331
'9/4/2012 9:00'	8.81	99.4	2.938	327.1
'9/4/2012 10:00'	8.92	99.5	2.925	334
'9/4/2012 11:00'	9.38	99.4	2.556	341.5
'9/4/2012 12:00'	9.26	99.5	3.429	31.82
'9/4/2012 13:00'	8.98	98.7	5.36	65.52
'9/4/2012 14:00'	8.93	95.2	5.096	71.04
'9/4/2012 15:00'	9.04	93.2	4.647	72.88
'9/4/2012 16:00'	9.54	90.7	3.735	75.28
'9/4/2012 17:00'	9.2	95.5	3.779	45.33
'9/4/2012 18:00'	9.29	98.4	2.262	38.52
'9/4/2012 19:00'	9.18	99.1	2.076	347.8
'9/4/2012 20:00'	9.07	99.5	1.59	320
'9/4/2012 21:00'	9.01	99.5	0.983	329.4
'9/4/2012 22:00'	9.08	99.4	0.633	74.83
'9/4/2012 23:00'	8.76	99.2	2.889	106.8
'9/5/2012 0:00'	8.75	93.9	3.592	126.2
'9/5/2012 1:00'	8.53	93.6	5.043	133.8
'9/5/2012 2:00'	8.37	94.2	5.496	153
'9/5/2012 3:00'	8.12	94.9	4.457	164

Appendix 2. Hourly Meteorological Data Used in the Baseline Calibration Model

Date	Average Air Temperature ˚C	Relative Humidity %	Average Wind Speed m/s	Average Wind Direction ˚(clockwise from North)
'9/5/2012 4:00'	7.99	95.1	4.117	156.8
'9/5/2012 5:00'	8.01	94.7	4.066	161.4
'9/5/2012 6:00'	7.933	95.2	5.486	171.4
'9/5/2012 7:00'	7.924	96	4.927	175.3
'9/5/2012 8:00'	7.843	95.8	4.717	155.4
'9/5/2012 9:00'	7.611	97	4.653	143.1
'9/5/2012 10:00'	7.539	96.3	4.832	146.3
'9/5/2012 11:00'	8.25	94.7	5.648	150.6
'9/5/2012 12:00'	9.47	91.2	6.389	153.2
'9/5/2012 13:00'	10.99	85.8	5.945	144.6
'9/5/2012 14:00'	12.52	82.2	5.771	162.4
'9/5/2012 15:00'	14.26	75.11	5.448	195.4
'9/5/2012 16:00'	14.78	70.01	5.391	190
'9/5/2012 17:00'	16.52	61.93	5.297	203.3
'9/5/2012 18:00'	17.25	57.81	6.619	225.1
'9/5/2012 19:00'	16.14	58.72	6.636	218.3
'9/5/2012 20:00'	14.66	64.58	6.29	204.7
'9/5/2012 21:00'	13.25	69.37	8.11	207
'9/5/2012 22:00'	12.63	69.8	8.26	208.9
'9/5/2012 23:00'	12.02	71.33	8.23	210.9
'9/6/2012 0:00'	12	69.6	8.56	211.7
'9/6/2012 1:00'	11.63	67.3	8.31	214.4
'9/6/2012 2:00'	11.51	65.64	7.723	213.5
'9/6/2012 3:00'	11.38	65.87	6.283	204.4
'9/6/2012 4:00'	11.22	66.38	6.31	211.1
'9/6/2012 5:00'	10.84	69.35	9.61	206.5
'9/6/2012 6:00'	10.32	75.57	9.33	195.7
'9/6/2012 7:00'	9.99	78.35	7.124	173.4
'9/6/2012 8:00'	10.96	76.91	6.081	176.5
'9/6/2012 9:00'	12.44	72.13	9.5	203.9
'9/6/2012 10:00'	13.52	68.22	10.95	198.2
'9/6/2012 11:00'	14.44	63.58	11.99	193.1
'9/6/2012 12:00'	16.1	57.76	13.46	190
'9/6/2012 13:00'	17.24	54.39	11.73	184.1
'9/6/2012 14:00'	17.95	52.51	12.47	181.5
'9/6/2012 15:00'	18.57	48.15	13.01	195.8
'9/6/2012 16:00'	18.81	47.26	13.21	217.5
'9/6/2012 17:00'	18.88	47.76	9.95	228.6
'9/6/2012 18:00'	18.64	49.39	8.46	231.4
'9/6/2012 19:00'	18.22	52.87	6.597	233.5
'9/6/2012 20:00'	17.27	57.77	4.705	250.9
'9/6/2012 21:00'	15.79	62.91	4.779	275.3
'9/6/2012 22:00'	13.05	76.47	6.453	319.3
'9/6/2012 23:00'	11.34	87.1	3.661	323.6
'9/7/2012 0:00'	11.32	89.7	2.985	320.8
'9/7/2012 1:00'	11.1	89.6	3.925	319.9
'9/7/2012 2:00'	10.46	90.5	3.657	315.4
'9/7/2012 3:00'	10.16	91.3	5.128	311.5
'9/7/2012 4:00'	9.7	95.1	4.856	318
'9/7/2012 5:00'	9.12	96.8	7.135	325.5

Appendix 2. Hourly Meteorological Data Used in the Baseline Calibration Model

Date	Average Air Temperature °C	Relative Humidity %	Average Wind Speed m/s	Average Wind Direction °(clockwise from North)
'9/7/2012 6:00'	8.82	97.7	6.971	332.1
'9/7/2012 7:00'	8.93	94.2	9.32	327.4
'9/7/2012 8:00'	9.15	89	9.21	325.8
'9/7/2012 9:00'	9.39	88.2	7.516	331.3
'9/7/2012 10:00'	9.71	83.6	8.39	327.9
'9/7/2012 11:00'	10.5	75.71	8.77	332.6
'9/7/2012 12:00'	11.05	73.56	8	351.8
'9/7/2012 13:00'	11.29	72.04	6.585	1.262
'9/7/2012 14:00'	10.99	73.12	3.968	355.8
'9/7/2012 15:00'	13.48	57.11	8.74	325
'9/7/2012 16:00'	14.39	49.16	8.89	322.7
'9/7/2012 17:00'	13.68	53.92	7.295	314.6
'9/7/2012 18:00'	13.49	55.78	5.659	295.3
'9/7/2012 19:00'	13.78	54.44	6.205	287.7
'9/7/2012 20:00'	12.54	48.34	7.492	289
'9/7/2012 21:00'	11.1	53.02	7.318	276.1
'9/7/2012 22:00'	10.68	55.55	7.059	273
'9/7/2012 23:00'	10.13	59.68	7.551	273.4
'9/8/2012 0:00'	8.83	66.64	9.14	266.1
'9/8/2012 1:00'	8.08	71.84	8.51	269.3
'9/8/2012 2:00'	7.358	76.9	7.424	248.3
'9/8/2012 3:00'	8.11	75.25	7.527	252.6
'9/8/2012 4:00'	7.535	75.28	6.347	240.9
'9/8/2012 5:00'	7.264	75.11	7.915	242.8
'9/8/2012 6:00'	6.97	74.52	8.15	241.2
'9/8/2012 7:00'	6.245	78.67	8.3	232.4
'9/8/2012 8:00'	6.697	75.7	8.16	229.9
'9/8/2012 9:00'	8.54	70.26	6.853	234.2
'9/8/2012 10:00'	9.39	67.5	6.981	233.3
'9/8/2012 11:00'	11.3	60.69	7.352	231.1
'9/8/2012 12:00'	12.41	51.02	8.16	237.7
'9/8/2012 13:00'	12.68	51.12	8.29	234.7
'9/8/2012 14:00'	12.92	52.42	5.319	230.4
'9/8/2012 15:00'	12.57	54.11	4.854	285.8
'9/8/2012 16:00'	10.91	60.99	3.498	299.1
'9/8/2012 17:00'	8.89	73.86	4.899	318.5
'9/8/2012 18:00'	9.76	65.44	2.26	307.4
'9/8/2012 19:00'	9.12	75.74	3.866	333
'9/8/2012 20:00'	8.41	76.44	3.502	326
'9/8/2012 21:00'	7.485	83	5.261	320.1
'9/8/2012 22:00'	7.109	84.1	4.421	323.4
'9/8/2012 23:00'	6.913	85.4	3.843	314.7
'9/9/2012 0:00'	6.427	89.7	4.15	328
'9/9/2012 1:00'	6.039	89.4	3.513	320.9
'9/9/2012 2:00'	5.696	88.9	3.421	323.2
'9/9/2012 3:00'	5.688	87.4	1.58	320.3
'9/9/2012 4:00'	5.83	85.2	0.862	255.8
'9/9/2012 5:00'	5.719	84.9	1.256	283.5
'9/9/2012 6:00'	5.418	86.3	2.427	248.1
'9/9/2012 7:00'	4.972	89.2	3.838	225.3

Appendix 2. Hourly Meteorological Data Used in the Baseline Calibration Model

Date	Average Air Temperature °C	Relative Humidity %	Average Wind Speed m/s	Average Wind Direction °(clockwise from North)
'9/9/2012 8:00'	5.104	90.6	4.188	222.7
'9/9/2012 9:00'	5.857	89.2	2.221	182
'9/9/2012 10:00'	6.742	84.3	3.049	184.7
'9/9/2012 11:00'	7.242	82.3	4.17	163.6
'9/9/2012 12:00'	8.05	83.4	3.699	135.3
'9/9/2012 13:00'	9.53	64.22	2.43	182.5
'9/9/2012 14:00'	10.37	53.69	2.261	196.3
'9/9/2012 15:00'	10.49	55.33	4.782	224.3
'9/9/2012 16:00'	11.16	52.99	2.199	234.1
'9/9/2012 17:00'	11.22	51.64	1.32	318.4
'9/9/2012 18:00'	10.49	59.73	1.751	136.4
'9/9/2012 19:00'	10.6	58.2	2.062	135.2
'9/9/2012 20:00'	9.79	59.11	2.435	141.1
'9/9/2012 21:00'	9.07	65.83	2.34	172.6
'9/9/2012 22:00'	7.288	73.57	3.009	327.1
'9/9/2012 23:00'	7.178	73.99	5.062	321.7
'9/10/2012 0:00'	6.736	75.57	5.361	326.9
'9/10/2012 1:00'	6.282	78.01	5.25	326.1
'9/10/2012 2:00'	6.07	78.41	4.508	322
'9/10/2012 3:00'	5.451	78.83	4.227	320.6
'9/10/2012 4:00'	4.907	80.3	3.638	310.5
'9/10/2012 5:00'	4.516	82.6	3.286	311.3
'9/10/2012 6:00'	4.575	81.2	3.294	317.2
'9/10/2012 7:00'	4.635	81.3	2.869	325.8
'9/10/2012 8:00'	4.709	86.3	2.466	326.9
'9/10/2012 9:00'	5.277	85.2	1.943	333.1
'9/10/2012 10:00'	5.6	84.7	3.025	352.6
'9/10/2012 11:00'	5.826	83.6	2.343	348.3
'9/10/2012 12:00'	6.283	81.3	2.139	349.6
'9/10/2012 13:00'	6.663	80.8	2.763	9.3
'9/10/2012 14:00'	7.078	79.41	3.082	355
'9/10/2012 15:00'	7.989	75.48	3.36	345.1
'9/10/2012 16:00'	7.776	79.87	4.596	344.2
'9/10/2012 17:00'	7.681	78.25	5.022	333.3
'9/10/2012 18:00'	7.741	76.54	5.267	329.7
'9/10/2012 19:00'	7.726	76.58	5.652	325
'9/10/2012 20:00'	7.787	76.8	6.719	326.8
'9/10/2012 21:00'	7.774	74.92	6.951	326.2
'9/10/2012 22:00'	7.325	77.8	6.904	325.6
'9/10/2012 23:00'	7.105	78.51	7.399	326.3
'9/11/2012 0:00'	7.012	78.49	7.453	325.8
'9/11/2012 1:00'	6.95	79.33	7.87	326.7
'9/11/2012 2:00'	6.678	79.71	7.848	329.3
'9/11/2012 3:00'	6.533	81.1	6.487	345
'9/11/2012 4:00'	6.073	82.4	6.921	47.85
'9/11/2012 5:00'	5.41	75.26	8.88	53.93
'9/11/2012 6:00'	5.12	76.33	6.563	42.57
'9/11/2012 7:00'	4.942	78.69	7.274	52.14
'9/11/2012 8:00'	4.771	79.57	7.134	51.72
'9/11/2012 9:00'	4.669	79.7	6.57	47.31

Appendix 2. Hourly Meteorological Data Used in the Baseline Calibration Model

Date	Average Air Temperature °C	Relative Humidity %	Average Wind Speed m/s	Average Wind Direction °(clockwise from North)
'9/11/2012 10:00'	4.809	76.91	7.403	46.88
'9/11/2012 11:00'	4.503	81	7.01	36.69
'9/11/2012 12:00'	4.762	75.63	8.88	46.75
'9/11/2012 13:00'	4.545	74.99	9.15	46.43
'9/11/2012 14:00'	4.652	73.02	8.35	37.99
'9/11/2012 15:00'	5.135	68.26	8.38	43.71
'9/11/2012 16:00'	5.68	61.58	8.72	42.05
'9/11/2012 17:00'	6.062	57.77	10.04	48.4
'9/11/2012 18:00'	5.721	59.02	10.06	55.04
'9/11/2012 19:00'	5.33	60.34	8.91	54.28
'9/11/2012 20:00'	4.533	69.08	8.28	45.21
'9/11/2012 21:00'	3.316	76.86	7.819	53.9
'9/11/2012 22:00'	2.591	80.9	7.093	54.14
'9/11/2012 23:00'	2.13	85.1	5.043	64.54
'9/12/2012 0:00'	1.69	90.6	4.812	53.29
'9/12/2012 1:00'	1.553	92.6	4.236	49.13
'9/12/2012 2:00'	1.455	94.2	4.406	58.02
'9/12/2012 3:00'	0.929	93.1	4.257	58.07
'9/12/2012 4:00'	0.486	91.6	4.142	62.09
'9/12/2012 5:00'	0.058	92.3	3.519	69.97
'9/12/2012 6:00'	0.458	85.3	2.916	66.17
'9/12/2012 7:00'	0.344	86.7	3.76	67.74
'9/12/2012 8:00'	0.078	90.2	3.058	98.4
'9/12/2012 9:00'	0.494	86.5	2.695	123
'9/12/2012 10:00'	1.191	80.2	3.095	110.3
'9/12/2012 11:00'	1.84	74.53	3.436	122.1
'9/12/2012 12:00'	2.379	69.3	3.234	132.3
'9/12/2012 13:00'	2.807	67.73	2.923	136.8
'9/12/2012 14:00'	3.373	64.92	3.652	152.4
'9/12/2012 15:00'	3.87	63.6	3.817	160.8
'9/12/2012 16:00'	3.978	62.93	3.822	158.3
'9/12/2012 17:00'	4.284	63.17	4.849	159.4
'9/12/2012 18:00'	4.193	65.04	4.812	181.3
'9/12/2012 19:00'	3.844	67.17	4.948	183
'9/12/2012 20:00'	3.603	69.5	5.099	166.5
'9/12/2012 21:00'	3.71	71.41	6.109	167.8
'9/12/2012 22:00'	4.117	71.93	6.232	157.9
'9/12/2012 23:00'	4.343	72.4	6.123	153.6
'9/13/2012 0:00'	4.423	73.23	6.782	160.8
'9/13/2012 1:00'	4.169	79.35	5.996	159
'9/13/2012 2:00'	3.788	85.2	7.556	162.9
'9/13/2012 3:00'	3.623	89.5	7.272	158.4
'9/13/2012 4:00'	3.798	92.8	7.089	156.3
'9/13/2012 5:00'	3.71	95.4	5.742	152.8
'9/13/2012 6:00'	3.948	96.3	5.462	154
'9/13/2012 7:00'	4.538	96.9	4.53	168.8
'9/13/2012 8:00'	5.445	94.2	3.997	221.4
'9/13/2012 9:00'	6.336	90.5	4.453	265.1
'9/13/2012 10:00'	6.585	89.5	4.882	308
'9/13/2012 11:00'	5.584	90.4	9.66	295.4

Appendix 2. Hourly Meteorological Data Used in the Baseline Calibration Model

Date	Average Air Temperature °C	Relative Humidity %	Average Wind Speed m/s	Average Wind Direction °(clockwise from North)
'9/13/2012 12:00'	5.465	83.8	10.84	293.5
'9/13/2012 13:00'	5.533	78.22	10.55	290
'9/13/2012 14:00'	5.891	72.13	9.44	292.7
'9/13/2012 15:00'	6.289	65.8	8.88	294.2
'9/13/2012 16:00'	6.384	61.1	8.99	291.8
'9/13/2012 17:00'	6.333	62.77	8.7	294.4
'9/13/2012 18:00'	6.234	64.76	8.01	295.1
'9/13/2012 19:00'	5.589	71.22	7.477	295.2
'9/13/2012 20:00'	4.79	70.68	6.241	287.7
'9/13/2012 21:00'	4.183	72.69	7.297	276.5
'9/13/2012 22:00'	3.685	77.74	9.43	269.6
'9/13/2012 23:00'	3.691	78.98	9.79	273
'9/14/2012 0:00'	3.546	79.73	5.476	317.5
'9/14/2012 1:00'	3.047	80.6	3.767	316.8
'9/14/2012 2:00'	2.861	80.8	3.846	319.8
'9/14/2012 3:00'	3.267	76.62	6.925	291.1
'9/14/2012 4:00'	2.772	78.72	7.064	285
'9/14/2012 5:00'	2.591	82.2	7.258	290.2
'9/14/2012 6:00'	2.521	84	6.647	291.4
'9/14/2012 7:00'	2.273	84	6.997	288
'9/14/2012 8:00'	2.603	82.2	6.523	280.1
'9/14/2012 9:00'	2.79	81.8	4.739	301.1
'9/14/2012 10:00'	3.244	74.73	4.946	306.7
'9/14/2012 11:00'	3.54	71.26	5.077	297.6
'9/14/2012 12:00'	4.487	64.87	4.6	324.9
'9/14/2012 13:00'	4.897	63.28	5.858	342.6
'9/14/2012 14:00'	4.239	73.47	5.071	341
'9/14/2012 15:00'	4.447	74.22	5.789	355.5
'9/14/2012 16:00'	4.532	71.14	6.083	358.4
'9/14/2012 17:00'	4.743	69.66	5.857	352.1
'9/14/2012 18:00'	4.575	69.48	5.416	5.702
'9/14/2012 19:00'	3.506	79.66	6.084	346.2
'9/14/2012 20:00'	3.364	80.4	6.334	1.89
'9/14/2012 21:00'	3.011	82.9	5.718	353.5
'9/14/2012 22:00'	2.817	84.3	6.77	12.08
'9/14/2012 23:00'	1.962	90.6	6.403	333.7
'9/15/2012 0:00'	1.317	93.7	6.807	324.3
'9/15/2012 1:00'	1.273	93.9	7.189	321.4
'9/15/2012 2:00'	1.17	93.3	6.522	324.2
'9/15/2012 3:00'	0.767	94.7	5.667	321.7
'9/15/2012 4:00'	1.276	88.8	5.802	327
'9/15/2012 5:00'	1.273	90.9	4.853	337.7
'9/15/2012 6:00'	1.801	85.7	4.251	332.8
'9/15/2012 7:00'	1.944	83.3	5.974	323.4
'9/15/2012 8:00'	2.067	83.5	5.2	317.5
'9/15/2012 9:00'	2.367	88.1	6.127	320.3
'9/15/2012 10:00'	2.44	88.2	7.189	330.6
'9/15/2012 11:00'	3.331	80.6	8.08	334.5
'9/15/2012 12:00'	3.674	79.41	8.09	334.1
'9/15/2012 13:00'	3.692	81.9	7.701	334.9

Appendix 2. Hourly Meteorological Data Used in the Baseline Calibration Model

Date	Average Air Temperature °C	Relative Humidity %	Average Wind Speed m/s	Average Wind Direction °(clockwise from North)
'9/15/2012 14:00'	3.704	83.6	7.504	346.4
'9/15/2012 15:00'	4.243	80.1	5.732	356.6
'9/15/2012 16:00'	4.653	79.13	5.921	358.6
'9/15/2012 17:00'	4.902	74.9	7.003	347.7
'9/15/2012 18:00'	4.047	81.3	6.853	318.5
'9/15/2012 19:00'	3.83	81.5	7.198	304
'9/15/2012 20:00'	3.391	80.9	6.577	307.1
'9/15/2012 21:00'	3.098	82.4	5.821	311.1
'9/15/2012 22:00'	3.053	83.9	4.836	305.6
'9/15/2012 23:00'	2.914	81.2	4.177	297.6
'9/16/2012 0:00'	2.9	82.4	3.256	291.7
'9/16/2012 1:00'	2.69	84.2	3.54	275.2
'9/16/2012 2:00'	2.39	85	4.475	262.6
'9/16/2012 3:00'	1.937	81.3	5.014	255.6
'9/16/2012 4:00'	2.55	76.95	5.382	256.4
'9/16/2012 5:00'	2.907	76.96	2.858	279.3
'9/16/2012 6:00'	2.781	79.27	2.435	215.1
'9/16/2012 7:00'	3.016	78.74	1.953	231.9
'9/16/2012 8:00'	2.91	82.2	1.567	213.1
'9/16/2012 9:00'	3.373	79.28	1.04	184.7
'9/16/2012 10:00'	4.555	75.22	1.514	210.9
'9/16/2012 11:00'	5.04	71.53	1.659	242
'9/16/2012 12:00'	5.005	73.17	1.9	317.9
'9/16/2012 13:00'	4.831	79.33	1.637	248.5
'9/16/2012 14:00'	5.095	78.75	1.976	216.1
'9/16/2012 15:00'	5.789	69.99	1.213	352.2
'9/16/2012 16:00'	5.195	77.62	4.457	22.23
'9/16/2012 17:00'	4.526	83.1	2.839	78.41
'9/16/2012 18:00'	4.603	81.7	1.677	88.5
'9/16/2012 19:00'	4.689	78.9	0.853	48.49
'9/16/2012 20:00'	4.272	76.57	3.64	76.92
'9/16/2012 21:00'	3.802	73.06	3.337	89.7
'9/16/2012 22:00'	3.655	69.23	2.698	115
'9/16/2012 23:00'	3.469	65.8	2.997	112.5
'9/17/2012 0:00'	2.944	67.84	2.47	117
'9/17/2012 1:00'	2.055	72.88	2.19	138.2
'9/17/2012 2:00'	2.126	70.63	3.122	154.2
'9/17/2012 3:00'	1.676	74.27	3.37	175.6
'9/17/2012 4:00'	1.261	68.96	4.244	165.6
'9/17/2012 5:00'	0.752	77.32	4.875	198
'9/17/2012 6:00'	0.834	75.07	4.698	183.9
'9/17/2012 7:00'	0.453	81	4.504	178.9
'9/17/2012 8:00'	0.99	78.76	4.715	178.3
'9/17/2012 9:00'	1.69	81.7	3.901	172.5
'9/17/2012 10:00'	2.654	79.06	4.386	172.3
'9/17/2012 11:00'	2.376	83.3	5.55	195.9
'9/17/2012 12:00'	3.301	79.34	6.349	202
'9/17/2012 13:00'	4.127	72.79	6.347	207.9
'9/17/2012 14:00'	5.092	65.73	6.84	195.2
'9/17/2012 15:00'	5.458	63.03	6.834	194.9

Appendix 2. Hourly Meteorological Data Used in the Baseline Calibration Model

Date	Average Air Temperature °C	Relative Humidity %	Average Wind Speed m/s	Average Wind Direction °(clockwise from North)
'9/17/2012 16:00'	5.913	60.68	6.932	182.7
'9/17/2012 17:00'	5.934	62.57	7.121	177
'9/17/2012 18:00'	5.495	66.58	6.638	171.2
'9/17/2012 19:00'	5.325	67.75	6.379	166.5
'9/17/2012 20:00'	5.013	68.13	7.421	175.8
'9/17/2012 21:00'	4.542	69.62	7.824	172.1
'9/17/2012 22:00'	4.53	70.13	7.74	169.9
'9/17/2012 23:00'	4.553	71.6	7.836	169.8
'9/18/2012 0:00'	4.33	75.37	7.03	167.6
'9/18/2012 1:00'	3.525	87.4	6.498	150.9
'9/18/2012 2:00'	3.138	89.7	7.837	152.2
'9/18/2012 3:00'	3.308	92	6.882	151.9
'9/18/2012 4:00'	3.219	93.7	7.24	152.7
'9/18/2012 5:00'	3.113	94.6	7.142	152.3
'9/18/2012 6:00'	3.286	95.4	5.448	151.8
'9/18/2012 7:00'	3.138	95.3	4.958	150.1
'9/18/2012 8:00'	3.104	95.4	5.197	153.8
'9/18/2012 9:00'	3.595	94.5	5.049	157.2
'9/18/2012 10:00'	3.795	96.5	2.673	145.9
'9/18/2012 11:00'	4.461	97.9	2.318	142.1
'9/18/2012 12:00'	4.875	98.1	1.216	124.4
'9/18/2012 13:00'	5.225	98.4	2.07	342.1
'9/18/2012 14:00'	5.687	99	5.398	327.4
'9/18/2012 15:00'	5.826	99.4	7.367	325.8
'9/18/2012 16:00'	5.839	99.1	8.05	321.2
'9/18/2012 17:00'	5.442	97.2	9.64	334.8
'9/18/2012 18:00'	4.689	94.6	10.98	329.7
'9/18/2012 19:00'	4.355	92.9	9.35	338.5
'9/18/2012 20:00'	4.068	92.4	8.48	322.1
'9/18/2012 21:00'	3.737	94.6	7.734	322.6
'9/18/2012 22:00'	3.584	95.6	7.869	315.7
'9/18/2012 23:00'	3.645	92.2	8.1	312
'9/19/2012 0:00'	3.508	93.1	7.05	313.2
'9/19/2012 1:00'	3.578	92.4	6.457	313.2
'9/19/2012 2:00'	3.314	94.8	6.353	314.1
'9/19/2012 3:00'	3.171	96.3	6.052	312.2
'9/19/2012 4:00'	3.033	98.4	5.252	320.5
'9/19/2012 5:00'	2.983	99.1	4.866	327.6
'9/19/2012 6:00'	2.889	99.4	3.555	328
'9/19/2012 7:00'	2.444	99.5	1.608	22.32
'9/19/2012 8:00'	2.097	99.6	1.112	118.2
'9/19/2012 9:00'	2.175	99.6	1.325	111.9
'9/19/2012 10:00'	2.403	99.6	0.622	101.9
'9/19/2012 11:00'	2.811	99.6	0.895	57.23

Appendix 3

Diesel Fuel Oil (Canada) Chemical Reference Sheet

Rescan™
an ERM company

Diesel Fuel Oil (Canada)

Synonyms: Automotive Gas Oil

Reference ID

Grade 1-D: straight-run fractions including kerosenes to intermediate distillates from mixed-base crudes; used for mobile service such as trucks, railroads and submarines.
Grade 2-D: similar to Grade 1-D but with lower volatility.; used for industrial and heavy mobile service.
Grade 4-D: residual fuel oils blended with more viscous distillates; used for larger stationary installations.

Data from EETD 85 are for a diesel sample purchased from a service station in the summer of 1984.

Data from Shell 1999 were taken from MSDS Number 322-110.

For additional fuel specifications refer to ASTM D975.

ASTM D 975

API Gravity

39.4		EETD 84

Equation(s) for Predicting Evaporation

Short term (<5 days): $\%Ev = (0.31 + 0.018T)\sqrt{(t)}$
Long term: $\%Ev = (5.8 + 0.045T)\ln(t)$
Where %Ev = weight percent evaporated; T = surface temperature (°C); t = time (minutes)

ESD 96

Sulphur (weight %)

0.10		EETD 86
0.16	(a)	

(a) winter diesel

Flash Point (°C)

>40	Shell 99a

Flammability Limits in Air (volume %)

1 to 6	Shell 99a

Ignition Temperature (°C)

250	Shell 99a

Reid Vapour Pressure (kPa)

2	ESD 91

Density (g/mL)

Evaporation (weight %)	Temperature (°C)		
0	0	0.8380	EETD 84
	15	0.8245	ESD 96
		<0.876	Shell 99a
	25	0.8171	ESD 96
	40	0.8063	
28	0	0.8450	EETD 89
	15	0.8350	

Pour Point (°C)

-30	EETD 86

Dynamic Viscosity (mPa·s or cP)

Temperature (°C)		
0	4	EETD 85
15	2	ESD 96
25	2	
40	1	

Diesel Fuel Oil (Canada)

Kinematic Viscosity (mm²/s or cSt)

Temperature (°C)		Reference ID
40	1.3 to 4.1	Shell 99a

Hydrocarbon Groups (weight %)

Waxes	1	ESD 91

Surface Tension (mN/m or dynes/cm)

Temperature (°C)		
0	27.7	EETD 84
15	26.5	ESD 96
25	23.8	
40	22.7	

Oil/Salt Water Interfacial Tension (mN/m or dynes/cm)

Temperature (°C)		
0	28.2	EETD 85
15	28.0	

Oil/Fresh Water Interfacial Tension (mN/m or

Temperature (°C)		
0	30.1	EETD 85
15	29.4	

(a) estimated

Boiling Point Distribution (weight %)

Boiling Point (°C)	Weight %	
40	1	ESD 95
60	1	
80	1	
100	1	
120	1	
140	3	
160	11	
180	23	
200	34	
250	65	
300	91	
350	99	

Boiling Point Distribution (°C)

Weight %	Boiling Point (°C)	
5		ESD 95
10		
15		
20		
25		
30		
35		
40		
45		
50		
55		

Diesel Fuel Oil (Canada)

Boiling Point Distribution (°C)

Weight %	Boiling Point (°C)	Reference ID
60		ESD 95
65		
70		
75		
80		
85		
90		
95		

Boiling Range (°C)

		Reference ID
246 to 388		Shell 99a

Metals (ppm)

		Reference ID
Barium	<0.3	Cao 92
Chromium	<1.5	
Copper	<0.6	
Iron	4.6	
Lead	<3	
Magnesium	12.3	
Molybdenum	<0.6	
Nickel	<1	
Titanium	<0.6	
Vanadium	<0.6	
Zinc	1.2	

Aqueous Solubility (mg/L)

Temperature (°C)			Reference ID
20 (approx.)	39	(a)	MacLean 89
22	3	(a)	Suntio 86
	2	(b) (d)	Murray 84
	8	(b) (e)	
20 (approx.)	60	(c)	MacLean 89

(a) fresh water; (b) distilled water; (c) salt water
(d) Gulf P20 diesel; (e) Gulf P40 diesel

Acute Toxicity of Water Soluble Fraction (mg/L)

	Test Organism			Reference ID
48h EC50	Daphnia magna	4	(a)	MacLean 89
		0	(b)	EETD 89
	Artemia spp.	22	(a)	MacLean 89
		1	(b)	EETD 89
48h LC50	Daphnia magna	7	(a)	MacLean 89
		1	(b)	EETD 89
	Artemia spp.	24	(a)	MacLean 89
		1	(b)	EETD 89
	Rainbow trout larvae	2	(c)	Lockhart 87
		3	(d)	

(a) results based on fluorescence spectroscopy; (b) results based on GC purge-and-trap analysis; (c) closed container; (d) open container

Appendix 4-1

Bathurst Inlet Wind Roses, Selected Modelling Data 2007 to 2012

Rescan™
an ERM company

2007

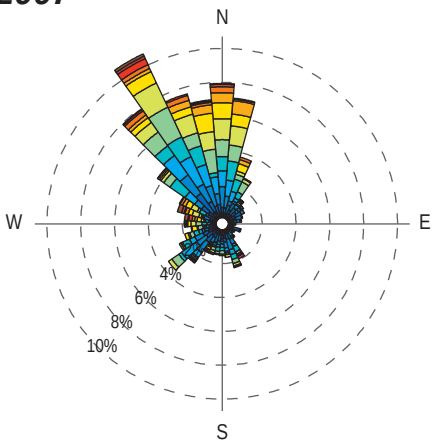

2011

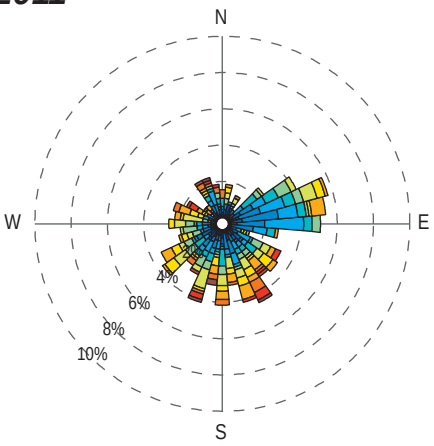

2008

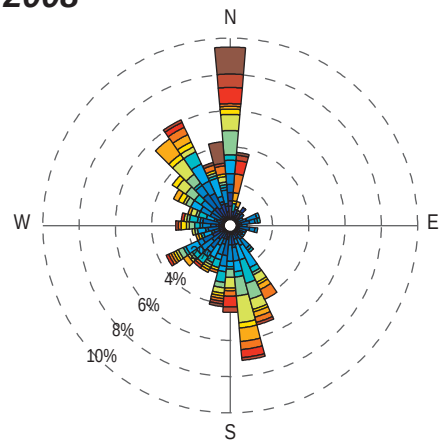

2012

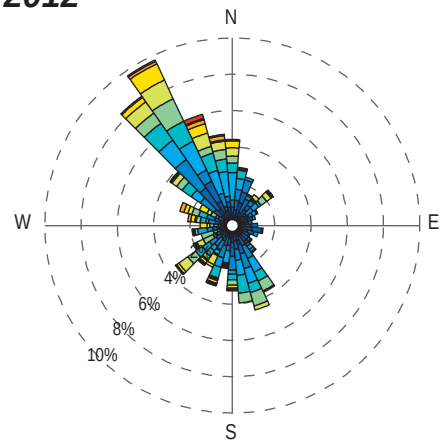

2010

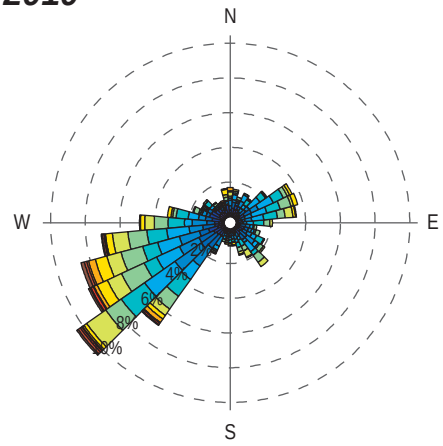

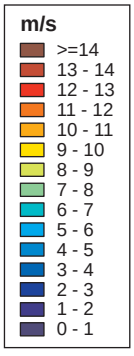

Notes: Wind direction is given as the direction FROM which the wind is blowing.

Figure A4-1

Bathurst Inlet Wind Roses, Selected Modelling Data 2007 to 2012

Sabina GOLD & SILVER CORP.

Rescan Engineers & Scientists

Appendix 4-2

Daily Average Wind Data Used in the Marine Diesel Fuel Spill Modelling

Rescan™
an ERM company

Appendix 4-2. Daily Average Wind Data Used in the Marine Diesel Fuel Spill Modelling

Date	Average Wind Speed m/s	Average Wind Direction °(clockwise from North)
'17-Jul-2007'	1.585598056	341.1381664
'18-Jul-2007'	4.884709253	219.3756106
'19-Jul-2007'	5.511254271	170.2089989
'20-Jul-2007'	7.148738571	199.0983412
'21-Jul-2007'	7.166126207	291.6768948
'22-Jul-2007'	8.589656098	273.4250242
'23-Jul-2007'	4.954443656	325.1184961
'24-Jul-2007'	3.982707544	340.5904965
'25-Jul-2007'	7.898540825	343.6991696
'26-Jul-2007'	4.217532847	342.3944977
'27-Jul-2007'	3.819377387	1.497897226
'28-Jul-2007'	4.268869696	344.9910709
'29-Jul-2007'	1.276927086	183.7371434
'30-Jul-2007'	3.231264083	310.3138041
'31-Jul-2007'	10.40633963	356.0385055
'01-Aug-2007'	1.150529353	344.3628187
'02-Aug-2007'	1.777573429	357.050773
'03-Aug-2007'	5.014755304	351.8554182
'04-Aug-2007'	5.016867174	339.4052104
'05-Aug-2007'	2.583632172	272.0852992
'06-Aug-2007'	4.568927205	354.8654296
'07-Aug-2007'	7.012074561	313.2227871
'08-Aug-2007'	11.58034644	288.0901067
'09-Aug-2007'	9.789538486	298.2260929
'10-Aug-2007'	7.493040251	353.7747262
'11-Aug-2007'	10.08013559	342.4001156
'12-Aug-2007'	6.968148824	347.8701245
'13-Aug-2007'	7.682492133	344.0066917
'14-Aug-2007'	9.368856179	351.8558365
'15-Aug-2007'	7.231000436	355.3008495
'16-Aug-2007'	0.585385511	340.4002738
'17-Aug-2007'	3.903226689	227.0710897
'18-Aug-2007'	2.545119556	235.8402052
'19-Aug-2007'	4.803928825	340.3605432
'20-Aug-2007'	6.457645247	4.404379999
'21-Aug-2007'	6.948423561	343.4337981
'22-Aug-2007'	8.769779657	351.2411546
'23-Aug-2007'	9.285424041	354.8747748
'24-Aug-2007'	9.139099303	8.139295992
'25-Aug-2007'	8.273296182	351.7428686
'26-Aug-2007'	7.958436455	348.7086297
'27-Aug-2007'	7.026889517	328.1880822
'28-Aug-2007'	8.186070519	331.861216
'29-Aug-2007'	6.395396304	334.4239954
'30-Aug-2007'	3.789429734	212.4943301
'31-Aug-2007'	2.743017243	186.8775479
'01-Sep-2007'	5.123227469	357.3575288
'02-Sep-2007'	4.645208813	264.9707117
'03-Sep-2007'	7.521988128	312.5229956
'04-Sep-2007'	3.774304495	14.68244222

Appendix 4-2. Daily Average Wind Data Used in the Marine Diesel Fuel Spill Modelling

Date	Average Wind Speed m/s	Average Wind Direction °(clockwise from North)
'05-Sep-2007'	1.007648261	352.4392207
'06-Sep-2007'	5.166751573	242.904143
'07-Sep-2007'	5.974752099	339.195474
'08-Sep-2007'	3.981546622	329.9656924
'09-Sep-2007'	7.249219922	332.6960168
'10-Sep-2007'	0.805025761	207.6981163
'11-Sep-2007'	4.020240267	243.2754847
'12-Sep-2007'	6.805615493	358.7804756
'13-Sep-2007'	5.654821483	345.3201717
'14-Sep-2007'	5.621125302	326.2084126
'15-Sep-2007'	6.90791482	24.91857188
'16-Sep-2007'	4.005169466	326.2844104
'17-Sep-2007'	5.001960429	321.4588887
'18-Sep-2007'	2.483832747	327.0512499
'19-Sep-2007'	2.786097205	175.1943559
'20-Sep-2007'	4.936711238	158.7923048
'21-Sep-2007'	1.847587582	135.6982181
'22-Sep-2007'	2.198162119	146.9328691
'23-Sep-2007'	4.018601194	14.06366209
'24-Sep-2007'	3.789905056	65.76219543
'25-Sep-2007'	4.086033721	32.99274319
'26-Sep-2007'	4.895109815	346.9070588
'27-Sep-2007'	5.641924264	264.2016135
'28-Sep-2007'	0.823165484	151.0953828
'29-Sep-2007'	8.095992372	16.58302886
'30-Sep-2007'	5.366620368	260.826098
'01-Oct-2007'	5.913601112	167.9950933
'02-Oct-2007'	2.81092486	319.4556812
'03-Oct-2007'	11.56299053	328.330665
'04-Oct-2007'	4.912524471	280.2690812
'05-Oct-2007'	3.296099136	235.0693285
'06-Oct-2007'	2.648332973	313.765461
'07-Oct-2007'	1.982793002	15.66902292
'08-Oct-2007'	6.210915874	207.6430312
'16-Sep-2008'	8.382106683	313.7607164
'17-Sep-2008'	2.24962173	1.226328345
'18-Sep-2008'	7.343369624	322.452425
'19-Sep-2008'	5.036522753	280.774844
'20-Sep-2008'	3.508681282	189.7508186
'21-Sep-2008'	4.155858654	161.0627835
'22-Sep-2008'	5.556438665	345.2905002
'23-Sep-2008'	11.99954259	3.665217712
'24-Sep-2008'	14.17433539	359.3810612
'25-Sep-2008'	10.14380563	343.3856609
'26-Sep-2008'	2.871663914	244.4271798
'27-Sep-2008'	4.665539192	186.7759244
'28-Sep-2008'	1.339635535	291.0323572
'29-Sep-2008'	3.281281338	81.74507356
'30-Sep-2008'	3.94707107	121.6198984
'01-Oct-2008'	7.516278471	166.3896888

Appendix 4-2. Daily Average Wind Data Used in the Marine Diesel Fuel Spill Modelling

Date	Average Wind Speed m/s	Average Wind Direction °(clockwise from North)
'02-Oct-2008'	0.982112043	195.0594143
'03-Oct-2008'	10.09732456	176.1449206
'04-Oct-2008'	1.559917236	258.3637083
'05-Oct-2008'	6.18899572	155.0443491
'06-Oct-2008'	6.47548293	245.3478666
'07-Oct-2008'	3.812591302	264.1468718
'08-Oct-2008'	3.711010807	304.1208448
'09-Oct-2008'	3.945556439	357.4395412
'10-Oct-2008'	4.641471885	170.6489596
'11-Oct-2008'	6.217005058	247.6381327
'12-Oct-2008'	1.829714641	266.8767822
'13-Oct-2008'	5.201280076	200.268245
'14-Oct-2008'	5.944945443	59.22852476
'29-Jun-2010'	5.261429161	59.27486245
'30-Jun-2010'	4.455280038	4.223057268
'01-Jul-2010'	1.885287332	34.31053757
'02-Jul-2010'	1.1951708	306.6137494
'03-Jul-2010'	7.51860093	359.1263789
'04-Jul-2010'	7.070374043	332.7613328
'05-Jul-2010'	7.461283317	263.6624785
'06-Jul-2010'	6.248632204	250.4520621
'07-Jul-2010'	4.423108401	248.9147752
'08-Jul-2010'	5.622056507	244.3392406
'09-Jul-2010'	2.729268527	199.9204486
'10-Jul-2010'	1.20172781	338.7885327
'11-Jul-2010'	6.993523875	64.31403897
'12-Jul-2010'	5.516542529	249.2236996
'13-Jul-2010'	0.16762909	284.2464377
'14-Jul-2010'	2.572402095	241.1236081
'15-Jul-2010'	4.241638125	243.9549882
'16-Jul-2010'	5.509667129	272.4005948
'17-Jul-2010'	5.5356343	244.5747652
'18-Jul-2010'	3.715203987	250.3545411
'19-Jul-2010'	3.194302665	157.5237115
'20-Jul-2010'	3.980971995	247.9514846
'21-Jul-2010'	3.562555051	260.5507626
'22-Jul-2010'	2.417615774	71.592824
'23-Jul-2010'	5.671076326	74.77712992
'24-Jul-2010'	0.55852601	37.17714722
'25-Jul-2010'	6.506523985	307.5918071
'26-Jul-2010'	1.886486149	290.8443437
'27-Jul-2010'	2.55955234	240.2321493
'28-Jul-2010'	1.55657353	23.16743605
'29-Jul-2010'	2.724959077	83.12341812
'30-Jul-2010'	4.211124169	232.038233
'31-Jul-2010'	3.481244794	239.4707778
'01-Aug-2010'	7.652115906	221.1289218
'02-Aug-2010'	6.385165693	216.7961837
'03-Aug-2010'	8.827192754	240.8539629
'04-Aug-2010'	2.408329185	255.9384062

Appendix 4-2. Daily Average Wind Data Used in the Marine Diesel Fuel Spill Modelling

Date	Average Wind Speed m/s	Average Wind Direction °(clockwise from North)
'05-Aug-2010'	3.39314092	152.321369
'06-Aug-2010'	6.83051139	77.89375327
'07-Aug-2010'	6.300058324	72.53190423
'08-Aug-2010'	1.403793748	91.5078499
'09-Aug-2010'	4.54735725	83.75748252
'10-Aug-2010'	4.864052298	121.804218
'11-Aug-2010'	7.669018133	241.3864848
'12-Aug-2010'	7.19723525	252.9584739
'13-Aug-2010'	4.515946576	244.2131541
'14-Aug-2010'	4.037657554	247.7996678
'15-Aug-2010'	7.894641675	247.2353024
'16-Aug-2010'	8.051028643	243.5933314
'17-Aug-2010'	4.21808486	248.9098402
'18-Aug-2010'	5.339016668	247.8130813
'19-Aug-2010'	6.865867699	231.4559072
'20-Aug-2010'	2.650866047	152.9162419
'21-Aug-2010'	2.461696211	167.5496959
'22-Aug-2010'	1.132284742	143.4955585
'23-Aug-2010'	4.604932451	237.9463774
'24-Aug-2010'	5.816693559	236.0649069
'25-Aug-2010'	4.879509522	245.3166917
'26-Aug-2010'	6.499698717	268.3814287
'27-Aug-2010'	7.026192255	271.8726806
'28-Aug-2010'	4.304600905	217.6657805
'29-Aug-2010'	2.960172799	74.21864417
'30-Aug-2010'	2.604471309	169.2238784
'31-Aug-2010'	3.356149287	258.304568
'01-Sep-2010'	1.967079883	97.80331258
'02-Sep-2010'	5.116579673	119.6744765
'03-Sep-2010'	6.991853941	75.78926597
'04-Sep-2010'	1.042031262	96.41452104
'05-Sep-2010'	4.104458013	203.7126714
'06-Sep-2010'	6.103080434	223.1423839
'07-Sep-2010'	1.956951055	324.368269
'08-Sep-2010'	5.265636063	58.59973408
'09-Sep-2010'	1.221873496	249.4866825
'10-Sep-2010'	5.871847173	230.409561
'11-Sep-2010'	7.484029707	250.0623062
'12-Sep-2010'	4.753469264	172.5423314
'13-Sep-2010'	4.592843493	162.8239702
'14-Sep-2010'	11.94184835	238.4378297
'15-Sep-2010'	6.116223825	180.9635119
'16-Sep-2010'	1.895865045	133.054298
'17-Sep-2010'	4.71246684	236.6454387
'18-Sep-2010'	5.198736982	230.805091
'19-Sep-2010'	2.475996763	212.4992041
'11-Sep-2011'	6.849069446	237.3978677
'12-Sep-2011'	7.277386144	248.1556831
'13-Sep-2011'	5.433074969	179.6123952
'14-Sep-2011'	3.662285118	148.1329434

Appendix 4-2. Daily Average Wind Data Used in the Marine Diesel Fuel Spill Modelling

Date	Average Wind Speed m/s	Average Wind Direction °(clockwise from North)
'15-Sep-2011'	3.085507018	302.1530202
'16-Sep-2011'	6.652929515	58.17527173
'17-Sep-2011'	3.322130871	3.474471567
'18-Sep-2011'	3.985373758	23.09589221
'19-Sep-2011'	4.989020537	102.2014932
'20-Sep-2011'	7.062491359	114.6665415
'21-Sep-2011'	7.918062784	121.5658969
'22-Sep-2011'	8.175474338	161.1519234
'23-Sep-2011'	6.552278969	205.0994826
'24-Sep-2011'	6.587974835	194.8959272
'25-Sep-2011'	2.561969201	213.3269866
'26-Sep-2011'	9.244775792	338.5287693
'27-Sep-2011'	8.927308697	280.217041
'28-Sep-2011'	5.789278034	222.4129318
'29-Sep-2011'	2.832851866	141.9827367
'30-Sep-2011'	7.118349151	24.7116853
'01-Oct-2011'	6.833931099	291.9269702
'02-Oct-2011'	7.023855458	142.8431186
'03-Oct-2011'	6.962553884	144.7750095
'04-Oct-2011'	7.624169414	75.19036758
'05-Oct-2011'	4.655708659	168.4751314
'06-Oct-2011'	2.861662856	146.0052395
'07-Oct-2011'	4.428301123	73.97722317
'25-Jul-2012'	3.314383446	281.5682081
'26-Jul-2012'	7.670197453	336.941114
'27-Jul-2012'	5.323211441	322.3199961
'28-Jul-2012'	4.441160488	321.4953303
'29-Jul-2012'	3.560912147	355.8830517
'30-Jul-2012'	2.515114485	92.44389922
'31-Jul-2012'	1.451391934	135.9463924
'01-Aug-2012'	1.498289993	34.91972427
'02-Aug-2012'	2.224530187	195.6985933
'03-Aug-2012'	4.533735063	172.0177298
'04-Aug-2012'	7.872670598	336.1816711
'05-Aug-2012'	3.454082702	343.0713046
'06-Aug-2012'	1.891282577	217.9943571
'07-Aug-2012'	5.020182919	242.4538925
'08-Aug-2012'	1.859725332	296.4788306
'09-Aug-2012'	4.935092089	354.7686501
'10-Aug-2012'	4.765900159	351.4222135
'11-Aug-2012'	5.447035459	337.1584026
'12-Aug-2012'	1.838945899	260.4230573
'13-Aug-2012'	5.998417655	330.5802622
'14-Aug-2012'	4.14539482	327.8802718
'15-Aug-2012'	0.85625299	306.2638455
'16-Aug-2012'	2.541906021	209.047308
'17-Aug-2012'	4.29297733	168.5995096
'18-Aug-2012'	1.656997078	195.9260664
'19-Aug-2012'	7.10255794	302.2410161
'20-Aug-2012'	7.092120853	303.8819584

Appendix 4-2. Daily Average Wind Data Used in the Marine Diesel Fuel Spill Modelling

Date	Average Wind Speed m/s	Average Wind Direction °(clockwise from North)
'21-Aug-2012'	5.061596386	316.8605373
'22-Aug-2012'	3.738776632	343.3921384
'23-Aug-2012'	1.986914281	346.2670561
'24-Aug-2012'	3.554513397	171.9396414
'25-Aug-2012'	4.180804724	197.7514731
'26-Aug-2012'	5.860045677	179.1011753
'27-Aug-2012'	1.721958504	297.0279183
'28-Aug-2012'	3.476298697	359.7771213
'29-Aug-2012'	7.363077741	353.4917263
'30-Aug-2012'	3.848088511	257.1136918
'31-Aug-2012'	4.602536549	272.3426723
'01-Sep-2012'	2.725416197	153.3506094
'02-Sep-2012'	5.752293511	174.077223
'03-Sep-2012'	2.62277331	342.6276307
'04-Sep-2012'	3.618220441	159.1476376
'05-Sep-2012'	9.005689744	201.5586718
'06-Sep-2012'	5.762230254	322.0809037
'07-Sep-2012'	6.521363455	254.7711777
'08-Sep-2012'	1.43878434	270.0441033
'09-Sep-2012'	2.713172315	331.7267845
'10-Sep-2012'	6.030541286	19.76306444
'11-Sep-2012'	3.479457902	80.00316238
'12-Sep-2012'	2.93367827	224.4727116
'13-Sep-2012'	5.527170632	302.4393393
'14-Sep-2012'	6.17936843	337.4180643
'15-Sep-2012'	2.368316551	283.7571941
'16-Sep-2012'	3.701691231	174.4781345
'17-Sep-2012'	3.192792071	163.8315152
'18-Sep-2012'	3.403983181	322.7485076
'19-Sep-2012'	3.10932605	322.8315254